STRUCTURE-FUNCTION STUDIES ON THE NOVEL ALPHA-KINASE FAMILY

by

MOJDEH SAMIMI GHARAEI

A thesis submitted to the Department of Biochemistry

In conformity with the requirements for

the degree of Master of Science

Queen's University

Kingston, Ontario, Canada

(February, 2010)

ABSTRACT

Dictyostelium myosin heavy chain kinase A (MHCK A) and mammalian transient receptor potential melastatin-related 7 (TRPM7) are two divergent members of a family of atypical protein kinases called the alpha kinases. The crystal structures of the alpha-kinase domains of MHCK A (A-CAT, residues 552-841) and mouse TRPM7 (TRPM7-CAT, residues 1548-1862) are very similar. In both cases a C-terminal tail (C-tail) sequence (A-CAT, residues 806-841 and TRPM7-CAT, residues 1819-1862) is missing from the crystal structure. Here I show that the unstructured C-tail is required for the catalytic activity of A-CAT and TRPM7-CAT. Truncation of the C-tail of A-CAT to residue 823 decreased kinase activity by ~98% and ATPase activity by ~97%. Truncation of the C-tail of TRPM7-CAT to residue 1827 decreased kinase activity by ~97% and ATPase activity by ~58%. Ligation of the C-tail sequence of MHCK B (residues 326-354) to A-CAT-802 (residues 552-802), fully rescued kinase activity. Alignment of the C-tail sequences of MHCK A-D revealed a conserved Gly-Thr-hydrophobic motif. Previous work has shown that in A-CAT, the conserved threonine (T825) is a site of autophosphorylation. Mutation of the T825 to alanine reduced A-CAT kinase and ATPase activities by 97%, whereas mutation to serine decreased kinase and ATPase rates by 85% and 60%, respectively. This result is consistent with the finding that A-CAT strongly prefers to phosphorylate threonine residues. Surprisingly, mutation of T825 to glutamic acid reduced kinase activity by ~93% and ATPase activity by ~96%. This result suggests that glutamic acid does not properly mimic phosphothreonine in this situation, or that the free hydroxyl group of T825 is required for the catalytic activity of A-CAT.

Mutation of T825 to alanine or glutamic acid in full-length MHCK A reduced kinase activity by ~90% and ATPase activity by ~40%. Further studies are required to determine if the C-tail of TRPM7-CAT also contains an essential threonine residue.

Acknowledgments

Firstly, I would like to express sincere gratitude to my supervisor, Dr. Graham P. Cote, for his encouragement, supervision and research ideas. I am indebted to Dr. Scott W. Crawley. Without his vision, mentorship, and guidance, this work would not have been possible. I would also like to thank my research committee members, Dr. Zongchao Jia and Dr. John Allingham, for their consultations, and helpful discussions. I am thankful to Dr. Qilu Ye, for helping in structural studies. I appreciate Mr. Kim Munro for providing me with the opportunity of performing CD analysis. My laboratory members, Dr. Emilia Kazmierczak and Yidai Yang deserve acknowledgement for their support.

I offer my special thanks to the friends who opened a new horizon for continuing my studies in Canada. I am appreciative to my dearest friend, Jane, for the encouragement which has been vital in the completion of this endeavor.

Last but not least, I wish to thank my mother for her unconditional immense love, support and encouragement throughout the pursuit of all of my goals in life and dedicate this research work to her.

Table of Contents

List of Tables

List of Figures

List of Abbreviations

A-CAT	Catalytic domain of MHCK A
AX3	Axenic Strain 3 (A *Dictyostelium discoideum* strain)
B-CAT	Catalytic domain of MHCK B
cAMP	Adenosine 3’5’-cyclic Monophosphate
CaM	Calmodulin
CaMKIII	Calcium/Calmodulin dependent Kinase III (eukaryotic elongation factor-2)
CD	Circular Dichroism
DMSO	Dimethyl Sulfoxide
DNAase I	Deoxyribonuclease I
DTT	Dithiothreitol
E.coli	*Escherichia coli*
EDTA	Ethylene Diamine Tetraacetic Acid
eEF2K	eukaryotic Elongation Factor 2 Kinase
G418	Geneticin
GST	Glutathione S-Transferase
IPTG	Isopropyl β-D-1-Thiogalactopyranoside
LB	Luria-Bertani Broth
MBP	Myelin Basic Protein
MHCK	Myosin Heavy Chain Kinase
N/D loop	Aspargine/Aspartate loop
PBS	Phosphate Buffered Saline
PCR	polymerase Chain Reaction
PLC	Phospholipase C

PMSF	Phenylmethylsulfonyl Fluoride
RMSD	Root Mean Square Deviation
SD	Standard Deviation
SDS	Sodium Dodecyl Sulfate
SDS-PAGE	Sodium Dodecyl Sulfate Polyacrylamide Gel Electrophoresis
TBS	Tris-(hydroxymethyl) Aminomethan Buffered Saline
Tris	Tris-(hydroxymethyl) Aminomethane
TRPM6	Transient Receptor Potential Cation Channel, Subfamily M, Member 6
TRPM7	Transient Receptor Potential Cation Channel, Subfamily M, Member 7
TRPM7-CAT	Catalytic domain of TRPM7
Tween 20	Polyoxyethylenesorbitan Monolaurate
VWF	Von Willebrand Factor
WD domain	WD (Triptophane/Aspartate)-Repeat Domain

CHAPTER 1

INTRODUCTION

There is a large superfamily of homologous kinases, called the Protein Kinase-like (PK-like) superfamily, that phosphorylate a variety of substrates and play important roles in various cellular functions. These kinases are phosphotransferases that cleave the γ-phosphate group from ATP and transfer it to proteins, lipids, and glycosides. They contribute to post-translational modification of downstream targets through the covalent addition of one or more negatively charged phosphate moieties. This type of modification can result in drastic changes to the cellular function of the substrate, changing either the enzymatic or structural properties of the molecule, and is fundamental to most signaling and regulatory processes in cells, including metabolism, transcription, cell cycle progression, cytoskeletal rearrangement, cell migration, apoptosis, and differentiation. Mutations and dysregulation of PK-like enzymes play causal roles in many human diseases including cancer, diabetes and inflammatory disorders. The possibility of developing agonists and antagonists of these enzymes for use in disease therapy, suggests why research in this area is so demanded. For identifying some novel specific inhibitors and facilitating translational research into the use of such drugs, a detailed understanding of the regulation and function of PK-like enzymes and their substrates is essential.

The PK-like superfamily consists of several families which share a common core domain consisting of regions required for ATP binding and catalysis of the phosphotransfer reaction [1]. One of the largest families within the PK-like superfamily,

commonly referred to as Conventional Protein Kinases (CPKs) [2], has received much experimental attention, both structurally and biochemically. CPKs comprise a large number of serine/threonine and tyrosine protein kinases. The other families of the PK-like superfamily, termed Atypical Protein Kinases (APKs), display little sequence similarity to CPKs and do not have the usual CPK sequence motifs conserved but retain structural homology with the catalytic core of CPKs. This suggests that they have a common ancestor [3], but diverged early in evolution to form a distinct phyletic group [1]. APKs include Actin-fragmin kinase, Phosphoinositide 3-kinase (PI3K), Rio1-like kinases, and Myosin Heavy Chain Kinase/Elongation Factor 2 kinase (MHCK/EF2K) that includes the Transient Receptor Potential cation channel (TRP) kinase. [4] The MHCK/EF2 kinase family is also called the alpha-kinase family [5].

The members of the alpha-kinase family phosphorylate serine/threonine residues on target proteins and are widely distributed in eukaryotes [1;2]. It seems that alpha-kinases developed to provide a novel signaling capacity within eukaryotic organisms [1].

1.1. The Alpha-Kinase Family

The alpha-kinases are a small but widespread family within the PK-like superfamily (Figure 1-1) which possess a novel protein kinase catalytic domain with no detectable sequence homology to CPKs [3;6]. Alpha-kinases acquired their name due to the proposal that these kinases prefer to target sites that are in the context of an alpha-helix [5]. This is in stark contrast to CPKs, which normally phosphorylate sites in β-turns, loops [7] or disordered regions [5]. However, as of yet, there is little direct

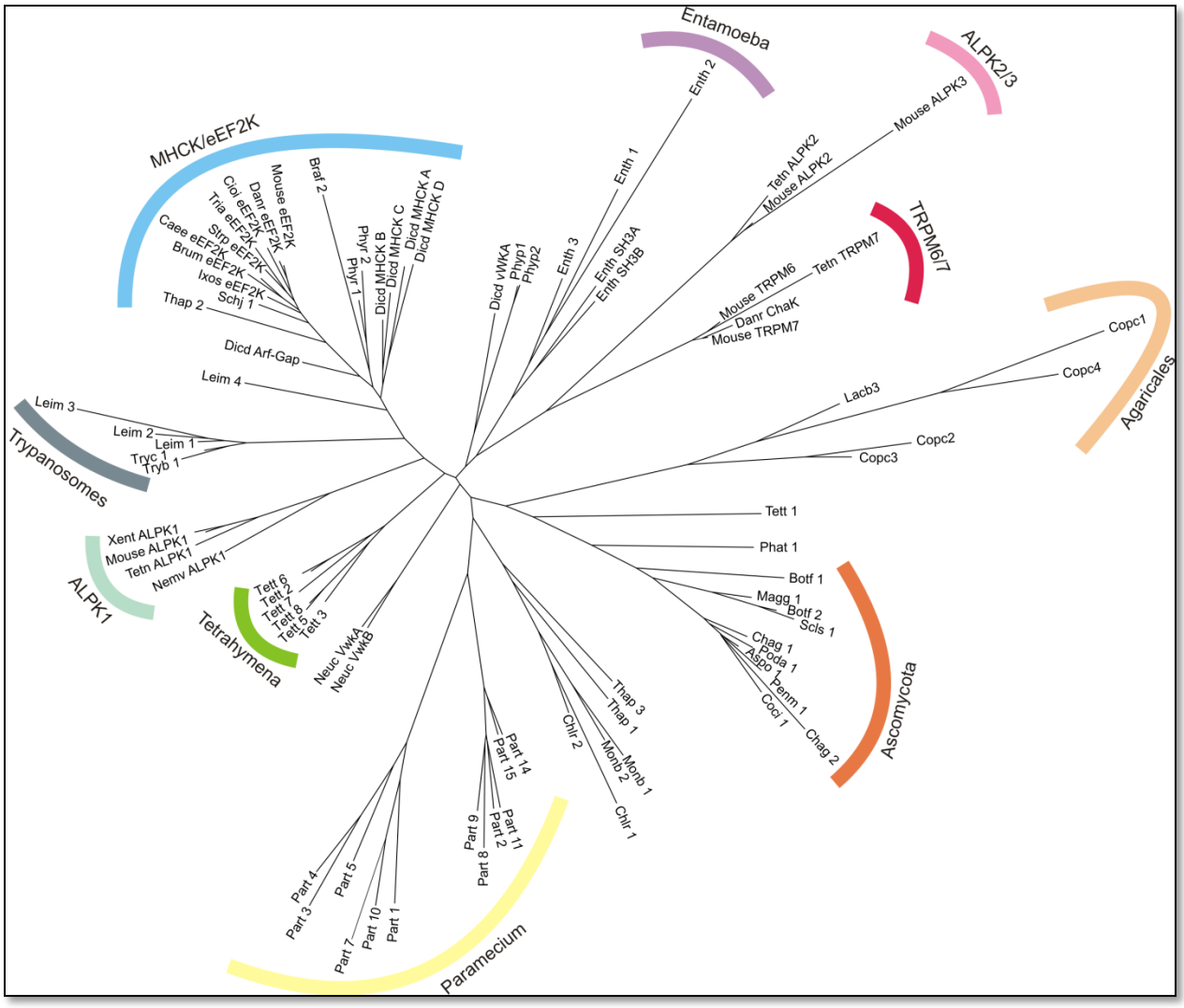

Figure 1-1. Evolutionary relationships of the alpha-kinases. A phylogenetic tree of alpha-kinase domains. Major groups of alpha-kinases are indicated by colored arcs. Branch length represents evolutionary time. [8]

empirical evidence to support this hypothesis about the alpha-kinases.

The novel alpha-kinase domain is found in numerous protein kinases that are involved in a diverse array of cellular activities. Representatives of the alpha-kinase family have been found in a wide variety of protozoa, fungi and animals but are missing from higher plants and insects [2]. Only a few alpha-kinases exist in each organism, suggesting that they perform some highly specific function. It is interesting that a small number of alpha-kinases have been highly conserved throughout evolution to regulate key cellular processes [8]. During evolution, the alpha kinase domains combined with many different functional subdomains such as von Willebrand factor-like motifs (vWKa) and even cation channels (TRPM6 and TRPM7). As a result, these kinases are implicated in a large variety of cellular processes such as protein translation, Mg^{2+} homeostasis, intracellular transport, cell migration, adhesion and proliferation (Table 1-1).

To date, six alpha-kinases in *Dictyostelium discoideum* and six in human have been identified. The most well characterized members of this novel family are the myosin heavy chain kinases (MHCKs) found in *Dictyostelium* [9-12]. MHCK A was purified to homogeneity as an activity capable of phosphorylating and disassembling myosin II filaments [9]. It was the cloning and analysis of the MHCK A gene that led to the discovery of the new and functionally diverse family of alpha-kinases [10;13]. The four closely related MHCKs (MHCK A, B, C and D) regulate the cellular activity of myosin II by controlling the formation of myosin II bipolar filaments [14]. The *Dictyostelium* alpha-kinase 1 (AK1) contains an N-terminal Arf-GAP domain [14] and is, like the MHCKs, specifically expressed by *Dictyostelium*. vWFa-Kinase (vWKa) is one

Table 1-1. Overview of alpha-kinases. The main characteristics of alpha-kinases and the domain architectures of these proteins. If known, substrate specificity is indicated together with the preference for threonines and/or serines. (Adapted from [15])

Name	Structure	Substrate	Function	Loss of Function Phenotype
TRPM6/ 7	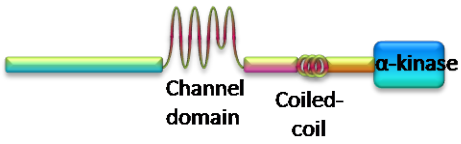	**TRPM6 & 7**. MHC: threonine & serine **TRPM6**. RACK1 **TRPM7**. Annexin 1	**TRPM6.** Whole body Mg^{2+} homeostasis. **TRPM7**. Cellular Mg^{2+} homeostasis. Ca^{2+} signaling and myosin II filament disassembly	**TRPM6**. Hypomagnesaemia with secondary hypocalcaemia **TRPM7**. Embryonic lethal, reduced cell proliferation and migration
ALPK2/3		---	**ALPK2**. --- **ALPK3**. Transcription regulation	**ALPK2**. --- **ALPK3**. Impaired cardiac myocyte differentiation
ALPK1		Myosin IA	Epithelial cell polarity and exocytic vesicular transport	Impaired vesicle delivery towards the apical membrane
eEF2k		eEF2: threonine	Inhibition of eEF2, regulation of the global rate of protein synthesis	Increased susceptibility to metabolic stress and stalled cell cycle
MHCK B/C		MHC: threonine	**MHCK B**. Myosin II filament disassembly in the contractile ring during cytokinesis **MHCK C**. Similar and in posterior regions of moving cells	Impaired cell migration and cytokinesis
MHCK A/D	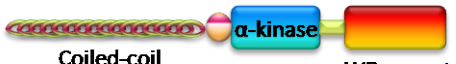	**MHCK A**. MHC: threonine **MHCK D**. ---	**MHCK A**. Myosin II filament disassembly at the leading edge of moving or dividing cells. **MHCK D**. ---	**MHCK A**. Impaired cell migration and cytokinesis. **MHCK D**. ---
AK-1	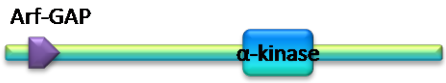	---	---	---
vWKa		(Not myosin II): threonine & serine	Myosin II expression and filament (dis)assembly	Impaired cytokinesis
SH3-containing		---	---	---
P53-like		---	---	---

of the more recently identified alpha-kinases in *Dictyostelium*, and is thought to play a role in regulating the periodic contractions of the contractile vacuole, which acts as part of the osmotic protective mechanism exhibited by *Dictyostelium* [16].

Other well characterized members of the alpha-kinase family include the transient receptor potential related ion channels, TRPM6 (Transient Receptor Potential cation channel, Melastatin subfamily, member 6), and TRPM7 (member 7) found in mammals [17;18]. They are bifunctional proteins that combine a Ca^{2+}- and Mg^{2+}-permeable cation channel with a C-terminal alpha-kinase domain. Other alpha-kinases found in mammals are the Elongation Factor-2 Kinase (eEF2K; previously known as calmodulin kinase III: CaMKIII) [19] and alpha-kinase 1 (Lymphocyte Alpha-Kinase: LAK or ALPK1), alpha-kinase 2 (Heart Alpha-Kinase: HAK or ALPK2) and alpha-kinase 3 (Muscle Alpha-Kinase: MAK or ALPK3) [5]. The mammalian alpha-kinases are widely distributed among all vertebrates. The eEF2K is also found in invertebrates such as *Caenorhabditis elegans,* the metazoan *Trichoplax adhaerens* and in the diatom *Thalassiosira pseudonana*, indicating that eEF2K represents the oldest alpha-kinase within the vertebrates (See http://pfam.sanger.ac.uk, Family: *Alpha_kinase* (PF02816), Species distribution).

1.2. Myosin II: Structure and Function

Myosin II is a molecular motor that plays an important role in a wide variety of contractile events in eukaryotic cells by supporting ATP-dependent movement of actin filaments in both muscle and nonmuscle cells [20]. Studies in *Dictyostelium* have

revealed that complex cellular processes such as cytokinesis [21], cellular migration, maintenance of cell cortical tension, cell surface receptor capping [20], protein transport, phagocytosis, exocytosis [22] and multicellular development depend on the proper function and regulation of myosin II [10]. The diversity of these myosin II-dependent processes demonstrates that cells must be able to affect highly localized reorganization of their myosin II filaments in response to specific signals that initiate specific contractile processes [20;23]. For example, myosin II is enriched at the rear of migrating cells, where it drives contraction and movement of the cell body forward [20], and at the cleavage furrow of a dividing cell, where it facilitates division and separation of the resulting daughter cells [24].

Myosin II is a hexameric protein complex composed of a pair of heavy chains (MHCII), a pair of essential chains and a pair of regulatory light chains [25-27]. The MHCII consists of: (i) a conserved motor domain at the N-terminus that drives the movement along actin filaments; (ii) a neck domain that serves as a rigid lever arm to generate movement of the motor domain and (iii) a non-conserved helical coiled-coil domain at the C-terminus, which terminates with a short non-helical tail (Figure 1-2) [28;29]. For the sake of clarity, the hexameric myosin II shall be referred to as monomeric myosin II throughout this thesis to distinguish it from myosin II that is in the form of bipolar filaments. The formation of myosin II thick filaments occurs through the spontaneous, self association of the myosin II tail domains [30]. It is the filamentous, cytoskeleton-associated form of myosin II that is the active form of myosin II in the cell, while individual monomeric myosin II molecules are cytosolic and inactive [31].

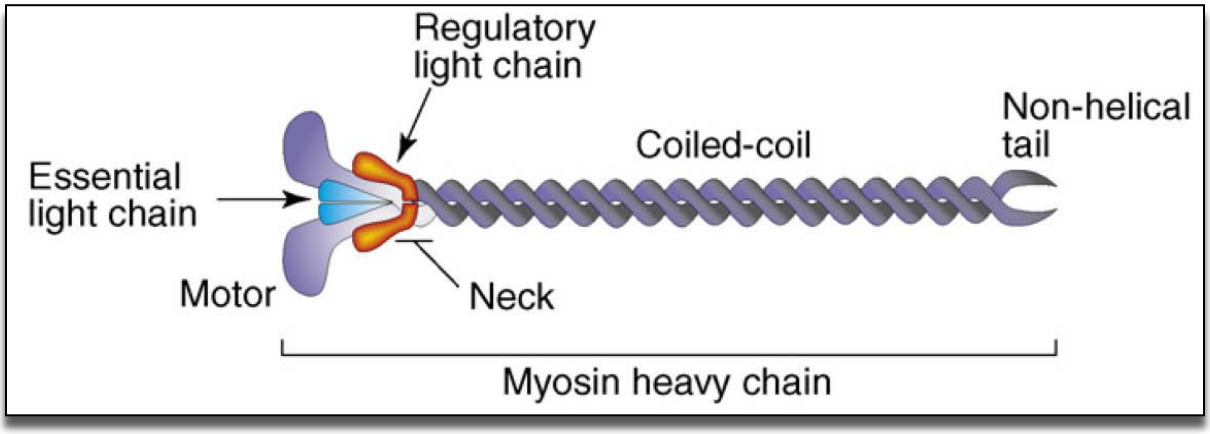

Figure 1-2. Schematic diagram of myosin II. Myosin II is a hexamer composed of two heavy chains and two sets of light chains. The different parts of the heavy chain, including the motor, neck, coiled-coil and nonhelical domains are indicated. [32]

1.3. Regulation of Myosin II

In *Dictyostelium* as well as in mammalian nonmuscle cells, myosin II exists in a dynamic equilibrium between a cytoplasmic pool of monomers and a cytoskeleton-associated assembly of bipolar filaments. Bipolar filament assembly appears to be required for the translocation of myosin II to the cortical actin cytoskeleton and thus is a critical process regulating myosin localization and activity in response to specific signals such as exposure of cells to chemoattractants [33;34]. Phosphorylation of the tail region of the myosin heavy chain II is the predominant mechanism controlling filament stability in *Dictyostelium* [35;36]. It is thought that phosphorylation of the tail causes a change in the net positive charge of this region which leads to disassembly of myosin thick filaments (Figure 1-3) [37], thereby preventing contraction of actin filaments, and promoting cytoskeleton relaxation [31;38;39].

1.4. The *Dictyostelium* MHCKs

Myosin Heavy Chain Kinase A (MHCK A) was identified from *Dictyostelium discoideum* as an activity capable of phosphorylating the myosin II heavy chain [10] both *in vitro* [9] and *in vivo* [40]. Mapping studies later elucidated that this kinase targets three key threonine residues in the tail of myosin II (T1823, T1833 and T2029) which, when phosphorylated, promote thick filament disassembly [41;42]. MHCK A has a molecular weight of 130 kDa [9], and consists of a N-terminal α-helical coiled-coil domain, a central novel alpha-kinase domain and a C-terminal WD (Trp/Asp) repeat domain (Figure 1-4) [10;43]. Cross-linking and gel filtration experiments indicate

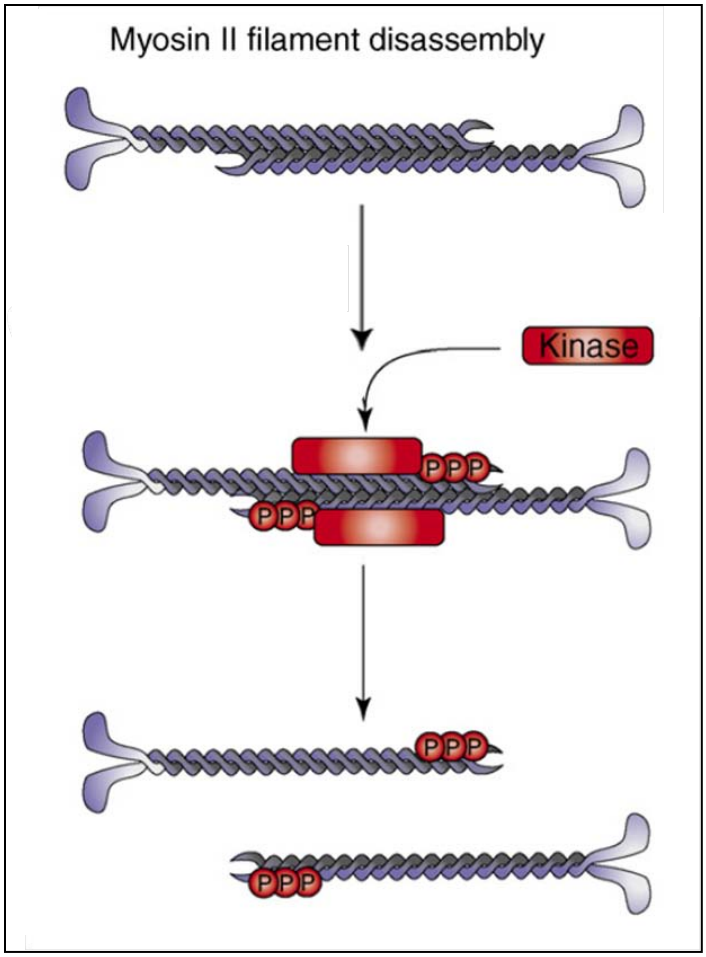

Figure 1-3. A schematic picture of phosphorylation of the myosin II heavy chain. Phosphorylation of the myosin II heavy chain destabilizes the electrostatic interactions between myosin II monomers, leading to filament disassembly. (adapted from [32])

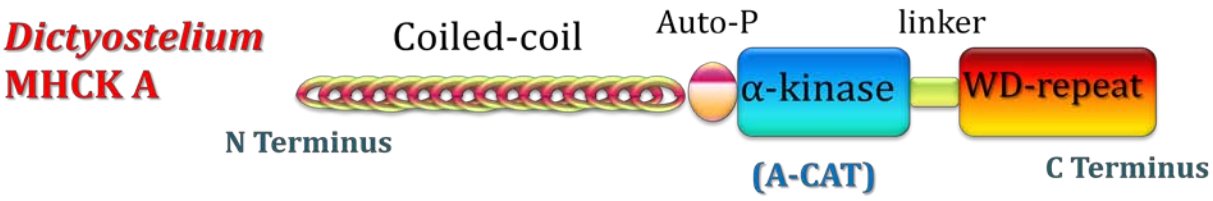

Figure 1-4. Schematic diagram of MHCK A. MHCK A domains: N-terminal α-helical coiled-coil domain, autophosphorylation domain, central alpha-kinase domain, linker and C-terminal WD repeat domain.

that native MHCK A is an oligomer with an approximate molecular size of 700 kDa [10]. Truncation analysis demonstrated that neither the coiled-coil domain nor the WD repeat domain are required for *in vitro* kinase activity, thereby identifying the protein kinase catalytic activity as residing solely in the 40-kDa MHCK A central domain [43;44]. The coiled-coil domain is responsible for oligomerization of the kinase [44], with 3-6 molecules coming together to form a homo-oligomer. The coiled-coil domain is also required for MHCK A to interact with actin filaments both *in vitro* and *in vivo*. Localization to actin-rich regions of the cell and translocation to the cell cortex in response to cAMP are abolished upon deletion of the coiled-coil domain [45]. This suggests that, in addition to driving myosin II disassembly, MHCK A may also affect the actomyosin cytoskeleton by crosslinking actin filaments. The C-terminal domain of MHCK A consists of seven WD repeat motifs which form a β-propeller domain that functions to target the kinase to myosin II filaments. Deletion of the WD repeat domain prevents myosin II phosphorylation by MHCK A *in vitro* and *in vivo* [46].

In vitro, the kinase activity of MHCK A is strongly enhanced by autophosphorylation. MHCK A incorporates up to 10 mol of phosphate/mol enzyme, although maximal activation is achieved after the incorporation of the first 3 molecules of phosphate per subunit [47]. Little is known concerning the signaling pathways that regulate MHCK A in the cell, but actin filaments, myosin II and acidic phospholipids stimulate the rate of autophosphorylation *in vitro* [34;48].

In addition to MHCK A, there are three more myosin heavy chain kinases with a similar domain structure in *Dictyostelium*, namely MHCK B, MHCK C and MHCK D. These kinases have an alpha-kinase domain located near their N-terminal end [2] and a

C-terminal WD repeat domain, but they lack an extended N-terminal coiled-coil domain. MHCK D contains a very short coiled-coil domain compared to MHCK A. Together MHCK A-D coordinate the assembly and disassembly of myosin II bipolar filaments within the cell [14], and play a key role in many complex processes in *Dictyostelium* such as cytoskeleton remodeling, cytokinesis, cellular migration, maintenance of cell cortical tension, and multicellular development. While each MHCK possesses a similar catalytic function, they are thought to act somewhat independently through differential localization during dynamic cellular processes such as cell migration and cytokinesis [12;14].

In migrating cells, MHCK A relocalizes to the actin rich cortex at sites of pseudopod formation in the anterior of the cell, where it presumably functions to phosphorylate and disassemble myosin II-based cross-linked actin filament networks which, in turn, may facilitate the reorganization of the actin cytoskeleton necessary for the formation of cellular extensions at the leading edge [49]. In contrast, MHCK C co-localizes with myosin II at the posterior region of locomoting cells, mediating contraction of the cell rear, and MHCK B distributes homogeneously in the cytoplasm [50]. In the early stage of cytokinesis, MHCK A (and sometimes MHCK C) localizes to the polar protrusions while MHCK B is always cytosolic throughout the cell. At the late stages of cytokinesis, MHCK C accumulates to the cleavage furrow and remains at this location to help disassemble myosin II thick filaments that have completed their role in furrow contraction [12;50].

MHCK A, B and C exhibit an unusually strong preference to phosphorylate threonine residues in protein and peptide substrates, but this preference is not shared by all alpha-kinases [51-54]. For instance vWKa phosphorylates both threonine and serine

residues [51] while TRPM7 prefers to phosphorylate mainly serine residues (Table 1-1) [53].

Pioneering studies performed in *Dictyostelium* on myosin II have clearly demonstrated the importance of MHCK A for proper regulation of the bipolar filament assembly equilibrium [14]. Disruption of the myosin II heavy chain gene in *Dictyostelium*, through homologous recombination, results in cells that display defects in cytokinesis and development [55-57]. Cells become large and multinucleated when grown in suspension due to the inability to close the contractile ring during cytokinesis. When subjected to starvation conditions in which wild type *Dictyostelium* amoeba undergo a developmental life cycle to form resistant spores, myosin II null cells are unable to progress past the loose aggregate stage. In a similar manner, overexpression of MHCK A leads to a myosin II null-like phenotype [40]. This is due to increased myosin II phosphorylation by the overexpressed kinase, which results in the conversion of active bipolar filaments into inactive monomers [40]. MHCK A-null cells have a decreased chemotactic efficiency caused by reduction in cell polarity and an inability to suppress lateral pseudopods and retract the uropod [58;59]. They also have a developmental defect, halting the developmental process shortly after cells have aggregated [40].

1.5. Mammalian TRPM6 and TRPM7

TRPM6 and TRPM7 belong to the Melastatin-related subfamily of TRP channels (TRPM: Transient Receptor Potential Melastatin cation channels), which consists of eight members (TRPM1–TRPM8) [60]. They display structural relatedness with the putative

tumor suppressor melastatin first identified in melanoma cells [61]. TRPM family displays a wide range of structural features, expression patterns, ion selectivity, gating properties and functions [62]. TRPMs are integral membrane proteins and possess a membrane topology similar to that of the well-studied voltage-gated potassium channels; each channel comprises six membrane-spanning segments with a pore-forming loop region between the fifth and sixth segments, and intracellular N- and C-termini [63]. TRPM7, and the highly related TRPM6, have a number of unusual features that distinguish them from other TRPMs. These include relatively a high conductivity to Mg^{2+} and an atypical protein kinase domain linked at the C-terminus to the channel domain [17;64;65].

TRPM7 is a 220 kDa Ca^{2+} and Mg^{2+}-permeable ion channel that has an alpha-kinase domain fused to the C-terminal cytoplasmic tail of the ion channel (Figure 1-5) [17;66]. TRPM7 was first identified in a yeast two-hybrid screen performed to identify binding partners of the C2 domain-containing COOH-terminus of PLC-β1 [17]. Subsequently TRPM6, a closely related homolog to TRPM7 (50% amino acid sequence identity for the full length protein and 75% when comparing the isolated kinase domains), was identified as the aberrant gene causing autosomal-recessive hypomagnesaemia with secondary hypocalcaemia found in humans [67]. In spite of these similarities between TRPM6 and TRPM7, they appear to be functionally non-redundant. While TRPM7 is ubiquitously expressed, TRPM6 expression is mostly limited to brain, intestine and kidneys [68]. Knockout studies have shown that both TRPM6 and TRPM7 are essential in development because loss of these channels is embryonic lethal [69;70]. Moreover, overexpression of TRPM6 cannot rescue cell growth arrest due to the ablation of TRPM7 [71]. TRPM7 has

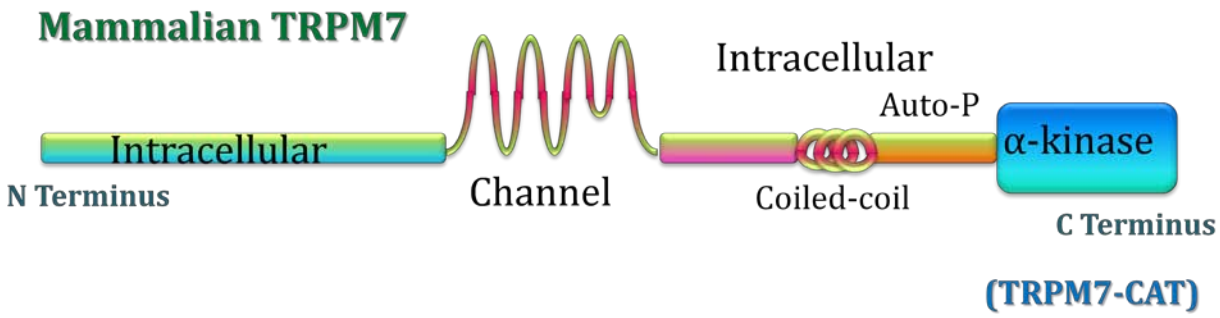

Figure 1-5. Schematic diagram of TRPM7. TRPM7 domains: N-terminal intracellular domain, transmembrane central ion channel domain, intracellular coiled-coil, autophosphorylation and C-terminal alpha-kinase domains.

been implicated in several pathological states including hypertension, anoxic neuronal death, hypopigmentation disorders and hearing impairment [72;73].

Like other TRPMs, TRPM7 and TRPM6 possess six transmembrane domains with N- and C-termini both residing in the cytosol and a pore loop region between transmembrane segments five and six. The alpha-kinase domain of TRPM6 and TRPM7 is located at the C-terminus [10;17;65;74] (Figure 1-5). To date, TRPM6 and TRPM7 are the only known ion channels to possess an intrinsic protein kinase domain. The question of whether or not autokinase activity regulates the channel activity of both TRPM6 and TRPM7 is still of great debate. The channel domain can be inhibited by physiological Mg.ATP concentrations [65;75;76]. The nucleotide-dependent regulation of TRPM7 appears to be mediated by a binding site within the endogenous kinase domain [77]. However, the general consensus is that mutations that eliminate kinase activity do not affect the channel activity of TRPM6 and TRPM7 but do influence the ability of free Mg^{2+} and nucleotides to suppress channel activity [52;78;79]. So, TRPM7 kinase and channel function are undoubtedly linked.

In an amazing conservation of function, evidence now suggests that both TRPM6 and TRPM7 may play a role in regulating myosin II filament assembly [80-82]. Both TRPM6 and TRPM7 are capable of phosphorylating the tail region of nonmuscle myosin II *in vitro*, which leads to filament disassembly [83]. Activation of TRPM7 in cells leads to a kinase-dependent inhibition of myosin II-based contractility and the remodeling of adhesion structures, such as focal adhesions and podosomes [81]. Apparently, this property of alpha-kinases has been preserved during evolution.

1.6. Regulation of Alpha-Kinase Activity

Research studies over the years have shown many different mechanisms for regulation of the activity of CPKs. For several kinases, intramolecular interactions with regulatory domains keeps them in an inactive state [84;85]. Transition to the active state can occur by association with regulatory proteins, such as calmodulin, lipids like PIP3, or second messengers such as cAMP [84;85]. Regulation may also occur through phosphorylation by upstream kinases or dephosphorylation by phosphatases [85] or by intermolecular or intramolecular autophosphorylation [86].

Initial studies undertaken to investigate the molecular mechanisms controlling the catalytic activity of alpha-kinases have revealed that regulatory mechanisms of the alpha-kinase family are similar to the ones that regulate CPKs. Generally two mechanisms appear to regulate several members of the alpha-kinase family: 1) autophosphorylation and 2) a requirement of additional domains beyond the catalytic core for efficient substrate phosphorylation [15]. Autophosphorylation is a regulatory mechanism for all alpha-kinases studied to date including MHCKs, eEF2K, TRPM6 and TRPM7 [46;47;50]. Studies show that MHCKs do not need complete autophosphorylation for activation because autophosphorylation of three sites (out of 10) is sufficient to activate MHCK A [47] and autophosphorylation of MHCK C and phosphorylation of myosin II proceeds in parallel [50]. In contrast, complete autophosphorylation of a Ser/Thr-rich domain next to the N-terminus of the catalytic domain of TRPM6 and TRPM7, helps these kinases to recognize myosin II as a substrate, however it is not needed for catalytic activity [53].

Notably, it has been found that the C-terminal WD repeat domain of MHCKs binds directly to *Dictyostelium* myosin II [46], which shows that MHCKs also require additional domains for substrate recognition. Upon deletion of this region, the rate of myosin II phosphorylation decreases but the kinetics of phosphorylation of a synthetic peptide are not affected [44;46]. The C-terminus of eEF2K plays a similar role for the activity of this enzyme [87;88]. In addition to autophosphorylation, eEF2K undergoes phosphorylation by upstream kinases like PKA which increases its enzymatic activity [89]. Another mechanism for activation of eEF2K is binding of Ca^{2+}/calmodulin to a region directly N-terminal of eEF2K catalytic domain [90;91].

Dimerization of the kinase domain of TRPM7 is essential for kinase activity [92-94]. Also the TRPM6 and TRPM7 kinase domain can heterodimerize to form a functional kinase [94]. The kinase activity of MHCK A requires Mg.ATP, and increases in the presence of 1-2 mM free Mg^{2+} or Mn^{2+} [43]. TRPM7 requires Mg^{2+} (optimum at 4–10 mM) or Mn^{2+} (optimum at 3–5 mM) for its activity. However, the kinase activity is about 2 orders of magnitude higher in the presence of Mn^{2+} than in the presence of Mg^{2+} [92].

1.7. Structural Overview of A-CAT

Despite the fact that alpha-kinases have no detectable sequence identity with CPKs, structural studies have shown that members of this novel kinase family possess a fold similar to CPKs [8;93]. Remarkably, the position of key amino acid residues important for catalysis appears to be very similar between the alpha-kinases and CPKs [2;93].

The crystal structures of the alpha-kinase domain from MHCK A reveal that, like

CPKs, the alpha-kinase domain is composed of a bilobed structure (Figure 1-6A) [8]. The N-terminal lobe of A-CAT is comprised mainly of a highly curved seven-stranded anti-parallel β sheet (β1-β3-β5-β6-β7-β9-β10), which rest on top of a large central α-helix (αC) which traverses both the N-terminal and C-terminal lobes. The C-terminal lobe contains one short stretch of anti-parallel β strands (β12-β15) and three α helices (αD-αF). The nucleotide-binding and active sites are formed by the cleft between the two lobes (Figure 1-7). There are three Mg^{2+} ions associated with the crystal structure of A-CAT-AMP: Mg^{2+}#1 is bound to the nucleotide, Mg^{2+}#2 is located very close to the nucleotide and Mg^{2+}#3 is coordinated by a loop called the N/D-loop (Figure 1-6A) [8]. The N/D-loop is a glycine-rich loop that contains a highly conserved aspartate or aspargine residue (Asp in 40% and Asn in 59% of alpha-kinases). It is proposed that the conformation of the N/D loop is altered upon binding of Mg^{2+}. Change in the conformation of the N/D loop, together with that of the P-loop, can alter the size and shape of an active-site pocket, that is proposed to be required for substrate binding [8].

While the fold of the N-terminal lobe of A-CAT bears a remarkable resemblance to CPKs, there are significant differences in the C-terminal lobe. One striking difference is the localization of the conserved GXGXXG motif which, in CPKs, is positioned within the catalytic P-loop and serves to bind the phosphate moieties of ATP. Although alpha-kinases do contain a similar glycine rich motif, it is not located within the P-loop but in the N/D loop.

Also of interest, A-CAT possesses a highly conserved zinc-binding motif near the C-terminus of its structure. A single zinc ion is tetrahedrally coordinated by two histidine and two cysteine residues (Figure 1-8) [8]. The zinc-binding module is crucial for the

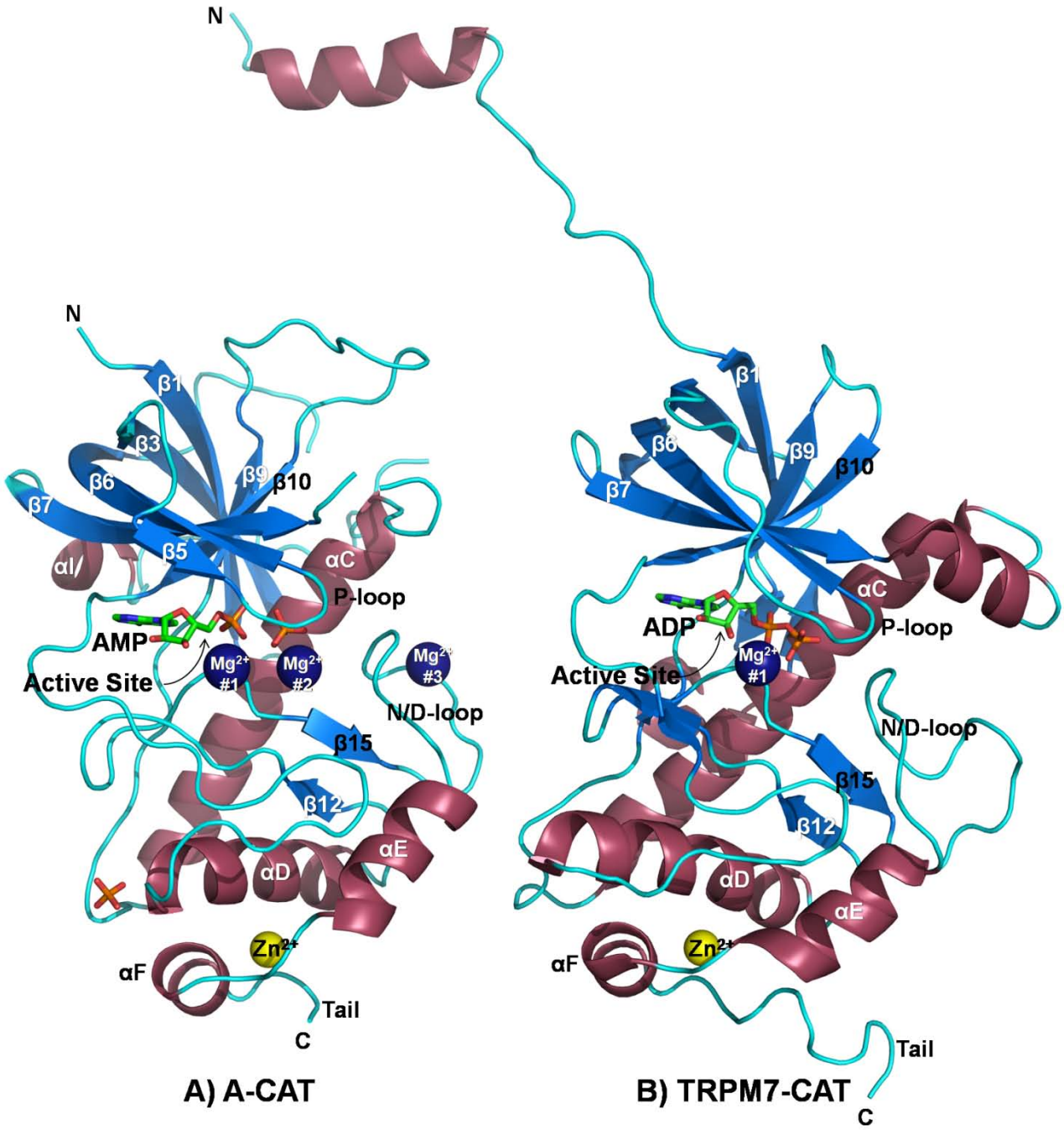

Figure 1-6. Structures of A-CAT and TRPM7-CAT. A) A stereoview of the A-CAT AMP complex, with β strands (blue) and α helices (raspberry). Mg^{2+} ions are rendered as dark blue spheres and the zinc atom as a yellow sphere. The nucleotide and Pi molecules are shown as sticks. N and T indicate the N and C-terminus [8]. B) A stereoview of the TRPM7-CAT-ADP complex (ID code in PDB: 1IAH). The colors are as introduced for A-CAT.

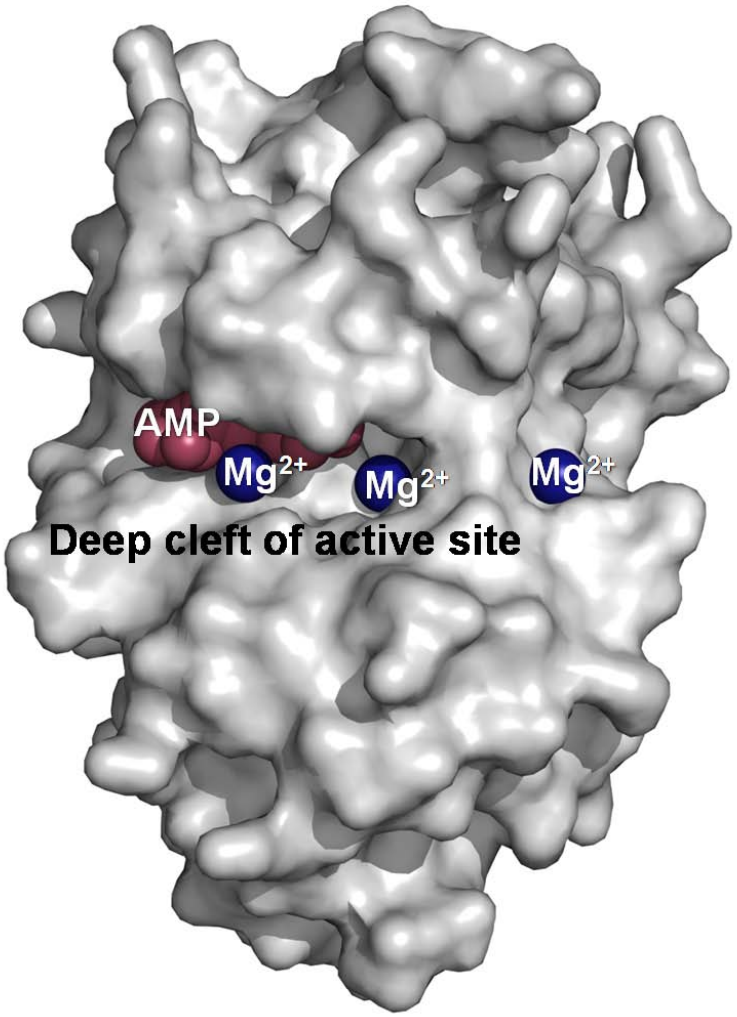

Figure 1-7. Molecular surface of A-CAT. The nucleotide and Pi molecules are rendered as raspberry spheres and the Mg^{2+} ions as dark blue spheres. (Adapted from [8])

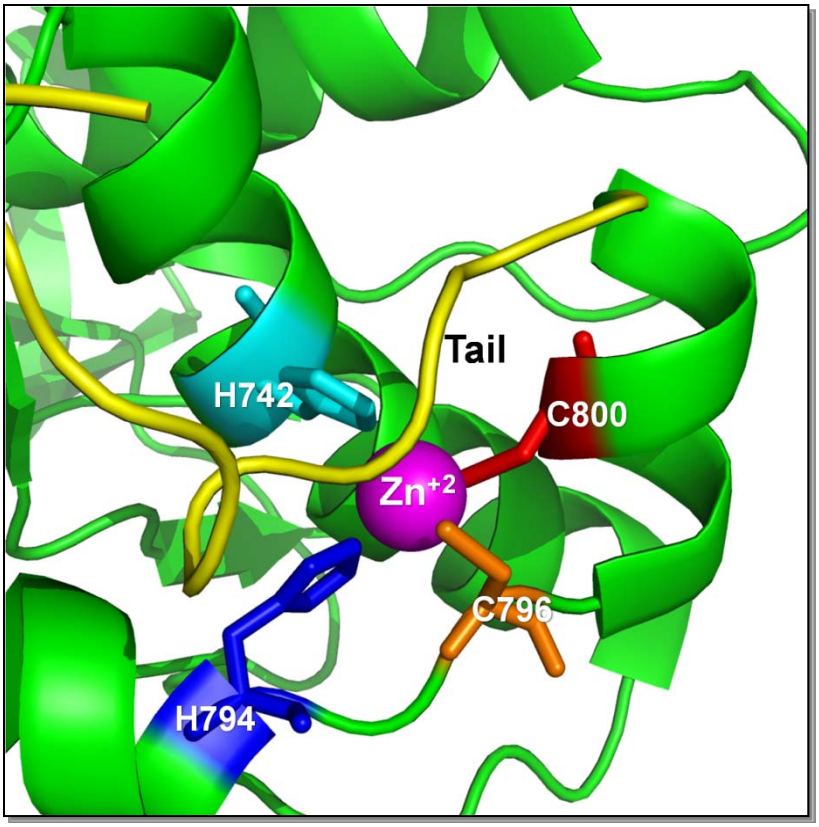

Figure 1-8. The zinc-binding module in the structure of A-CAT. The zinc ion is coordinated by H742, H794, C796 and C800, and is crucial for the structure stability.

stability of the kinase domain.

A-CAT primarily forms monomers, but some small amounts of dimer, tetramer and hexamer also exist in solution which shows the presence of weak intermolecular interactions. These weak intermolecular interactions found between A-CAT monomers most probably become physiologically relevant in native MHCKA, as the coiled-coil domain results in oligomerization of the full length molecule thereby placing 4-5 catalytic domains in close proximity [8;10].

1.8. Comparison of A-CAT and TRPM7-CAT

Although *Dictyostelium* MHCK A (Figure 1-6A) and mammalian TRPM7 (Figure 1-6B) are two divergent members of the alpha-kinase family, sharing only 24% sequence identity, they both possess a well-conserved common core kinase domain [8], composed of two similar lobes with an active site in between. The N/D loop is conserved in both structures (although five residues longer in TRPM7).

While an overlay of the structure of alpha-kinase domains of TRPM7 and MHCK A shows a high degree of similarity (Figure 1-9), there are some notably differences. The kinase domain of MHCK A is a functional monomer while TRPM7 forms a dimer as a consequence of a domain-swapping exchange of an N-terminal 27-residue "dimerization segment" that is partly helical (residues: 1551–1577). The dimerization segment of one molecule interacts extensively with the kinase domain of the other molecule in the dimer and is necessary for kinase activity [94].

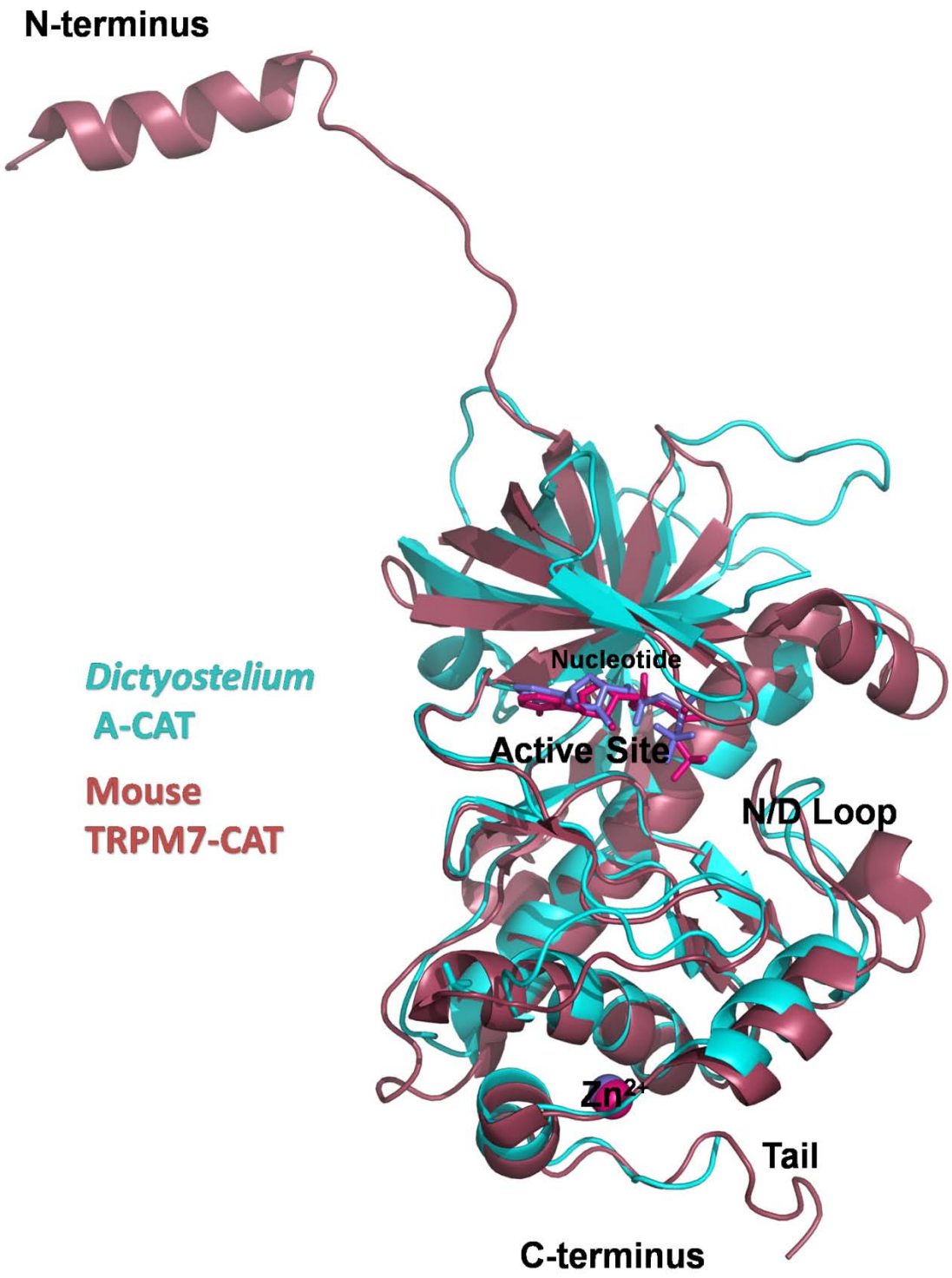

Figure 1-9. Front view of the superimposed structures of A-CAT and TRPM7-CAT. The structure of A-CAT has been shown in cyan and TRPM7-CAT in raspberry (PDB code 1IA9). The nucleotide (AMPPCP in A-CAT and AMPPNP in TRPM7-CAT) and zinc ion are colored blue and hot pink for A-CAT and TRPM7-CAT, respectively. [8]

1.9. Novel Insights into the Catalytic Mechanism of Alpha-Kinase Members

Studying the structures of A-CAT and TRPM7-CAT provides novel insights into the catalytic and regulatory properties of the alpha-kinases. Investigating these novel features may help to explain the reason for conservation of a small number of alpha-kinases throughout evolution for regulation of key cellular processes. Some of these novel insights into the catalytic mechanism of alpha-kinase members are as follows:

(a) Interestingly, in several crystal structures obtained of A-CAT, D766 in the active site was found to be phosphorylated suggesting the possibility that the γ-phosphate group of ATP is first covalently transferred to the enzyme before being transferred to the substrate (Figures 1-10 and 1-11). The aspartylphosphate is exposed to solvent within an active-site pocket, access to which is regulated by the N/D loop that functions as a Mg^{2+} ion binding site. The stability of the aspartylphosphate in the crystal structure is unusual. No member of the protein kinase-like superfamily has been found to employ a phosphoenzyme intermediate in its catalytic mechanism yet [8].

(b) Crystallization trials of A-CAT set up in the presence of ATP often resulted in structures in which the nucleotide bound was found to be AMP (Figure 1-12) or adenosine. This raises the intriguing possibility that along with possessing kinase activity, alpha-kinase domains may be able to hydrolyze nucleotides in the absence of substrate.

(c) At present, the mechanism(s) that regulate the kinase activity of both MHCK A and TRPM7 are unknown. Both enzymes, when purified, are active protein kinases that

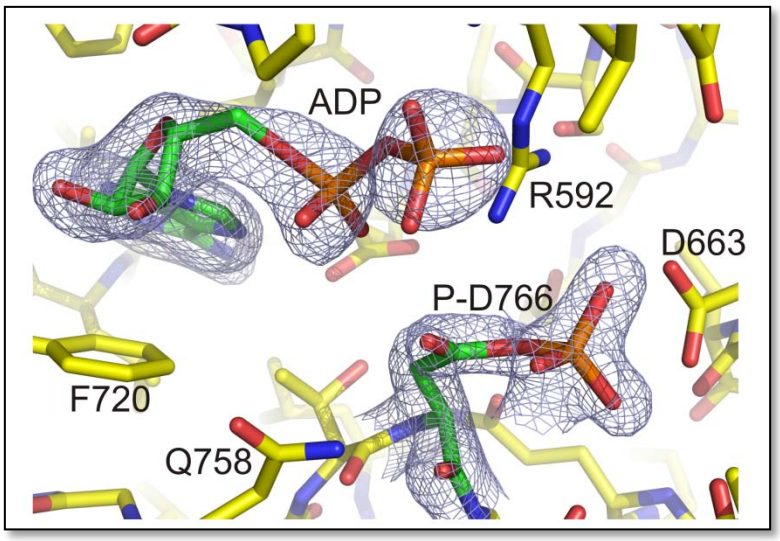

Figure 1-10. The phosphorylated D766 in the A-CAT active site. $2F_o$-F_c electron density map of ADP and the phosphorylated D766 (P-D766) contoured at 2σ (grey mesh). Residues are shown as yellow sticks, with ADP and D766 shown as green sticks. [8]

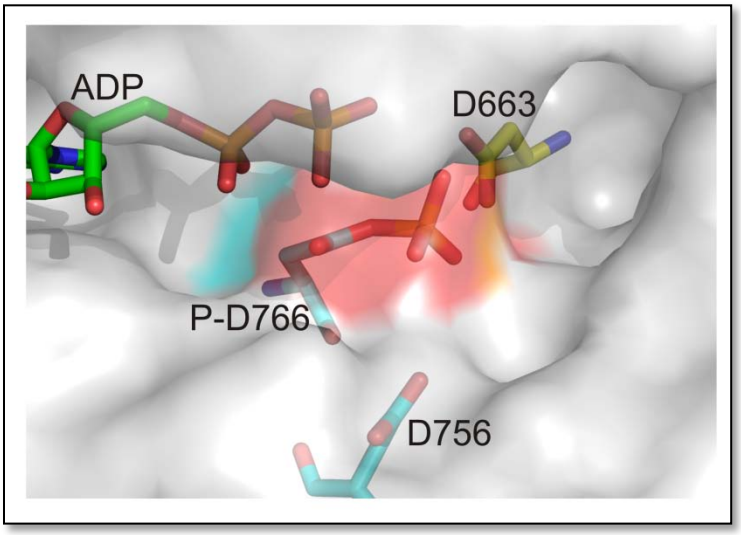

Figure 1-11. A surface representation of the phosphorylated D766 in the A-CAT active site. The surface representation shows that the phosphorylated D766 residue is positioned near to the entrance of the active-site pocket. The surface area contributed by the aspartylphosphate is colored red. [8].

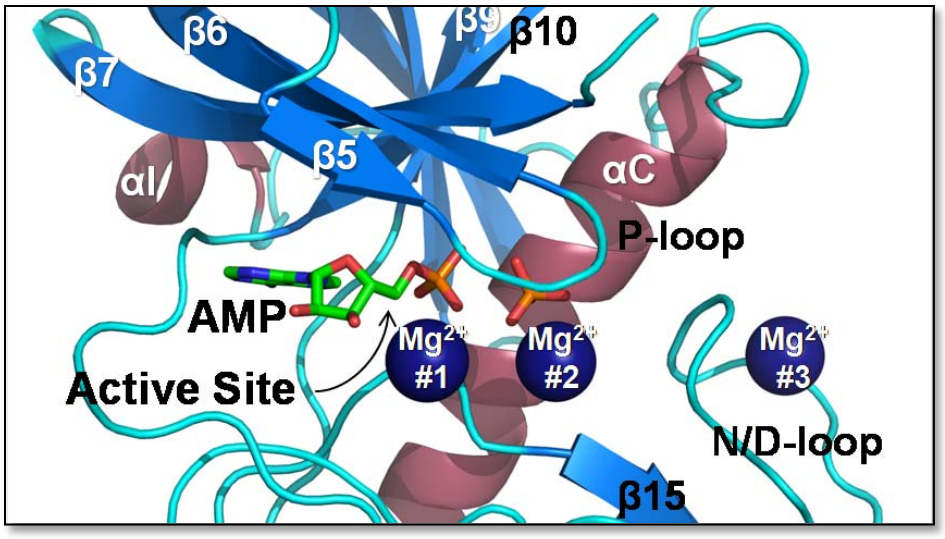

Figure 1-12. AMP bound to the nucleotide binding site of A-CAT. (Adapted from [8]).

need no cofactors beyond Mg^{2+}. Notably, both the crystal structure of A-CAT and TRPM7-CAT are missing the C-tail of the constructs indicating that this region may be unstructured and highly flexible (Figures 1-6A, 1-6B and 1-9) and also calling into question whether this is a necessary component of the alpha-kinase domain in general.

HYPOTHESES

This research work was focused on investigation of the following hypotheses: The alpha-kinase family can hydrolyze ATP in the absence of peptide/protein substrate; and the unstructured tail sequences C-terminal to the kinase domains of MHCK A and TRPM7 are important for catalytic activity.

Objectives

The goal of this project was to understand both the kinase catalytic mechanism and the regulatory mechanisms governing the alpha-kinase family. The major objectives were:

1. Test whether the alpha-kinase domains of MHCK A and TRPM7 possess ATPase and ADPase activity.

2. Determine whether truncation, deletion or mutation of residues in the C-terminal kinase tail sequence (C-tail) affects the catalytic activity of MHCK A and TRPM7.

CHAPTER 2

MATERIALS AND METHODS

2.1. Plasmid Constructs

All DNA manipulations were carried out using standard methods [95]. All constructs were verified by restriction digests and DNA sequencing.

The MHCK A (GenBankTM accession number 1170675) catalytic domain used in these studies, designated A-CAT, comprises residues 552–841 of MHCK A. A-CAT is identical to the previously described T-5 [43]. All A-CAT constructs were inserted into the pET-28a vector (Novagen), except for the C-tail construct which was created as a GST-fusion protein. The pET28a vectors that express A-CAT with an N-terminal hexahistidine tag and a TEV protease site (GENLYFQG) or a C-terminal hexahistidine tag were constructed. The constructs were cloned in frame into the *Nco*I and *Xho*I sites of the vector. DNA constructs encoding site-directed mutants of A-CAT were generated using the Quikchange XL-site-directed mutagenesis system (Stratagene). The truncation and deletion constructs were created using PCR (Table 2-1).

DNA encoding the C-tail region of A-CAT (residues 806-841) was generated by PCR using primers containing 5' *Bam*HI and 3' *Xho*I restriction sites and cloned into the pCR2.1 TA vector (Invitrogen). The A-CAT C-tail was then subcloned into pGEX-4T-3 (GE Healthcare) to generate the expression construct pGEX-4T3-A-CAT-Tail.

MHCK A (GenBankTM accession number 1170675) used in these studies comprises residues 1–1146. All MHCK A constructs (MHCK A, MHCK A-T825A and

Table 2-1. List of DNA Constructs

Construct Name	Protein Name	Residues	Specification	TAG	Vector
A-CAT	MHCK A	552-841	Kinase domain of MHCK A (A-CAT)	N-terminal His-TEV	pET-28a
A-CAT-831	MHCK A	552-831	A C-tail-truncated construct of A-CAT	N-terminal His-TEV	pET-28a
A-CAT-823	MHCK A	552-823	A C-tail-truncated construct of A-CAT	N-terminal His-TEV	pET-28a
A-CAT-809	MHCK A	552-809	A C-tail-truncated construct of A-CAT	N-terminal His-TEV	pET-28a
A-CAT-D766A	MHCK A	552-841	A mutated construct of A-CAT: D766A	N-terminal His-TEV	pET-28a
A-CAT-B-CAT-Tail-Chimera	MHCK A MHCK B	552-802 326-354	A chimera construct of A-CAT (without tail) And the C-tail of B-CAT	N-terminal His-TEV	pET-28a
A-CAT-T825A	MHCK A	552-841	A mutated construct of A-CAT: T825A	N-terminal His-TEV	pET-28a
A-CAT-T825S	MHCK A	552-841	A mutated construct of A-CAT: T825S	N-terminal His-TEV	pET-28a
A-CAT-T825E	MHCK A	552-841	A mutated construct of A-CAT: T825E	N-terminal His-TEV	pET-28a
A-CAT-Tail	MHCK A	806-841	The C-tail region of A-CAT	N-terminal GST	pGEX-4T-3
A-CAT-ΔVLS	MHCK A	552-811+ 815-841	A deletion construct of A-CAT The deleted residues: VLS: 812-814	N-terminal His-TEV	pET-28a
A-CAT-ΔGGVLSG	MHCK A	552-809+ 816-841	A deletion construct of A-CAT The deleted residues: GGVLSG: 810-815	N-terminal His-TEV	pET-28a

Construct Name	Protein Name	Residues	Specification	TAGs	Vector
A-CAT-ΔGGVLSGNNKK	MHCK A	552-809+ 820-841	A deletion construct of A-CAT The deleted residues: GGVLSGNNKK: 810-819	N-terminal His-TEV	pET-28a
A-CAT-5xAla	MHCK A	552-841	A mutated construct of A-CAT: S553A, T612A, T613A, T614A, and T634A	C-terminal His	pET-28a
MHCK A	MHCK A	1-1146	Full-length MHCK A	N-terminal FLAG	pTX-FLAG
MHCK A-T825A	MHCK A	1-1146	A mutated construct of full-length MHCK A: T825A	N-terminal FLAG	pTX-FLAG
MHCK A-T825E	MHCK A	1-1146	A mutated construct of full-length MHCK A: T825E	N-terminal FLAG	pTX-FLAG
TRPM7-CAT	TRPM7	1548-1862	Kinase domain of TRPM7 (TRPM7-CAT)	N-terminal His-TEV	pET-28a
TRPM7-CAT-1827	TRPM7	1548-1827	A C-tail-truncated construct of TRPM7-CAT	N-terminal His-TEV	pET-28a
TRPM7-CAT-1820	TRPM7	1548-1820	A C-tail-truncated construct of TRPM7-CAT	N-terminal His-TEV	pET-28a
TRPM7-CAT-T1827A	TRPM7	1548-1862	A mutated construct of TRPM7-CAT: T1827A	N-terminal His-TEV	pET-28a
TRPM7-CAT-S1838A	TRPM7	1548-1862	A mutated construct of TRPM7-CAT: S1838A	N-terminal His-TEV	pET-28a
TRPM7-CAT-S1839A	TRPM7	1548-1862	A mutated construct of TRPM7-CAT: S1839A	N-terminal His-TEV	pET-28a
TRPM7-CAT-S1838A-S1839A	TRPM7	1548-1862	A mutated construct of TRPM7-CAT: S1838A-S1839A	N-terminal His-TEV	pET-28a
TRPM7-CAT-S1848A	TRPM7	1548-1862	A mutated construct of TRPM7-CAT: S1848A	N-terminal His-TEV	pET-28a
TRPM7-CAT-S1857A	TRPM7	1548-1862	A mutated construct of TRPM7-CAT: S1857A	N-terminal His-TEV	pET-28a

MHCK A-T825E) were expressed as FLAG-tagged proteins using the plasmid pTX-FLAG vector [96] that had been adapted to the GATEWAY technology (Invitrogen). Briefly, the parent plasmid pTX-FLAG was digested by *Bam*HI and *Xho*I and blunted with T4 DNA polymerase, and the Gateway recombination cassette (reading frame cassette B) was cloned in, which resulted in the creation of the destination vector pTX-FLAG-GATE. Expression constructs containing the MHCK A gene were then created using pTX-FLAG-GATE according to the manufacturer's instructions. (Invitrogen).

DNA encoding the catalytic domain of mouse TRPM7 (NM_021450) (residues 1548–1862) (herein known as TRPM7-CAT) was obtained by PCR using a mouse-brain cDNA library (Clontech Laboratories Inc.) as a template. A pET28a vector that expresses TRPM7-CAT with an N-terminal hexahistidine tag and a TEV protease site within the *Nco*I and *Xho*I sites was constructed. DNA constructs encoding C-terminally truncated versions of the TRPM7-CAT were generated using PCR. For generation of site-directed mutants the Quikchange XL-site-directed mutagenesis system (Stratagene) was used.

2.2. Peptide Synthesis

The 16-residue peptide MH-3 (RKKFGEAEKTKAKEFL-amide) is based on the MHCK A target site on *Dictyostelium* myosin II at residue 2029 (underlined in peptide above) [47]. MH-3S has the same sequence as MH-3 except that the phosphorylated threonine is converted to a serine (RKKFGEAEKSKAKEFL-amide) [54]. MH-3 and MH-3S were synthesized using the HBTU/HObt coupling protocols on an Applied Bio-systems 431A peptide synthesizer in the Department of Biochemistry, Queen's

University. These two synthetic peptides were used for testing the threonine specificity of A-CAT and A-CAT-809.

2.3. Protein Expression and Purification

A-CAT was expressed in *Escherichia coli* BL21(DE3) (Novagen). Bacteria were grown overnight at 37°C to an A_{595} of more than 1.0 and cooled to 24°C prior to induction with isopropyl-β-D-thiogalactosidase (IPTG) (BioShop Canada Inc.) (1 mM final concentration). All steps of the purification were carried out at 4°C. Cells were lysed by sonication in 400 mM NaCl, 0.2% Triton X-100, and 20 mM Tris-HCl pH 8.0, containing 0.1 mg/ml lysozyme (BioShop Canada Inc.), 1 mM Phenylmethyl Sulphonyl Fluoride (PMSF) (BioShop Canada Inc.), 50 μg/ml protease inhibitor cocktail solution (Sigma) or one complete mini protease inhibitor tablet (Roche Diagnostics) per 50 ml of buffer, and 100 μg/ml Deoxyribonuclease I (DNAase I) (Sigma) and 5 mM $MgCl_2$. The lysate was centrifuged at 75,000 x *g* for 1 hour, and the resulting supernatant was applied to a column of His-Bind resin (Novagen) to isolate His-tagged A-CAT constructs. The material eluted with 100 mM NaCl, 200 mM imidazole, 1% glycerol, and 20 mM Tris-HCl pH 8.0 was collected, dialyzed against 50 mM NaCl, 1 mM EDTA, 20 mM Tris-HCl pH 7.5 buffer and passed over a column of DE-53 cellulose (Whatman) equilibrated in 50 mM NaCl, 1 mM EDTA, and 20 mM Tris-HCl pH 7.5 buffer. The flow-through was collected and passed over an SP Sepharose Fast Flow (Amersham Pharmacia Biotech) column equilibrated in the same buffer with pH 7.0. The flow-through was collected, concentrated using a 10,000 molecular weight cut-off Ultrafree-4 Centrifugal Filtration

Unit (Millipore), and dialyzed against a buffer containing 20 mM NaCl, and 50 mM Tris-HCl pH 7.4.

TRPM7-CAT and its mutant forms were expressed in *E. coli* strain BL21(DE3) as described for A-CAT. All steps of the purification were carried out at 4°C. Cells were lysed by sonication in 500 mM NaCl, 5 mM imidazole, and 20 mM Tris-HCl pH 7.9 containing 0.1 mg/ml lysozyme, 1 mM PMSF, 50 μg/ml protease inhibitor cocktail solution, 100 μg/ml DNAase I and 5 mM $MgCl_2$, and centrifuged at 75,000 x *g* for 1 hour. The resulting supernatant was applied to a column of His-Bind resin. The material was eluted with 500 mM NaCl, 1 M imidazole, 1% glycerol, and 20 mM Tris-HCl pH 7.9, collected, and dialyzed against a buffer containing 20 mM NaCl, and 50 mM Tris-HCl pH 7.4.

GST-A-CAT C-tail fusion protein was expressed at 37°C in *E. coli* BL21(DE3). Bacteria were grown at 37°C to an A_{595} of more than 1.0, then cooled to 24°C and induced using a final concentration of 1 mM IPTG. After 6 hours incubation at room temperature, cells were harvested by centrifugation and resuspended in ice-cold PBS buffer (137 mM NaCl, 2.7 mM KCl, 100 mM Na_2HPO4 and 2 mM KH_2PO4, pH 7.4) containing 0.1 mg/ml lysozyme, 50 μg/ml protease inhibitor cocktail solution, 1 mM PMSF, 100 μg/ml DNAase I and 5 mM $MgCl_2$. Cells were lysed by sonication and centrifuged at 75,000 x *g* for 1 hour to remove insoluble material. The soluble GST-fusion proteins were purified over a glutathione–Sepharose column (GE Healthcare), using an elution buffer containing PBS buffer and 20 mM glutathione. All steps of the purification were carried out at 4°C.

FLAG-tagged full-length MHCK A and its mutants were expressed in the *Dictyostelium discoideum* AX3 cell line [97]. Cells were cultured axenically on 9 cm plastic petri dishes in HL5-medium [98] supplemented with 10,000 U/ml penicillin, and 10 mg/ml streptomycin (Penicillin-Streptomycin Solution, Sigma Aldrich). Plasmids encoding FLAG-tagged full-length MHCK A and its mutants were introduced to AX3 cells by electroporation at 0.85 KV and 25 μF using a Bio-RAD Gene Pulser II Electroporation System [99]. Clonal cell lines were produced through selection by adding 20 μg/ml geneticin (G418) (Invitrogen) and dilution plating. The expression of the FLAG-tagged MHCK A and its mutants was confirmed by immunoblot analysis using M5 anti-FLAG antibody (Sigma Aldrich). All steps of the purification were carried out at 4°C. For extraction of the protein, the cells were collected and washed with PBS buffer pH 7.4, and homogenized in lysis buffer (500 mM NaCl, 1 mM EDTA, 0.3% Triton X-100, and 50 mM Tris-HCl pH 8.0) containing one complete mini protease inhibitor tablet (Roche Diagnostics) per 50ml of buffer at 4°C. The lysate was centrifuged at 12,000 x *g* for 1 hour to remove insoluble material. Immunoprecipitation of FLAG-tagged MHCK A constructs was performed according to the manufacturer's instructions using anti-FLAG M2 resin (ANTI-FLAG M2 Affinity Gel A2220 from Sigma). For elution, TBS buffer (150 mM NaCl, 50 mM Tris–HCl pH 7.4) containing 200 μg/ml FLAG peptide was applied. The eluted samples were dialyzed against a buffer containing 20 mM NaCl, and 50 mM Tris-HCl pH 7.4.

2.4. Kinase Assays

I*n vitro* kinase assays for A-CAT, TRPM7-CAT, and full-length MHCK A were carried out at 25°C in kinase buffer (2 mM $MgCl_2$, 1 mM dithiothreitol (DTT) (Sigma), 0.25 mM ATP (Sigma) and 20 mM TES, pH 7.0) containing [γ-^{32}P]ATP (NEN PerkinElmer Life Sciences) at a specific activity of 100–500 cpm/pmol ATP. Either 33 μM Myelin Basic Protein (MBP) (Sigma), or 300 μM MH-3 or MH-3S were used as the substrate. Assays were initiated by addition of 50 μg/ml A-CAT, 50 μg/ml TRPM7-CAT, or 5 μg/ml full-length MHCK A. Phosphorylation rates were determined by removing 20-μl aliquots of the reaction mixture at time points from 1 to 60 min. The time courses of 1, 2, 3, 4, and 5 minutes were used for A-CAT and full-length MHCK A, and 5, 10, 20, 30 and 60 minutes for TRPM7-CAT. Incorporation of ^{32}Pi into MH-3, MH-3S, or MBP was determined by spotting aliquots onto 2x2-cm squares of P81 phosphocellulose paper (Whatman) [100]. After washing in 1% phosphoric acid, the paper squares were dried and counted in a Beckman LS 9000 scintillation counter using ScintiVerse Universal LS Cocktail (Fisher Scientific).

2.5. Autophosphorylation Assays

In vitro autophosphorylation assays were carried out at 25°C in kinase buffer (2 mM $MgCl_2$, 1 mM DTT, 0.25 mM ATP and 20 mM TES, pH 7.0) containing [γ-^{32}P]ATP at a specific activity of 600 cpm/pmol ATP. Assays were initiated by addition of 500 μg/ml kinase and stopped after time courses of 1, 5, 10, 20, 40 and 60 minutes by adding 20 μl of the reaction sample to 5 μl of 5xSDS loading buffer and boiling it for 2 minutes at

100ºC. Samples were subjected to SDS polyacrylamide gel electrophoresis on a 12% gel to separate the kinase from the free [γ-^{32}P]ATP. The gels were dried and autoradiography was performed. Subsequently, bands were excised and the amount of incorporated ^{32}Pi in each band was counted in a Beckman LS 9000 scintillation counter using ScintiVerse Universal LS Cocktail (Fisher Scientific).

2.6. ATPase and ADPase Assays

Measurement of ATPase activity was performed by following the release of ^{32}Pi from [γ-^{32}P]ATP as described [101]. Assays contained 50 µg/ml A-CAT, 50 µg/ml TRPM7-CAT, or 5 µg/ml full-length MHCK A. Reactions were started by adding [γ-^{32}P]ATP buffer (2 mM $MgCl_2$, 1 mM DTT, 0.25 mM ATP, 20 mM TES, pH 7.0, and [γ-^{32}P]ATP (5 cpm/pmol)) and stopped at 5, 10, 20, and 40 minutes by addition of a mixture of silicotungstic acid and sulfuric acid, followed by 2-butanol-benzene and finally ammonium molybdate after vortexing [101]. The phases were separated by centrifugation and 500 µl of the organic (upper) phase was added to 5 ml ScintiVerse Universal LS Cocktail and counted in a Beckman LS 9000 scintillation counter.

Hydrolysis of ATP to ADP and AMP was measured in kinase buffer using [α-^{32}P] ATP (NEN PerkinElmer Life Sciences) at a specific activity of 15-30 cpm/pmol ATP. Aliquots of 300 µl were removed from the reaction and flash-frozen in a dry ice-ethanol bath. For analysis, aliquots were rapidly thawed by addition of an equal volume of an unlabelled mixture of 10 mM ATP, 10 mM ADP and 10 mM AMP and were then loaded onto a 1 ml HiTrap Q HP column (GE Healthcare). AMP, ADP and ATP were eluted

using a stepwise gradient of 50 mM, 115 mM and 300 mM of NaCl, respectively. Peaks were collected and aliquots were counted as described above to measure the amounts of ATP, ADP and AMP.

2.7. Far-UV Circular Dichroism Spectroscopy

Far-UV circular dichroism (CD) spectra were taken from 180 to 250 nm, on an Olis RSM 1000 spectrophotometer. Far-UV spectra were collected using 12.64 μM A-CAT and A-CAT-809 using a 0.1 mm path length cuvette, with a step size of 0.2 nm, a scan speed of 100 nm/min, a response time of 2.0 seconds, and a bandwidth of 2 nm.

CHAPTER 3

RESULTS

3-1. A-CAT Possesses ATPase and ADPase Activities

Despite the fact that crystal trials of the alpha-kinase domain of MHCK A (A-CAT; residues 552–841) were set up in the presence of ATP, the structures often contained AMP or adenosine in the nucleotide binding site [8]. To assess whether A-CAT possesses nucleotide hydrolyzing activity in the absence of substrate, A-CAT was expressed and purified. Purification resulted in a product migrating on SDS-PAGE slightly higher than the expected size (35 KDa) (Figure 3-1). This decrease in mobility is likely due to autophosphorylation of the construct.

When tested for the ability to hydrolyze [α-^{32}P]-ATP, A-CAT displayed an ATPase rate of 2.19×10^{-2} sec^{-1} which is approximately half the kinase rate toward the substrate MBP (4.44×10^{-2} sec^{-1}) (Figure 3-2 and Table 3-1). Mutation of the highly conserved D766 eliminated both kinase and ATPase activity of A-CAT (data not shown). A-CAT also showed ADPase activity (3.0×10^{-4} sec^{-1}), however it was ~100 times lower than the ATPase activity (Figure 3-2 and Table 3-1). Apparently, hydrolysis of the bond between the α- and β-phosphates of ATP is considerably less favored compared to the hydrolysis of the γ-phosphate. These results demonstrates that A-CAT possess ATPase and ADPase activities in addition to kinase activity.

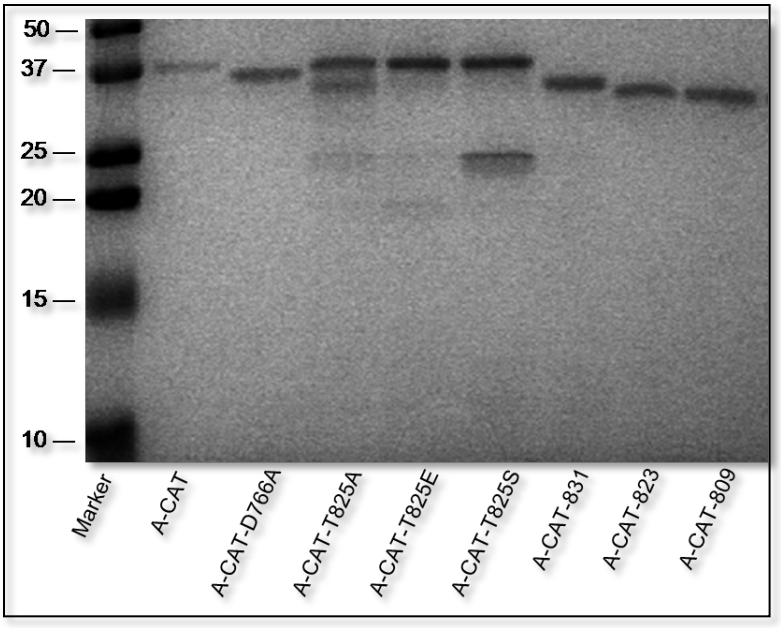

Figure 3-1. Coomassie Blue-stained SDS polyacrylamide gel of the purified bacterially-expressed A-CAT, and its mutated and truncated constructs. A-CAT, A-CAT-D766A, A-CAT-T825A, A-CAT-T825E and A-CAT-T825S all correspond to constructs containing residues 552-841. A-CAT-831: C-terminal truncation of A-CAT: residues 552-831; A-CAT-823: residues 552-823; A-CAT-809: residues 552-809.

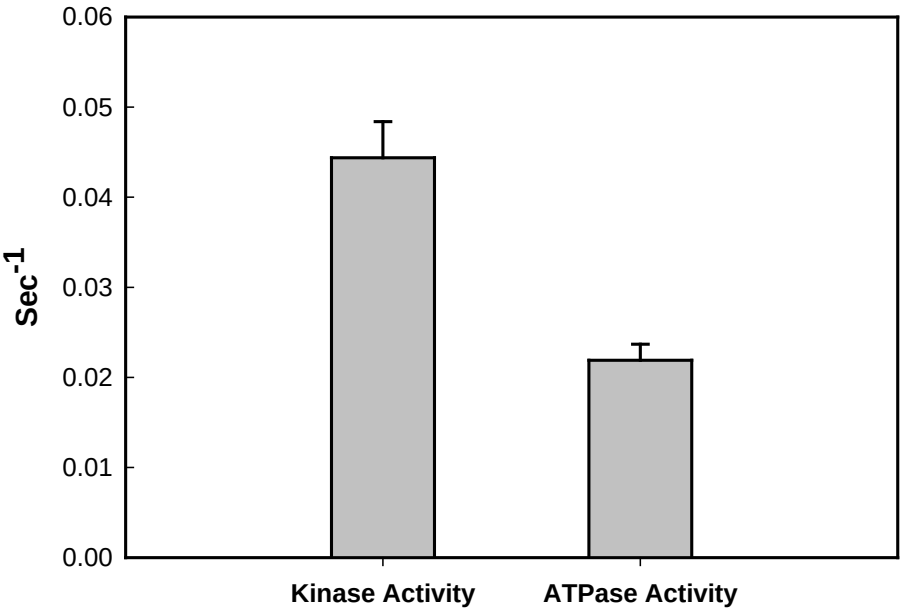

Figure 3-2. Kinase and ATPase activities of A-CAT. A-CAT showed an ATPase activity ~2 fold lower than the kinase activity with MBP as substrate. Assays were carried out as described in Materials and Methods.

Table 3-1. Kinase, ATPase and ADPase rates of A-CAT, full-length MHCK A and TRPM7-CAT. Kinase assays were performed using MBP as substrate as described in Materials and Methods except for those marked with a star (*) or diamond (♦) which contained MH-3 or MH-3S as the substrate, respectively. For each experiment, the number of determinations (No. of D.) is shown. Empty cells indicate that the related rates were not determined.

Construct Name	Kinase Rate (Sec^{-1})	Standard Deviation (Sec^{-1})	No. of D.	ATPase Rate (Sec^{-1})	Standard Deviation (Sec^{-1})	No. of D.	ADPase Rate (Sec^{-1})
A-CAT	4.44×10^{-2}	4.02×10^{-3}	17	2.19×10^{-2}	1.79×10^{-3}	10	3.00×10^{-4}
A-CAT *	1.01×10^{-1}	2.88×10^{-3}	3				
A-CAT ♦	7.85×10^{-4}	1.06×10^{-4}	3				
A-CAT-831	4.17×10^{-2}	6.98×10^{-4}	3	2.03×10^{-2}	4.00×10^{-4}	2	
A-CAT-823	8.58×10^{-4}	2.35×10^{-5}	5	5.65×10^{-4}	1.79×10^{-4}	2	
A-CAT-809	1.92×10^{-3}	1.07×10^{-4}	4	5.65×10^{-4}	2.00×10^{-4}	4	
A-CAT-809 *	1.12×10^{-2}	1.61×10^{-3}	3				
A-CAT-809 ♦	2.65×10^{-4}	2.29×10^{-5}	3				
A-CAT-B-CAT-Tail-Chimera	4.47×10^{-2}	1.85×10^{-3}	4	9.91×10^{-3}	2.85×10^{-4}	2	
A-CAT-T825A	1.34×10^{-3}	1.51×10^{-4}	4	5.63×10^{-4}	2.70×10^{-4}	2	
A-CAT-T825S	6.88×10^{-3}	3.54×10^{-4}	4	8.15×10^{-3}	1.79×10^{-4}	2	
A-CAT-T825E	3.06×10^{-3}	9.25×10^{-5}	4	8.45×10^{-4}	1.00×10^{-4}	2	
A-CAT-809 + A-CAT Tail	2.10×10^{-3}	3.04×10^{-4}	16				
A-CAT-ΔVLS	1.44×10^{-2}	4.17×10^{-4}	4	3.39×10^{-3}	8.04×10^{-5}	2	
A-CAT-ΔGGVLSG	1.47×10^{-2}	4.47×10^{-4}	4	5.99×10^{-3}	1.70×10^{-4}	2	
A-CAT-ΔGGVLSGNNKK	3.75×10^{-2}	5.57×10^{-4}	4	5.23×10^{-3}	1.61×10^{-4}	3	
A-CAT-5xAla	4.01×10^{-2}	6.08×10^{-3}	4	1.82×10^{-2}	8.44×10^{-4}		
MHCK A	1.87×10^{-1}	3.31×10^{-2}	6	3.21×10^{-2}	2.77×10^{-3}	2	
MHCK A-T825A	1.54×10^{-2}	1.44×10^{-3}	4	2.08×10^{-2}	1.71×10^{-3}	2	
MHCK A-T825E	1.66×10^{-2}	1.02×10^{-3}	4	1.98×10^{-2}	9.00×10^{-4}	2	
TRPM7-CAT	9.05×10^{-3}	8.25×10^{-4}	11	4.21×10^{-3}	1.53×10^{-4}	2	1.77×10^{-4}
TRPM7-CAT-1827	2.37×10^{-4}	9.66×10^{-5}	4	1.76×10^{-3}	7.66×10^{-5}	2	
TRPM7-CAT-1820	8.29×10^{-5}	8.35×10^{-5}	4	1.93×10^{-3}	4.35×10^{-5}	2	
TRPM7-CAT-T1827A	6.64×10^{-3}	9.18×10^{-4}	4				
TRPM7-CAT-S1838A	7.75×10^{-3}	2.01×10^{-4}	4				
TRPM7-CAT-S1839A	7.18×10^{-3}	6.13×10^{-4}	4				
TRPM7-CAT-S1838A-S1839A	6.64×10^{-3}	1.23×10^{-3}	4				
TRPM7-CAT-S1848A	8.25×10^{-3}	9.18×10^{-4}	6				
TRPM7-CAT-S1857A	8.63×10^{-3}	1.41×10^{-4}	6				

3.2. AMP and Adenosine Do not Act as Potent Competitive Inhibitors of A-CAT Kinase Activity

Structural studies revealed that the nucleotide binding site of A-CAT can bind both AMP and adenosine. To investigate whether these nucleotides act as competitive inhibitors of kinase activity by interfering with ATP binding, adenosine and AMP inhibition assays were performed. The effect of different concentrations (0-1 mM) of adenosine or AMP on the kinase activity of A-CAT toward the exogenous substrate MBP was assayed. The rate of A-CAT kinase activity was not affected by the presence of AMP up to a concentration of 1 mM (Figure 3-3, Upper panel). The presence of adenosine at higher concentrations (0.1-1 mM) slightly reduced the kinase activity (Figure 3-3, Lower panel).

3.3. The C-Tail Region of A-CAT Is Necessary for the Activity of the Kinase Domain

The crystal structure of A-CAT does not possess defined electron density for residues 812-841 of the C-tail (residues 806-841) indicating that this region is inherently disordered. To assess whether or not this region of the alpha-kinase domain is necessary for catalytic activity a number of truncated and mutated constructs were cloned, expressed, purified and tested for kinase and ATPase activities (Figure 3-4). The SDS polyacrylamide gel of the purified constructs is shown in Figure 3-1.

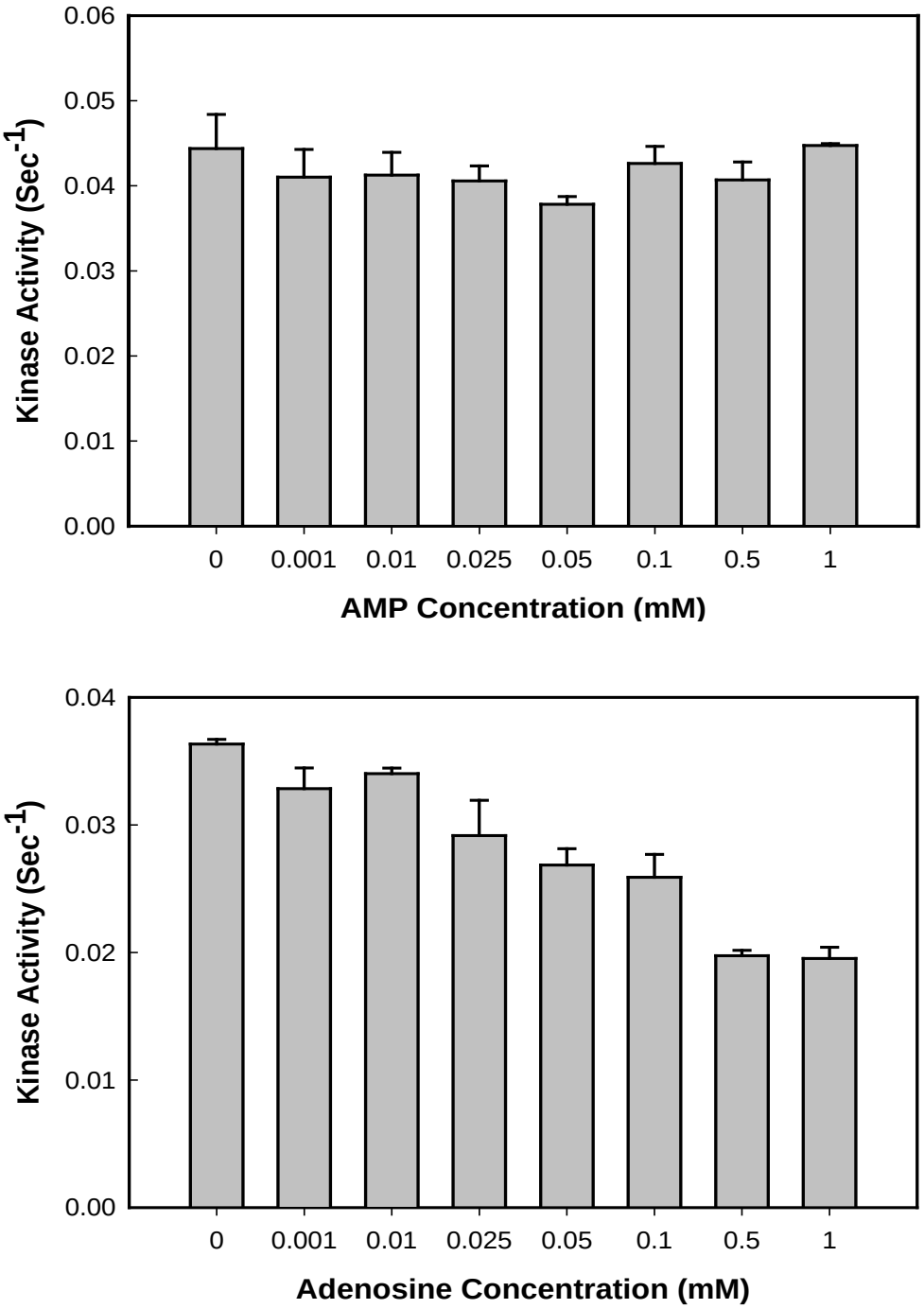

Figure 3-3. The kinase inhibitory effect of AMP and adenosine on the kinase activity of A-CAT. Upper panel: The inhibitory effect of AMP. Lower panel: The inhibitory effect of adenosine. Kinase activity toward MBP was measured for A-CAT at varying concentrations of AMP or Adenosine (0-1 mM). ATP was used at the concentration of 0.25 mM. Assays were carried out as described in Materials and Methods. The results are based on 3 determinations.

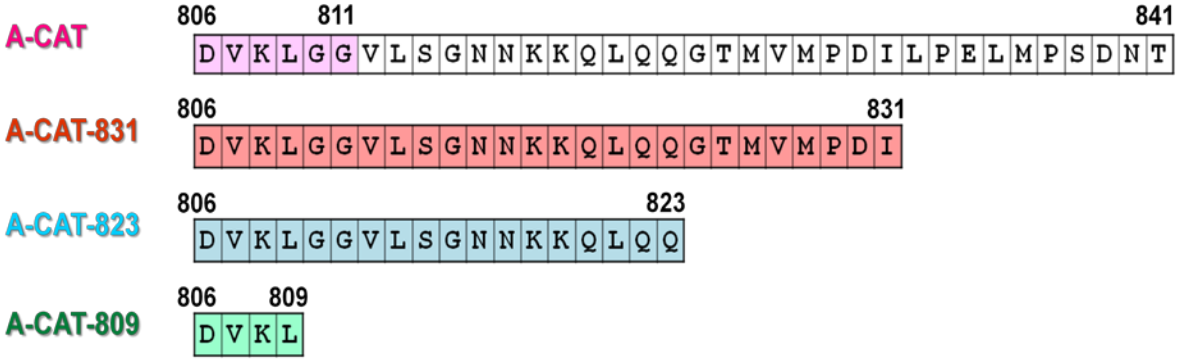

Figure 3-4. Sequences of the C-tail regions of A-CAT, A-CAT-831, A-CAT-823 and A-CAT-809. The crystal structure of A-CAT has no defined electron density for residues 812-841 of the C-tail.

Deletion of the last 10 amino acids of the C-tail (A-CAT-831) resulted in a kinase rate ($4.17x10^{-2}$ sec^{-1}) very close to A-CAT ($4.44x10^{-2}$ sec^{-1}) (Figure 3-5, Upper panel and Table 3-1) and an ATPase rate ($2.03x10^{-2}$ sec^{-1}) near to that of A-CAT ($2.19x10^{-2}$ sec^{-1}) (Figure 3-5, Lower panel and Table 3-1). Further truncation of the C-tail to residue 823 (A-CAT-823) caused a dramatic drop (~97-98%) in both activities (Figure 3-5 and Table 3-1). Deletion of the entire C-tail region of A-CAT (A-CAT-809) had the same result with the construct exhibiting only ~4.5% kinase and ~2.5% ATPase activities (Figure 3-5 and Table 3-1). Given that both the kinase and ATPase activities of A-CAT-823 and A-CAT-809 are both dramatically lowered, it is unlikely that the C-tail is involved in peptide substrate binding/orientation. Rather, the C-tail may be directly involved in the phosphotransfer mechanism. These results reveal that the C-tail sequence of A-CAT is necessary for the activity of the kinase domain and the region between amino acids 823 and 831 is a necessary component for the catalytic activity.

3.4. Truncated A-CAT Folds Properly

To rule out the possibility that the low activity of the C-tail deletion constructs was due to misfolding of the mutant proteins, far-UV CD analysis was performed on A-CAT and A-CAT-809. The far-UV CD spectra of A-CAT-809 had a larger positive signal at 190 nm and a larger negative signal at 210 nm compared to A-CAT, indicating that the C-tail deletion construct has overall more structure per folded unit (Figure 3-6). This is in agreement with the idea that the C-tail is inherently unstructured. Given that the C-tail constitutes approximately 12% of the total amino acids within A-CAT

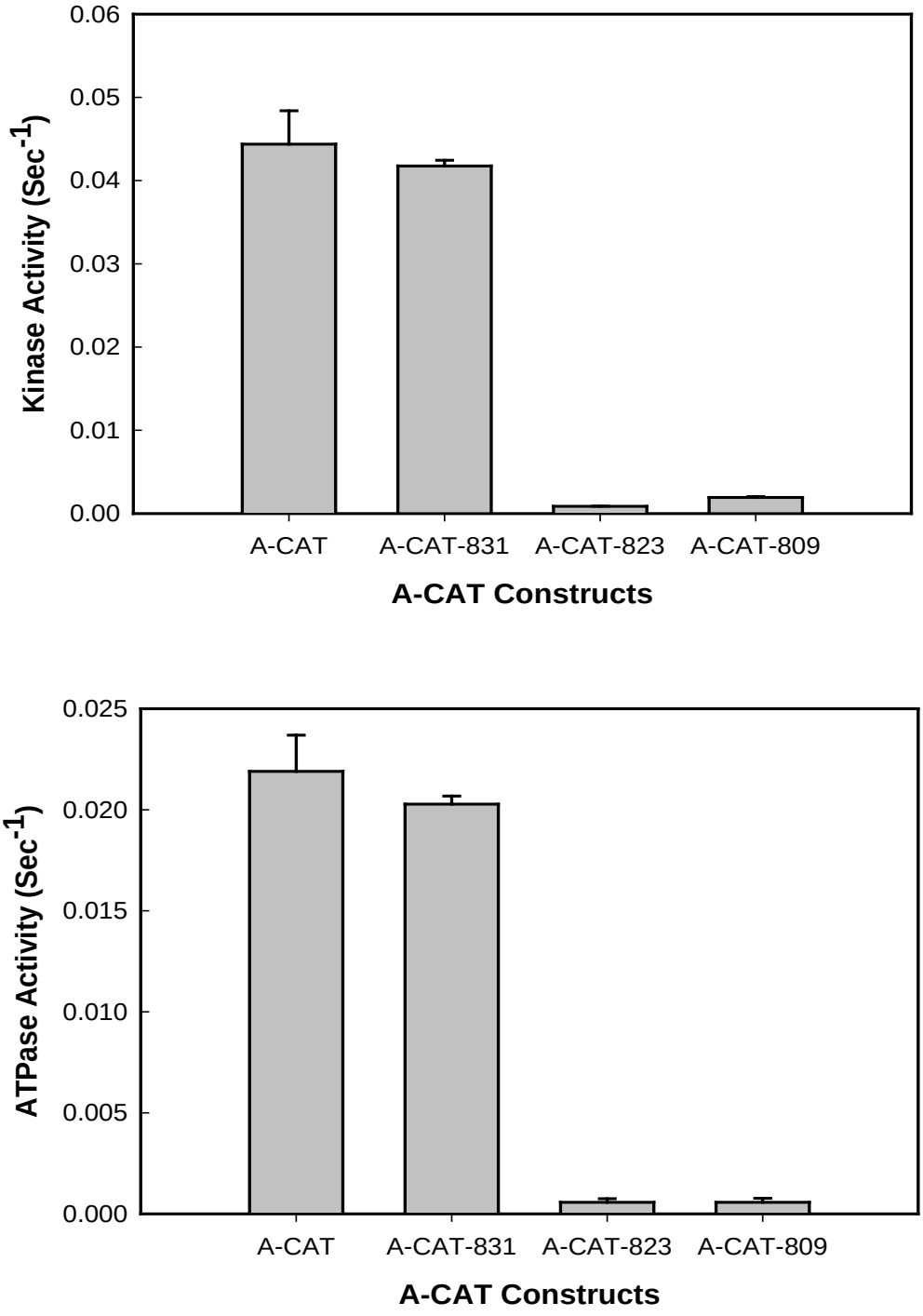

Figure 3-5. Kinase and ATPase activities of A-CAT, A-CAT-831, A-CAT-823 and A-CAT-809. Upper panel: Kinase activity. Lower panel: ATPase activity. Assays were carried out as described in Materials and Methods.

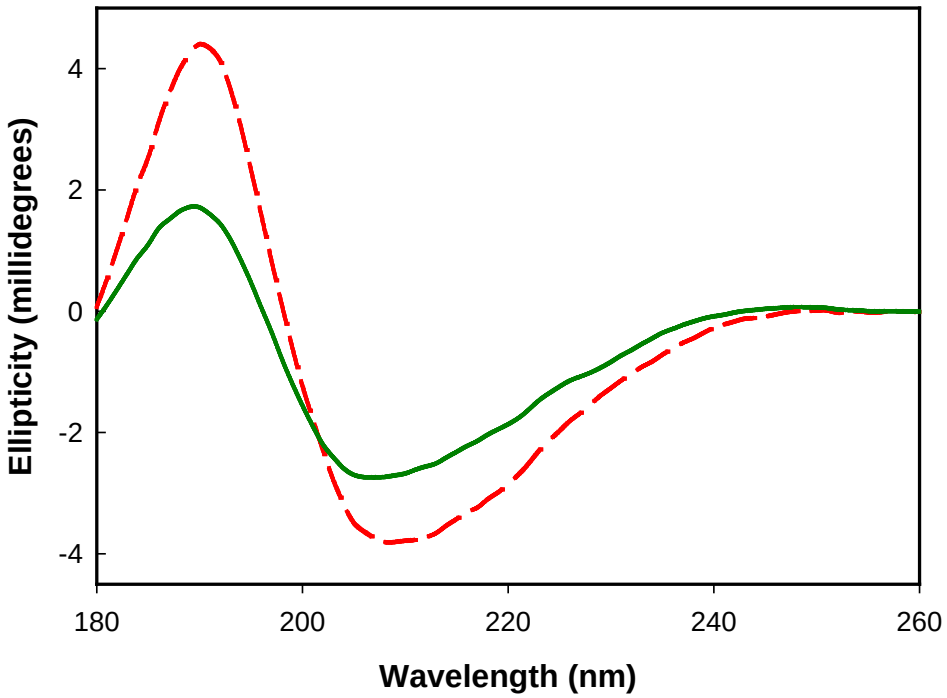

Figure 3-6. The far-UV CD spectra of A-CAT and A-CAT-809. The far-UV CD spectra of A-CAT (solid green line) and A-CAT-809 (dashed red line) were measured at 13 μM.

(36 out of 290), deletion of this region may cause the mutant protein to appear to have more structure by CD analysis (Figure 3-6).

Crystallization trials were performed using A-CAT-809 in order to address whether or not its lack of catalytic activity could be due to a small structural change in the fold of the protein. Interestingly, diffraction-quality crystals of A-CAT-809 were obtained in less time than that was necessary to obtain A-CAT crystals, indicating that the disorder of the flexible C-tail may be a limiting factor in the crystallization of A-CAT.

The structural analysis revealed a very low Root Mean Square Deviation (RMSD= 0.374) between A-CAT and A-CAT-809, which shows that the structures are nearly identical and that deletion of the C-tail does not cause any misfolding or change in the kinase domain structure (Figure 3-7). Surprisingly the X-ray structure of A-CAT-809 shows an ADP bound to the active site, which must be the result of the remaining ~2.5% ATPase activity. Mg^{2+}#2 and Mg^{2+}#3 are seen in this structure as in the A-CAT AMP structure (Figures 3-7 and 1-6A). However, Mg^{2+}#1 has been substituted with a water molecule. Comparison with the X-ray structure of A-CAT-ADP shows that the position of the ADP β-phosphate is different even though neither structures has Mg^{2+}#1 (Figure 3-7). The results of CD analysis and crystallization trial revealed that the low activity of the C-tail deletion constructs is not due to misfolding or secondary structural changes of the truncated proteins.

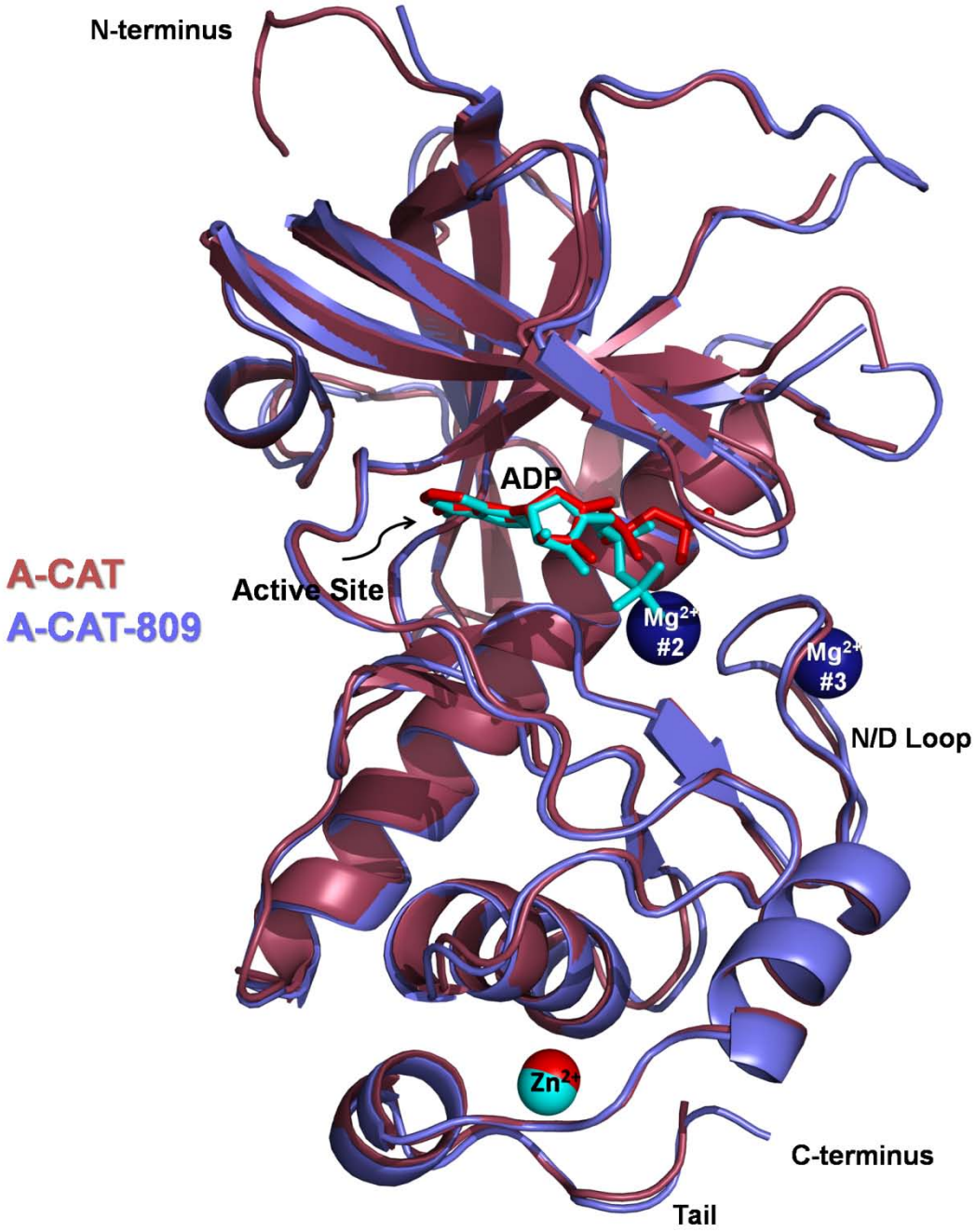

Figure 3-7. A-CAT and A-CAT-809 structures overlay. An overlay of the structures of A-CAT (raspberry) and A-CAT-809 (slate) has been shown. ADP and zinc atom are colored red and cyan for A-CAT and A-CAT-809, respectively. Mg^{2+}#2 and Mg^{2+}#3 (dark blue) are present in the structure of A-CAT-809. The alignment shows that the structures are virtually identical and that deletion of the C-tail does not cause misfolding of the structure.

3.5. The C-Tail Sequence of A-CAT Does not Play a Role in Mediating Threonine-Specificity

It has been previously shown that the catalytic domains of MHCK A, B, C and eEF2 kinase display a unique preference for the phosphorylation of threonine residues in substrates [51;54]. At present, the structural features of A-CAT that define this specificity are unknown. To test whether the C-tail sequence of A-CAT plays a role in mediating this threonine-specificity, A-CAT and A-CAT-809 were assayed with two different synthetic peptides: MH-3 and MH-3S. As previously found [102], MH-3 was an excellent substrate for A-CAT, whereas MH-3S was not appreciably phosphorylated (less than 1%) (Figures 3-8 and 3-9 and Table 3-1). Similarly, MH-3 was a substrate for A-CAT-809 (albeit, phosphorylated at a substantially lower rate compared to A-CAT) whereas MH-3S was not phosphorylated appreciably (Figures 3-8 and 3-9 and Table 3-1). These results suggest that the structural features that define the Thr-specificity of A-CAT are inherent to the main kinase fold (residues 552-805) and are not found within the kinase C-tail sequence (residues 806-841).

3.6. The C-Tail Region Is Conserved in the Members of the MHCK Family

The results of previous experiments showed that the C-tail is important for activity. To investigate the conservation of the C-tail region in the members of MHCK family, an alignment of the C-tail sequences of MHCK A, B, C and D (Figure 3-10) was made, which revealed how variable the C-tails are in length and sequence. However, a highly

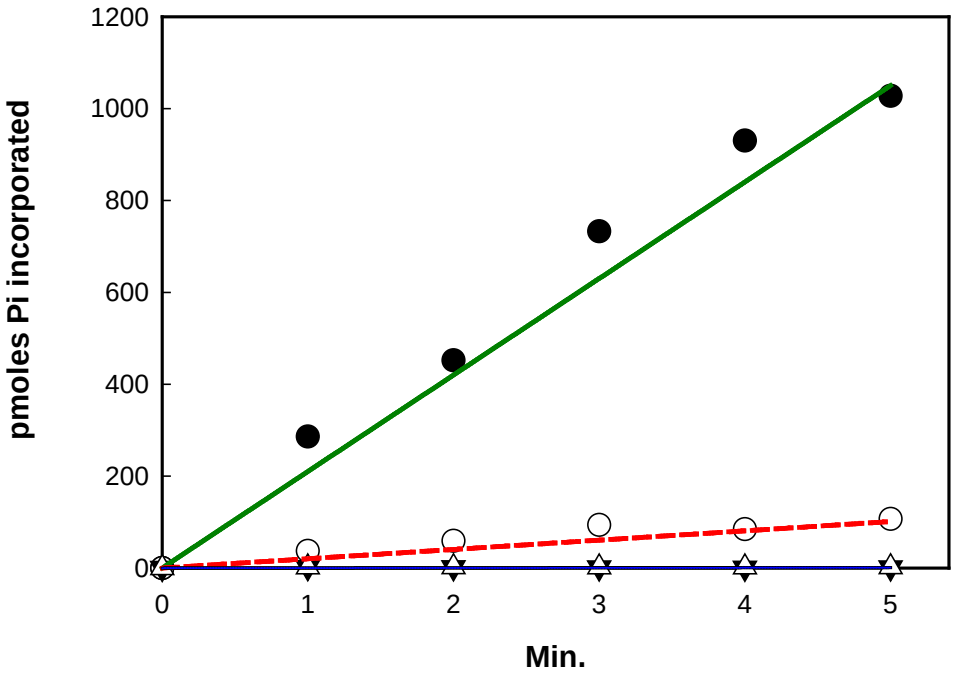

Figure 3-8. Threonine specificity of A-CAT and A-CAT-809. . A-CAT and A-CAT-809 were assayed with two synthetic peptides, MH-3 and MH-3S at 300μM. ●(solid green line) A-CAT with MH-3, ○(dashed red line) A-CAT-809 with MH-3, △(solid blue line) A-CAT with MH-3S, and ▼(solid blue line) A-CAT-809 with MH-3S.

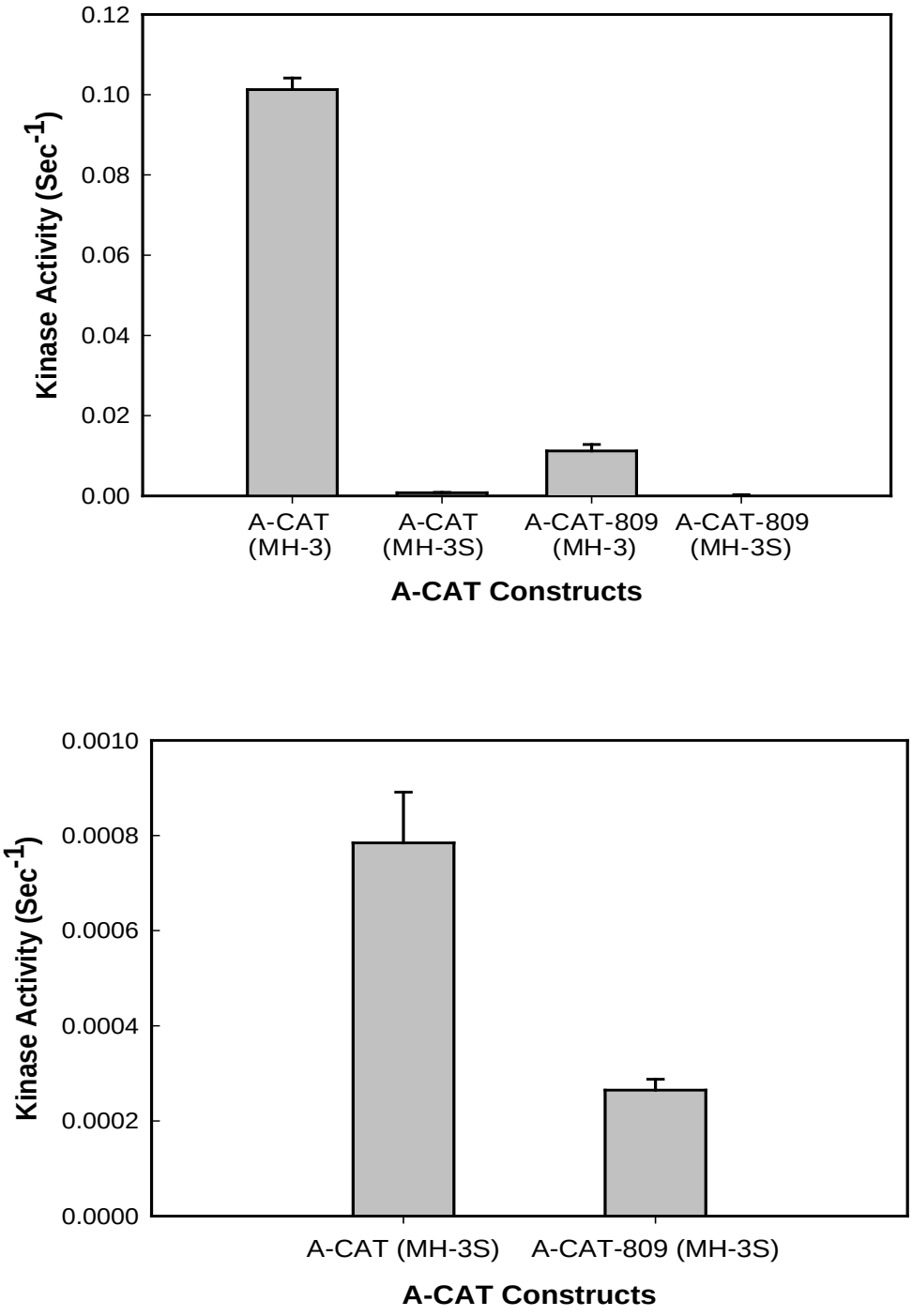

Figure 3-9. Kinase activity of A-CAT and A-CAT-809 showing threonine specificity. Upper panel: Kinase activity of A-CAT and A-CAT-809 using MH-3 and MH-3S as substrate. Lower panel: Kinase activity of A-CAT and A-CAT-809 using MH-3S as substrate, shown in the upper panel, is shown here with an expanded scale. Assays were carried out as described in Materials and Methods.

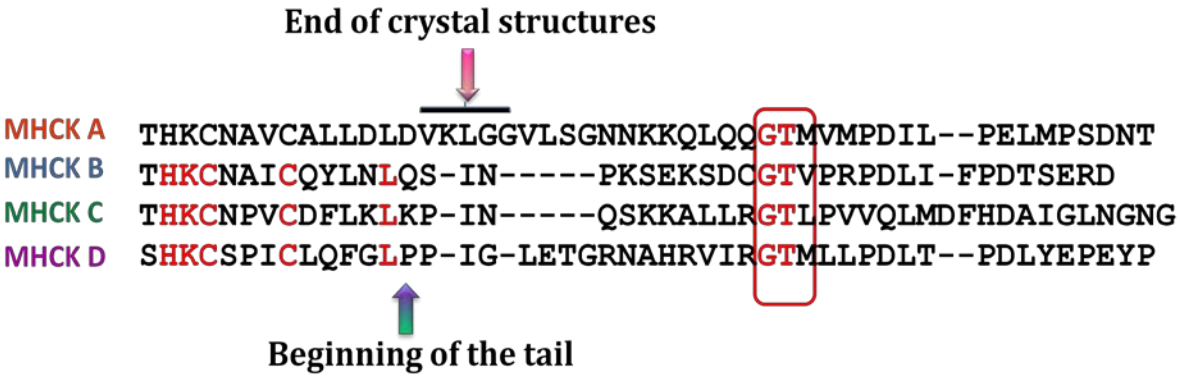

Figure 3-10. Alignment of the kinase C-tail sequences of MHCK A, MHCK B, MHCK C and MHCK D. The conserved Gly-Thr-hydrophobic motif is marked by a red box. The conserved threonine residue is T825 in MHCK A; T339 in MHCK B; T254 in MHCK C; and T597 in MHCK D.

conserved Gly-Thr-hydrophobic motif was found within the C-tails, which for A-CAT is at position 824-826. These conserved residues are located in the region previously found by truncation analysis to be critical for activity (residues 823-831). To determine if the A-CAT C-tail could functionally be substituted with the C-tail sequence of MHCK B kinase domain (B-CAT), a chimera version of A-CAT (residues 552-802) with the B-CAT C-tail (residues 326-354) was expressed and purified (Figures 3-11 and 3-12). Surprisingly, adding the C-tail domain sequence of B-CAT to the truncated A-CAT-809 fully rescued kinase activity (Figure 3-13, Upper panel). However, ATPase activity was rescued to a lesser extent (~45%) (Figure 3-13, Lower panel and Table 3-1). This result reveals that the MHCK C-tail regions contain a conserved sequence necessary for activity.

3.7. T825 is Critical for A-CAT Activity

The highly conserved threonine residue (T825) in the Gly-Thr-hydrophobic motif in the C-tail domain was analyzed to determine if it played a role in kinase activity. Mutation of T825 to alanine (T825A) resulted in a drop (~97%) in both kinase and ATPase activities. This loss of activity is similar in magnitude to that observed upon deletion of the entire C-tail (A-CAT-809) (Figure 3-14 and Table 3-1). This result shows that T825 is a critical residue in the C-tail region for A-CAT activity.

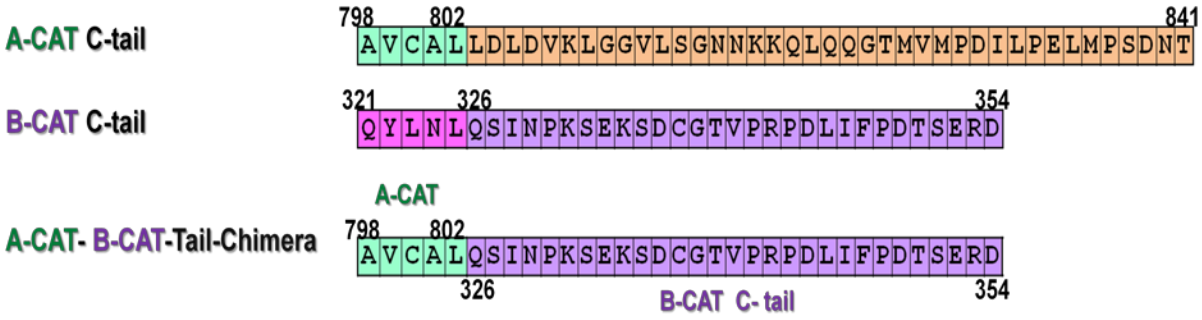

Figure 3-11. Sequences of the C-tail region of A-CAT, B-CAT and A-CAT–B-CAT-Tail-Chimera construct. A-CAT–B-CAT-Tail-Chimera consists of residues 552-802 of A-CAT and residues 326-354 of C-tail sequence of B-CAT.

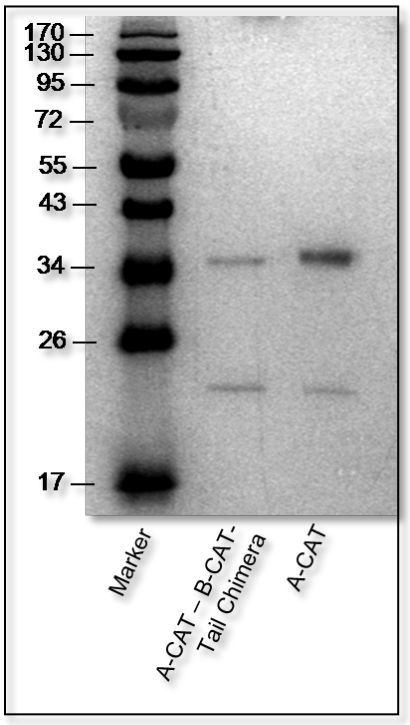

Figure 3-12. Coomassie Blue-stained SDS polyacrylamide gel of the purified bacterially-expressed A-CAT–B-CAT-Tail-Chimera and A-CAT.

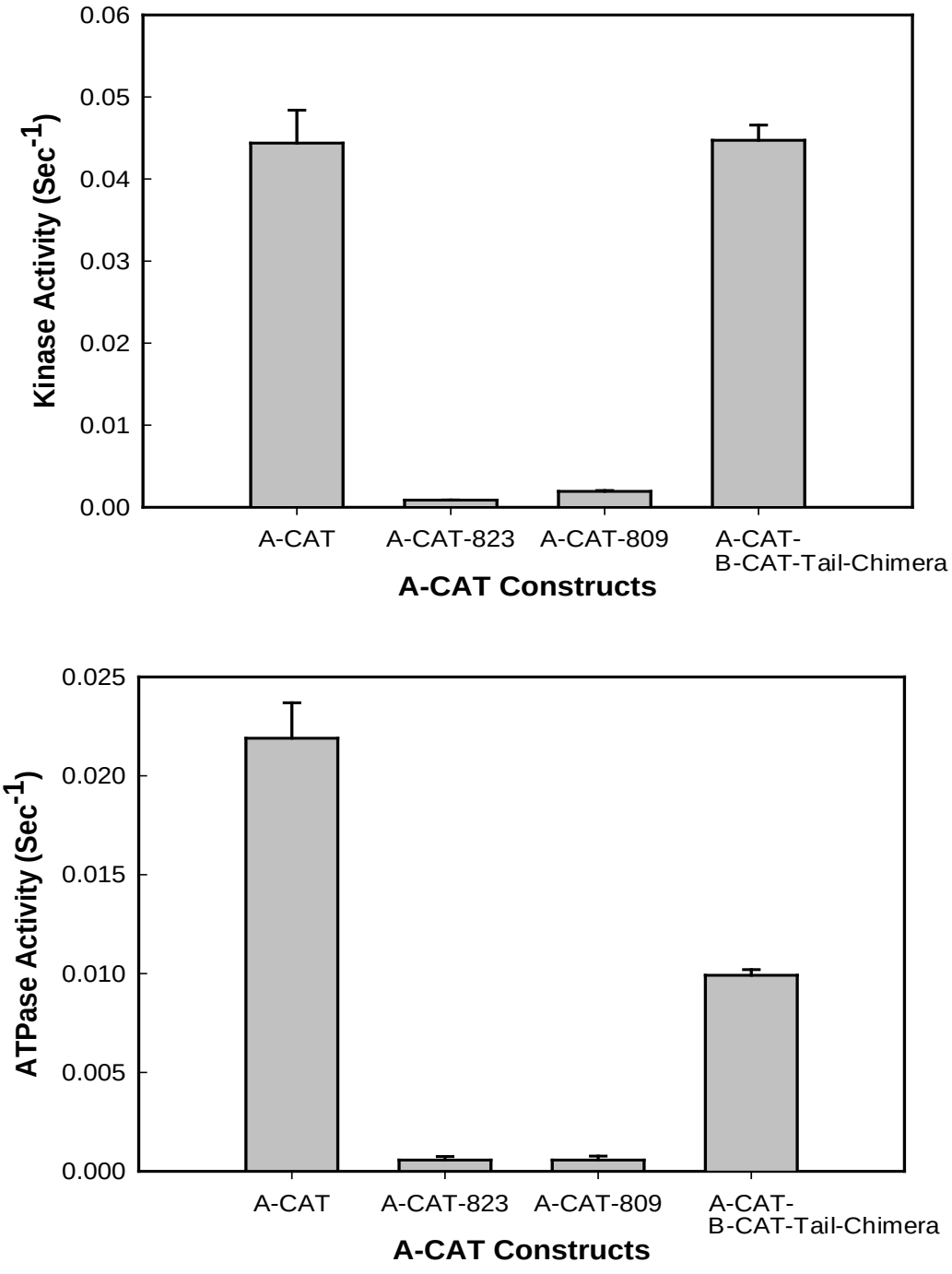

Figure 3-13. Kinase and ATPase activities of A-CAT-B-CAT-Tail-Chimera. Upper panel: Kinase activity. Lower panel: ATPase activity. Assays were carried out as described in Materials and Methods.

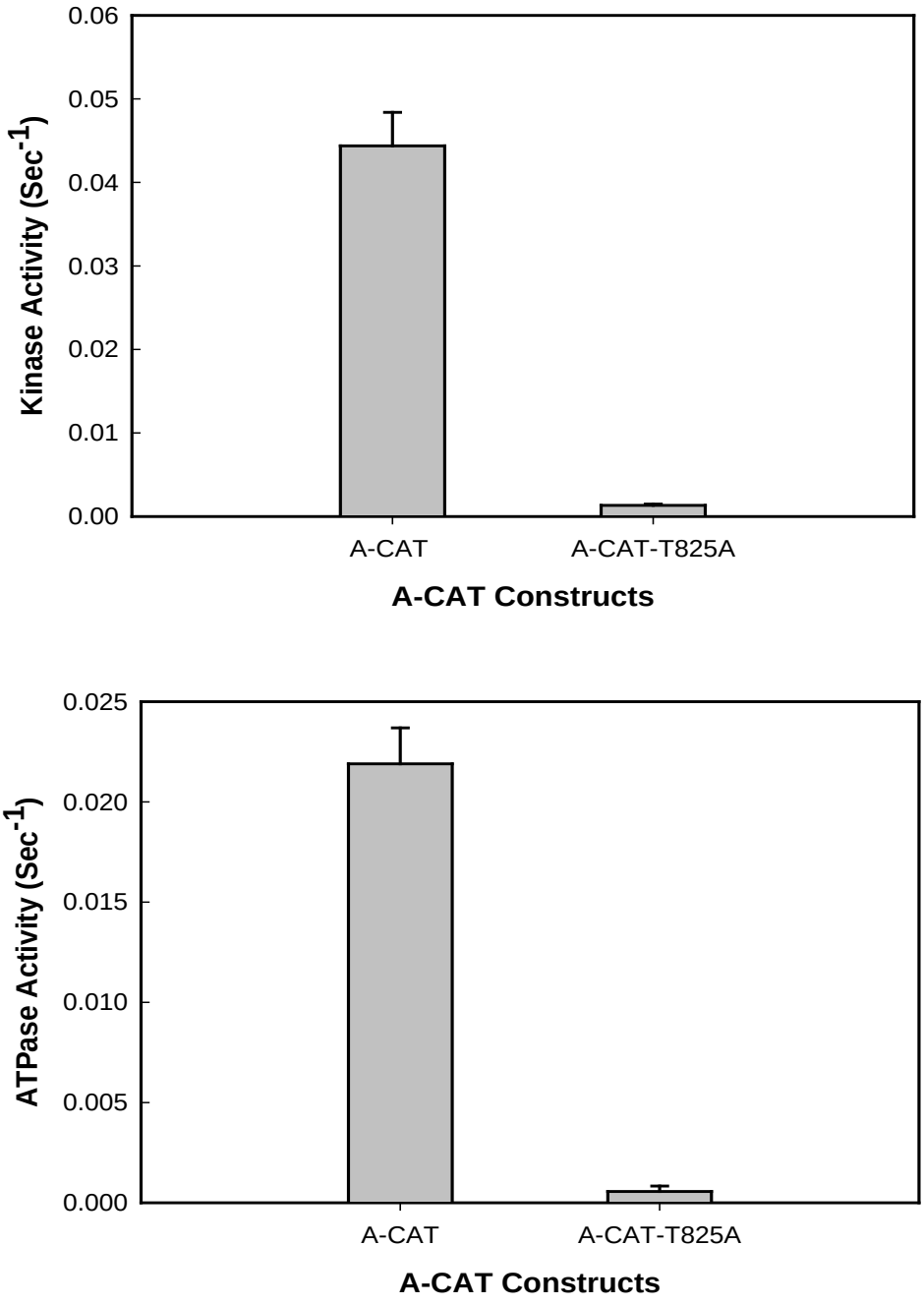

Figure 3-14. Kinase and ATPase activities of A-CAT and A-CAT-T825A. Upper panel: Kinase activity. Lower panel: ATPase activity. Assays were carried out as described in Materials and Methods.

3.8. Exogenous A-CAT C-Tail Cannot Rescue the Activity of A-CAT-809

To investigate the necessity for the C-tail to be in a specific position in relation to the active site, the C-tail region of A-CAT (residues 806-841) was expressed and purified as a GST-fusion protein (Figure 3-15). The GST-tail fragment was incubated for 1 hour with A-CAT-809, before addition of the substrate MBP, [γ-^{32}P]ATP and kinase buffer. Incubation of GST-A-CAT C-tail with A-CAT-809 at a ratio of 10:1 did not rescue the kinase activity of A-CAT-809 (Figure 3-16 and Table 3-1). This shows that the C-tail needs to be properly positioned in relation to the active site of the kinase to be functional, and cannot simply be added exogenously.

3.9. There Is an Optimal Length for the C-Tail Region of A-CAT

To investigate whether the length of the C-tail region is important for activity, a varying number of residues of the C-tail located before the critical T825 were deleted (Figures 3-17 and 3-18). The constructs were tested for kinase and ATPase activities (Figure 3-19). Deletion of 3 residues (812-814) in A-CAT-ΔVLS, and 6 residues (810-815) in A-CAT-ΔGGVLSG, before the critical threonine (T825) reduced the kinase activity by ~70% and the ATPase activity by ~70-85%. Deletion of 10 amino acids (810-819) in A-CAT-ΔGGVLSGNNKK reduced the ATPase activity by ~70%, but no remarkable drop (~15%) was seen in the kinase rate (Figure 3-19 and Table 3-1). These results show that changing the length of C-tail region of A-CAT affects its kinase and ATPase activities.

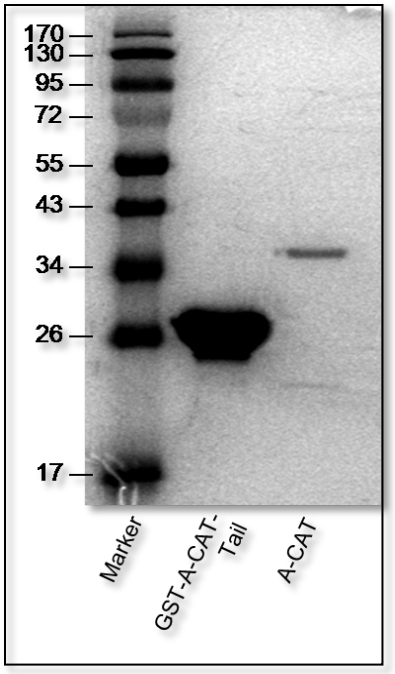

Figure 3-15. Coomassie Blue-stained SDS polyacrylamide gel of the purified bacterially-expressed GST-A-CAT-Tail and A-CAT.

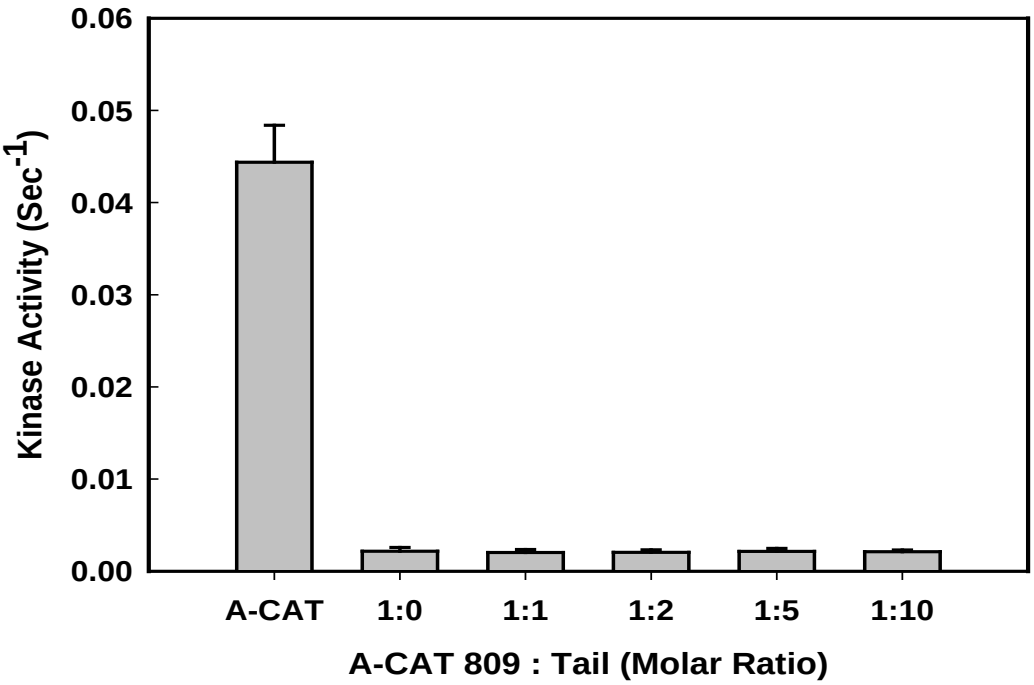

Figure 3-16. Kinase activity of A-CAT and, A-CAT-809 and the GST-A-CAT-Tail. The rate of kinase activity was measured using various proportions of the C-tail (0-10 times A-CAT-809 concentration) and 33 µM MBP as substrate. Assays were carried out as described in Materials and Methods.

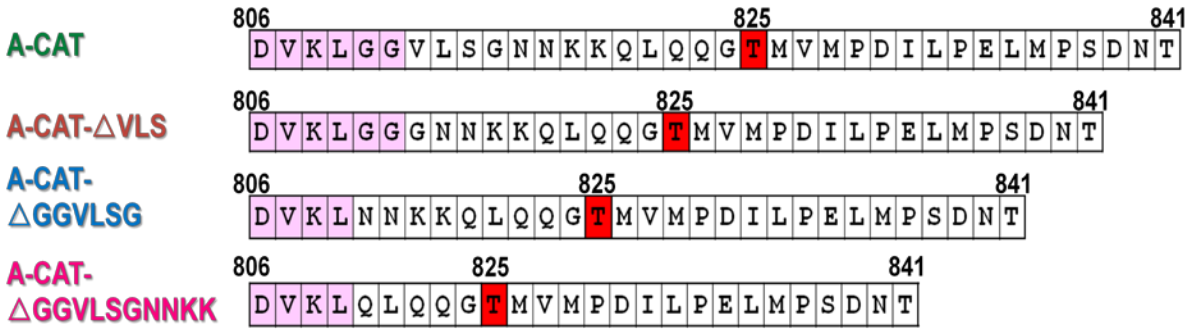

Figure 3-17. Sequences of the C-tail region of the A-CAT, A-CAT-△VLS, A-CAT-△GGVLSG and A-CAT-△GGVLSGNNKK deletion constructs. In A-CAT-△VLS residues 812-814, in A-CAT-△GGVLSG residues 810-815, and in A-CAT-△GGVLSGNNKK residues 810-819 are deleted.

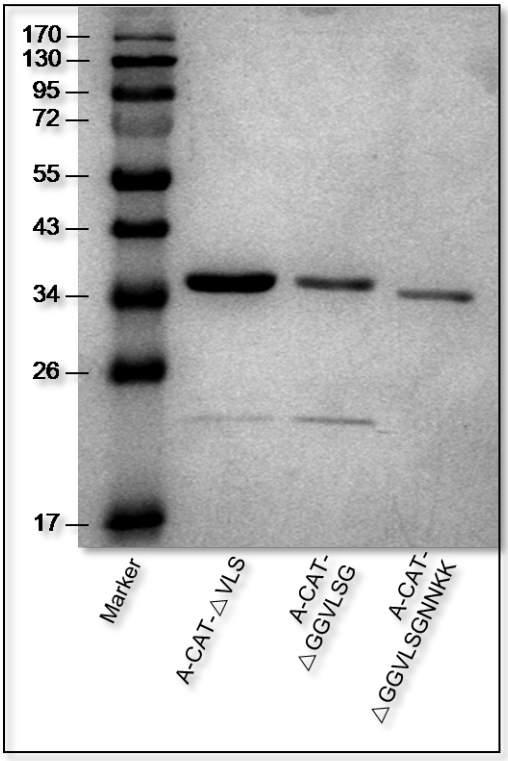

Figure 3-18. Coomassie Blue-stained SDS polyacrylamide gel of the purified bacterially-expressed A-CAT-△VLS, A-CAT-△GGVLSG and A-CAT-△GGVLSGNNKK deletion constructs.

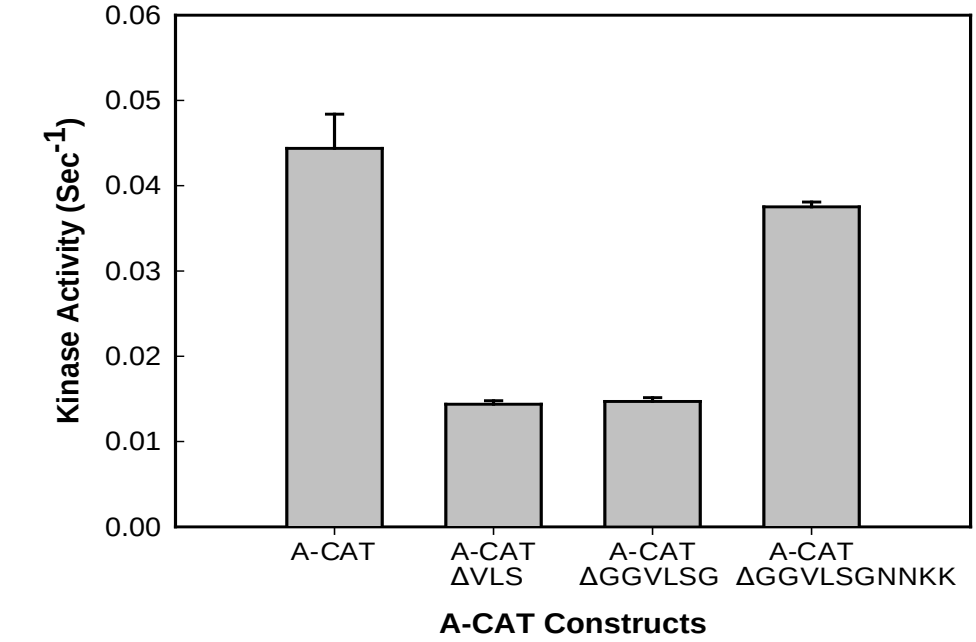

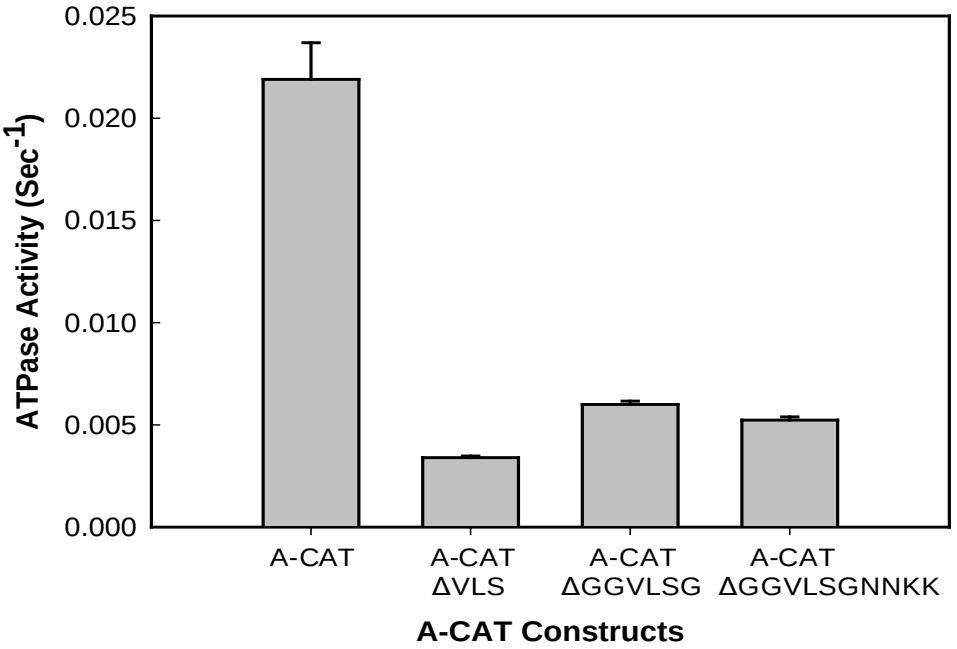

Figure 3-19. Kinase and ATPase activities of A-CAT, A-CAT-△VLS, A-CAT-△GGVLSG and A-CAT-△GGVLSGNNKK. Upper panel: Kinase activity. Lower panel: ATPase activity. Assays were carried out as described in Materials and Methods.

3.10. T825 is an Important Autophosphorylation Site in A-CAT

Six autophosphorylation sites in A-CAT have been identified: S553, T612, T613, T614, T634 and T825 [8]. In order to determine the significance of autophosphorylation of T825, all of the autophosphorylation sites were mutated to alanine except for T825 (S553A, T612A, T613A, T614A, and T634A) (Figure 3-20). The autophosphorylation of the mutated construct (A-CAT-5xAla) was measured and compared to the autophosphorylation of A-CAT (Figure 3-21). The result showed that T825 comprises ~30% of the total autophosphorylation of the protein (Figure 3-22).

It was previously demonstrated that T825 was critical for the kinase activity. To test whether any of the other auto-phosphorylation sites were necessary for the kinase activity, the A-CAT-5xAla construct was assessed for kinase and ATPase activities. A-CAT-5xAla showed kinase (4.01×10^{-2} sec^{-1}) and ATPase (1.82×10^{-2} sec^{-1}) activities very close to A-CAT (Figure 3-23 and Table 3-1). This is in contrast to A-CAT-T825A, in which all of the autophosphorylation sites except for T825 were intact (Figures 3-23). The results of this experiment reveal that T825 is the only critical autophosphorylation site.

3.11. Autophosphorylation of T825 Plays as a Regulatory Mechanism for A-CAT Kinase Activity

Since threonine and serine have the same polar side chain (hydroxyl group) and their structure differs only in one methyl group, the general expectation is that they can be

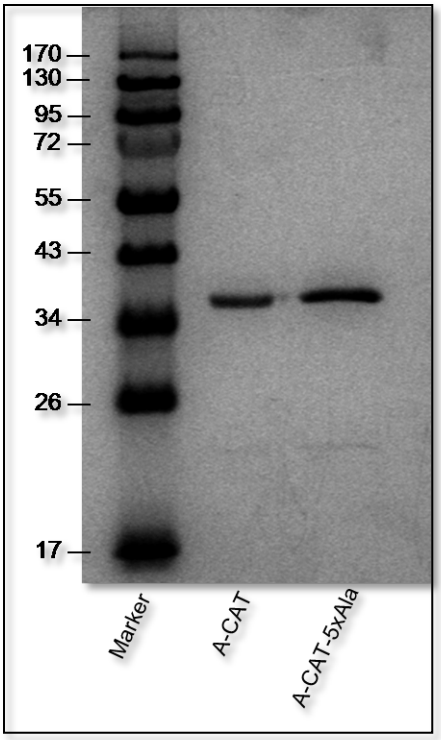

Figure 3-20. Coomassie Blue-stained SDS polyacrylamide gel of the purified bacterially-expressed A-CAT and A-CAT-5xAla.

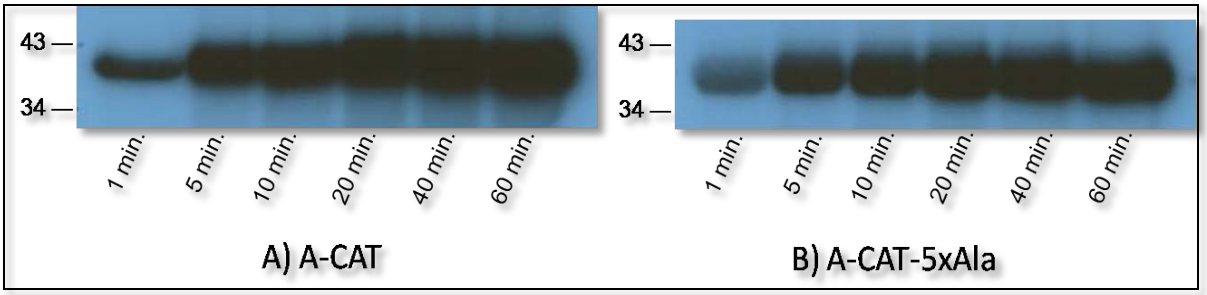

Figure 3-21. Autoradiograph pictures of autophosphorylation of A-CAT and A-CAT-5xAla. A) Autophosphorylation of A-CAT. B) Autophosphorylation of A-CAT-5xAla.

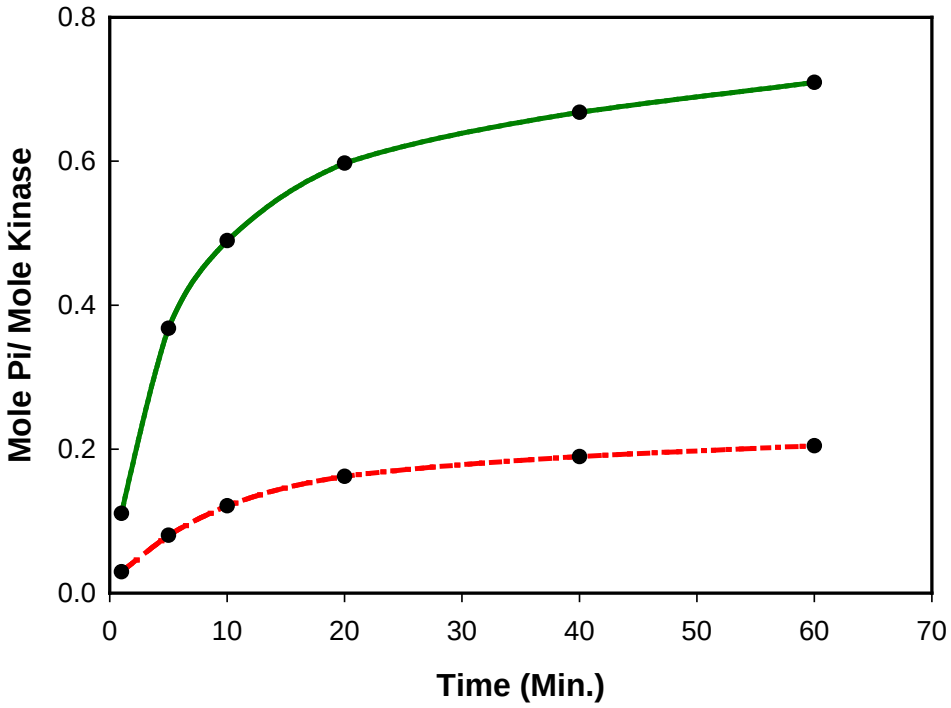

Figure 3-22. Autophosphorylation rates of A-CAT and A-CAT-5xAla. The autophosphorylation rate of A-CAT is shown with solid green and of the A-CAT-5xAla with dashed red line. A-CAT-5xAla shows ~30% of the total autophosphorylation of A-CAT.

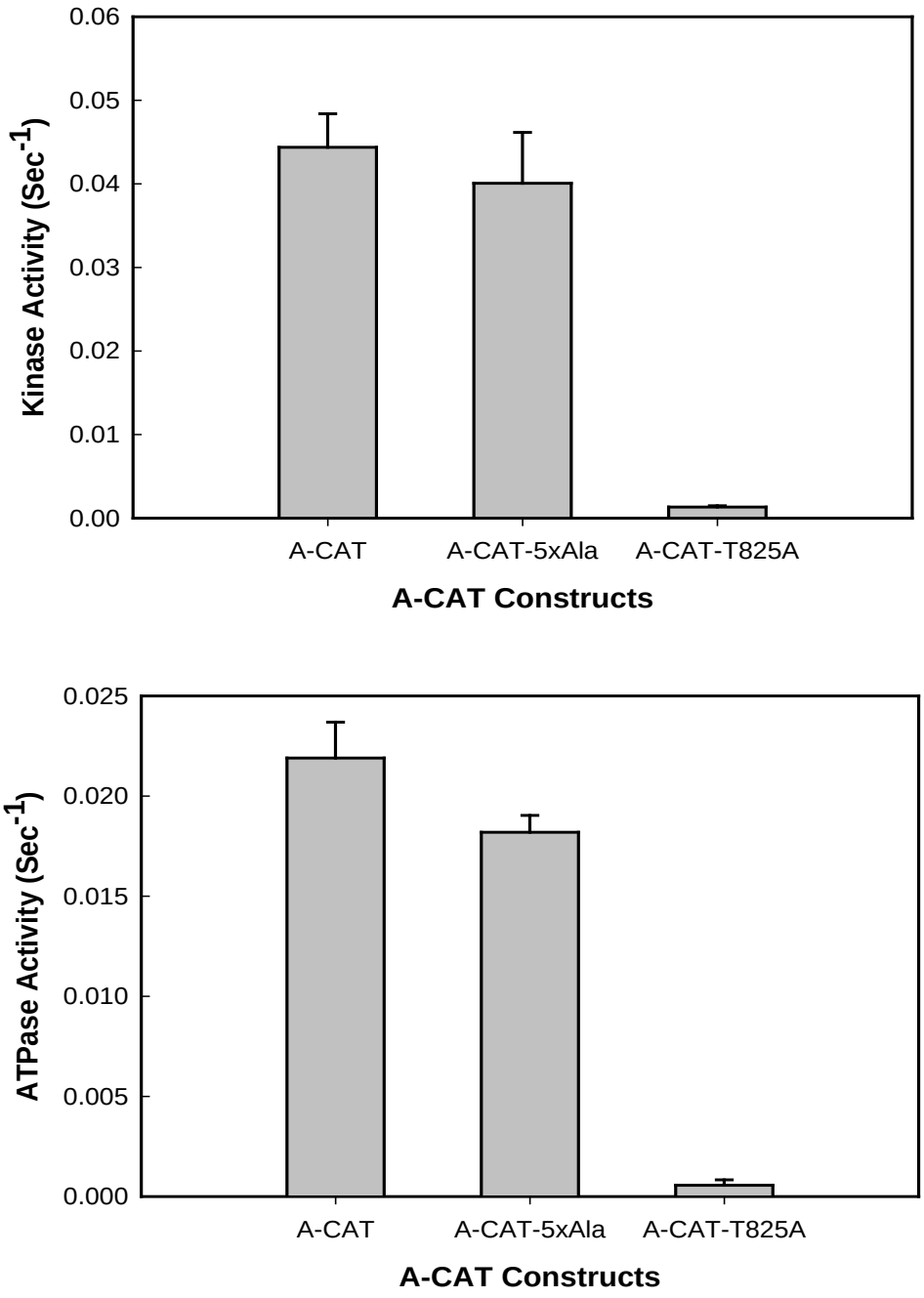

Figure 3-23. Kinase and ATPase activities of A-CAT, A-CAT-5xAla and A-CAT-T825A. Upper panel: Kinase activity. Lower panel: ATPase activity. Assays were carried out as described in Materials and Methods.

substituted in the structure of proteins. However, A-CAT has been shown to phosphorylate threonine residues specifically [54]. T825 was mutated to serine to investigate whether this replacement would impact catalytic function. Remarkably, the construct A-CAT-T825S showed lower kinase ($6.88x10^{-3}$ sec^{-1}) and ATPase ($8.15x10^{-3}$ sec^{-1}) activities compared to A-CAT (Figure 3-24 and Table 3-1). This experiment indicates that conversion of T825 to a serine makes it a poor auto-phosphorylation site and results in low activity.

To further test the role of autophosphorylation of this residue, T825 was mutated to glutamic acid. Surprisingly T825E possessed low kinase ($3.06x10^{-3}$ sec^{-1}) and ATPase ($8.45x10^{-4}$ sec^{-1}) activities (Figure 3-24 and Table 3-1). Previous experiments have shown that the activity of MHCK A increases with the overall autophosphorylation state of the kinase [47]. In this case it is possible that glutamic acid does not fully mimic a phosphorylated T825 residue. Another possibility is that reversible phosphorylation of T825 may be required for A-CAT activity.

3.12. T825 Plays an Important Catalytic Role in the Context of Full-Length MHCK A

At present, little is known about the mechanisms which regulate the activity of MHCK A *in vivo*. Mutation analysis of A-CAT indicates that both the kinase and ATPase activities can be potentially regulated through reversible modification of T825 within the C-tail sequence of the kinase domain. In MHCK A the C-tail is a part of the linker that connects A-CAT to the WD repeat domain (Figure 3-25). It was sought to determine

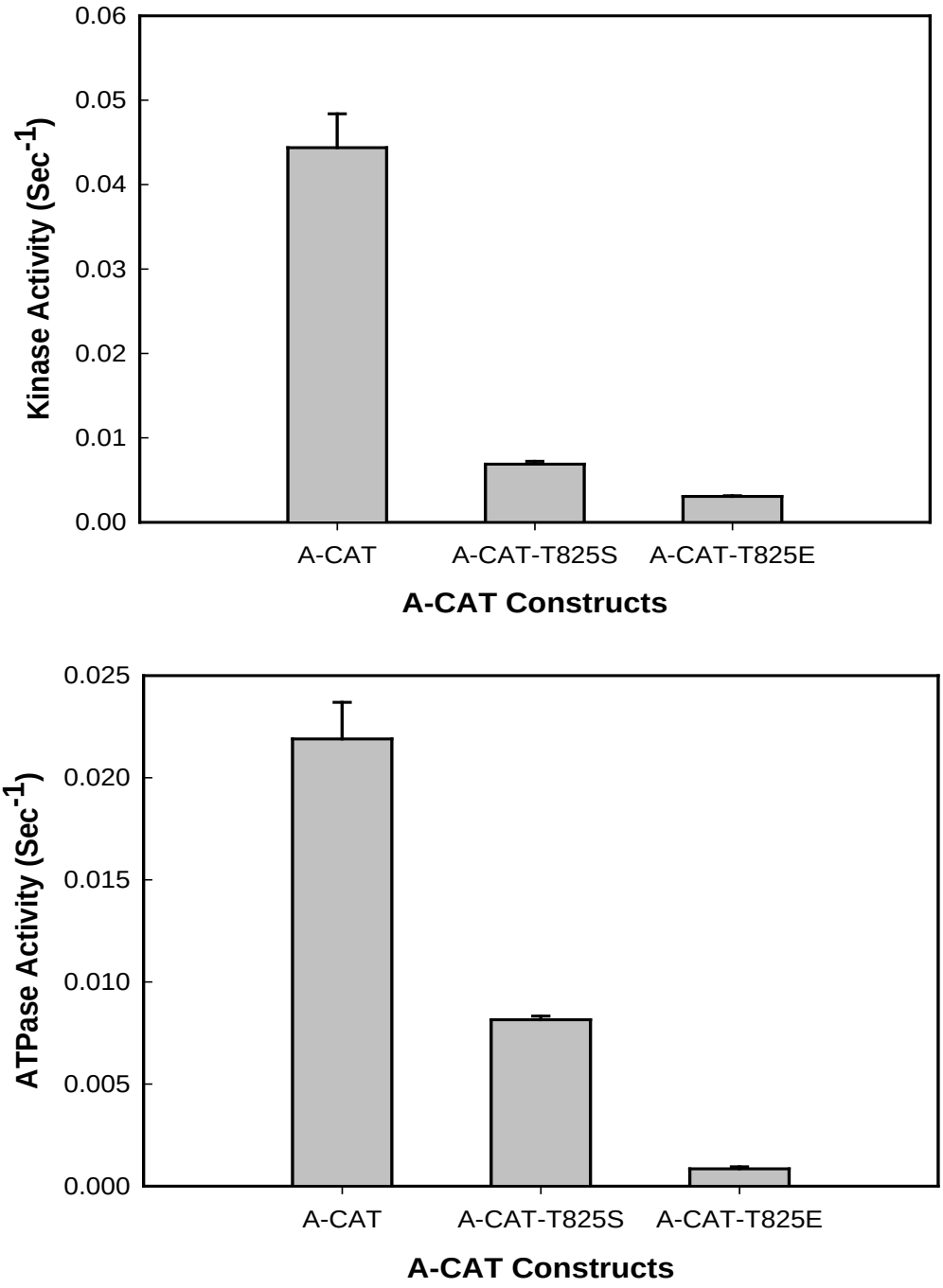

Figure 3-24. Kinase and ATPase activities of A-CAT, A-CAT-T825S and A-CAT-T825E. Upper panel: Kinase activity. Lower panel: ATPase activity. Assays were carried out as described in Materials and Methods.

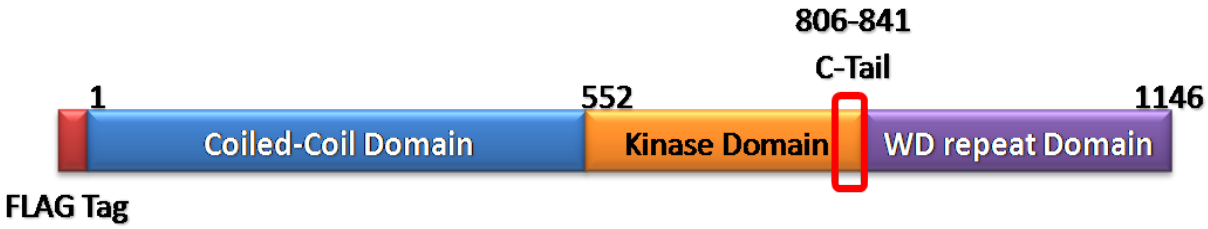

Figure 3-25. Schematic diagram of FLAG-TAG-MHCK A. The C-tail is a part of the linker that connects A-CAT to the WD repeat domain.

whether the C-tail sequence and specifically T825 plays an important catalytic role in the context of full-length MHCK A.

Full-length MHCK A, MHCK A-T825A and MHCK A-T825E were cloned and expressed in the *Dictyostelium* AX3 cell line. The purified proteins (Figure 3-26) were assessed for kinase and ATPase activities (Figure 3-27 and Table 3-1). Mutation of T825 to alanine (MHCK A-T825A) reduced kinase activity by ~92% (Figure 3-27, Upper panel). Mutation to glutamic acid (MHCK A-T825E) also reduced kinase activity by ~91%. This reduction was also seen in the ATPase activity but was not as substantial as the kinase activity (Figure 3-27, Lower panel). The results show that T825 is essential for the activity of full-length MHCK A.

Interestingly, the kinase activity of the full-length MHCK A ($1.87x10^{-1}$ sec^{-1}) is about 4 times more than that of A-CAT ($4.44x10^{-2}$ sec^{-1}) (Figure 3-28 and Table 3-1). This may be because MHCK A is an oligomer or has more autophosphorylation sites which produce more negative charge for attracting the substrate toward the catalytic domain.

3.13. TRPM7-CAT Possesses ATPase and ADPase Activities

To assess whether TRPM7-CAT possesses nucleotide hydrolyzing activity, TRPM7-CAT (residues 1548-1862) was expressed and purified (Figure 3-29). TRPM7-CAT was tested for the ability to hydrolyze [α-^{32}P]-ATP. TRPM7-CAT displayed a lower activity compared to A-CAT with a kinase rate of $9.05x10^{-3}$ sec^{-1} and an ATPase rate of $4.21x10^{-3}$ sec^{-1} (Figure 3-30 and Table 3-1). The ADPase rate of TRPM7-CAT is

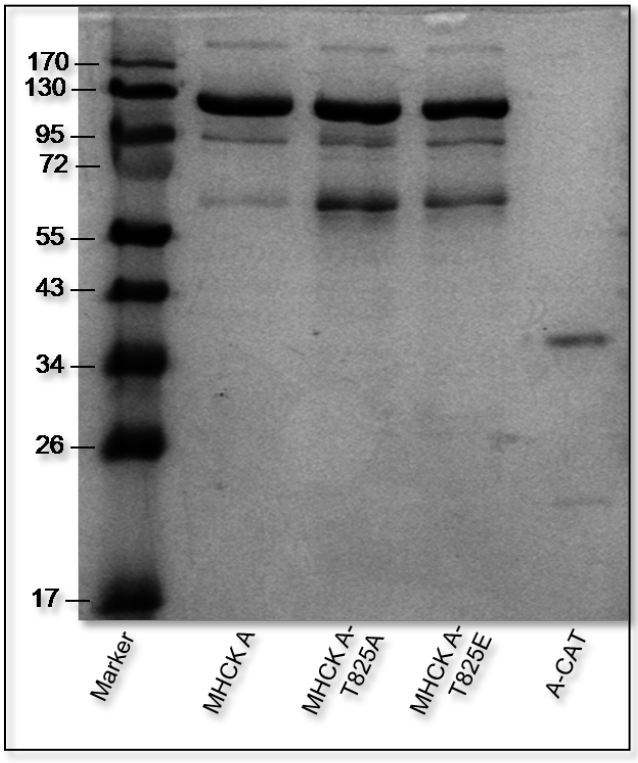

Figure 3-26. Coomassie Blue-stained SDS polyacrylamide gel of the purified expressed full-length MHCK A, MHCK A-T825A, MHCK-T825E and A-CAT in *Dictyostelium discoideum*.

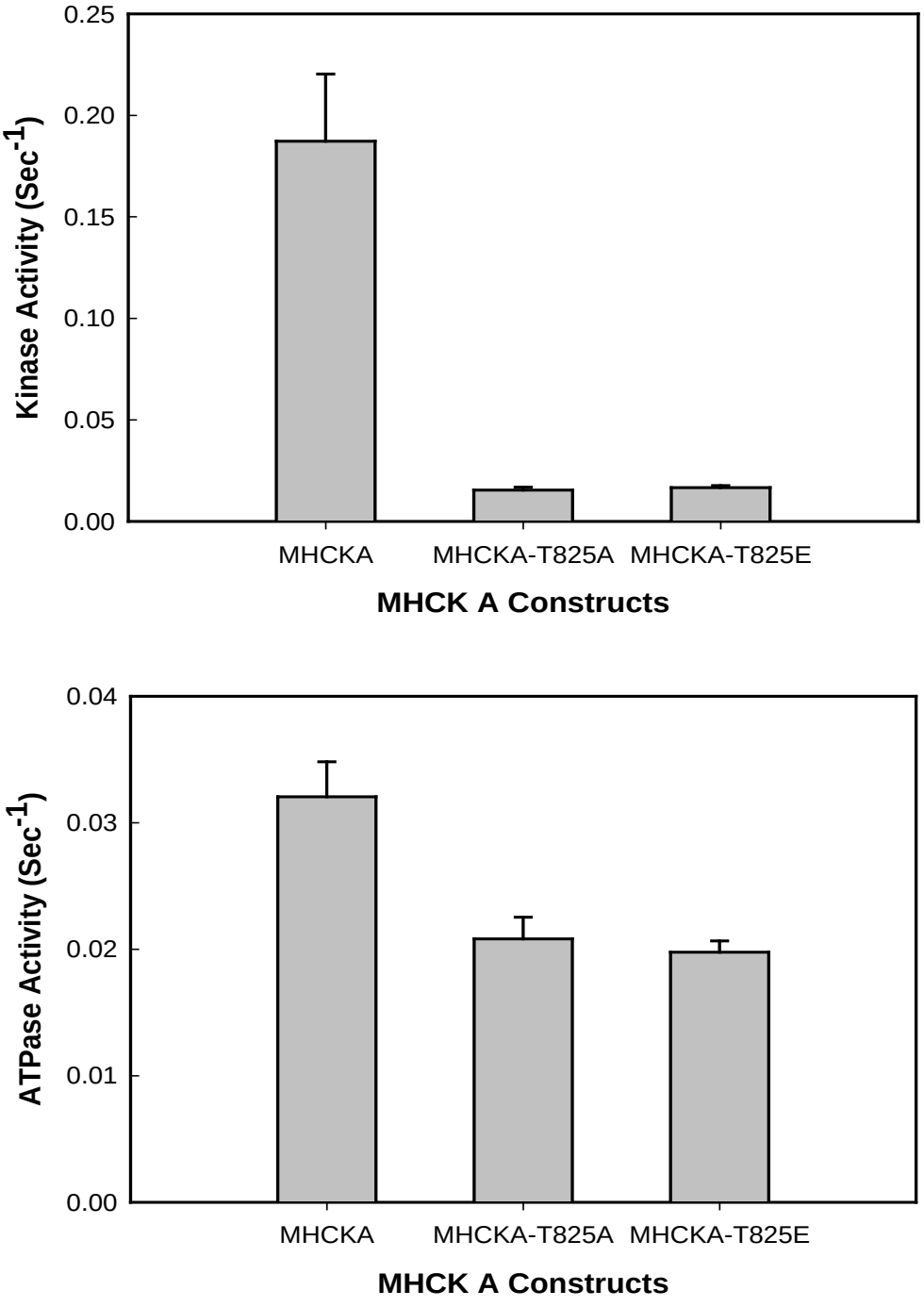

Figure 3-27. Kinase and ATPase activities of full-length MHCK A, MHCKA-T825A and MHCKA-T825E. Upper panel: Kinase activity. Lower panel: ATPase activity. Assays were carried out as described in Materials and Methods.

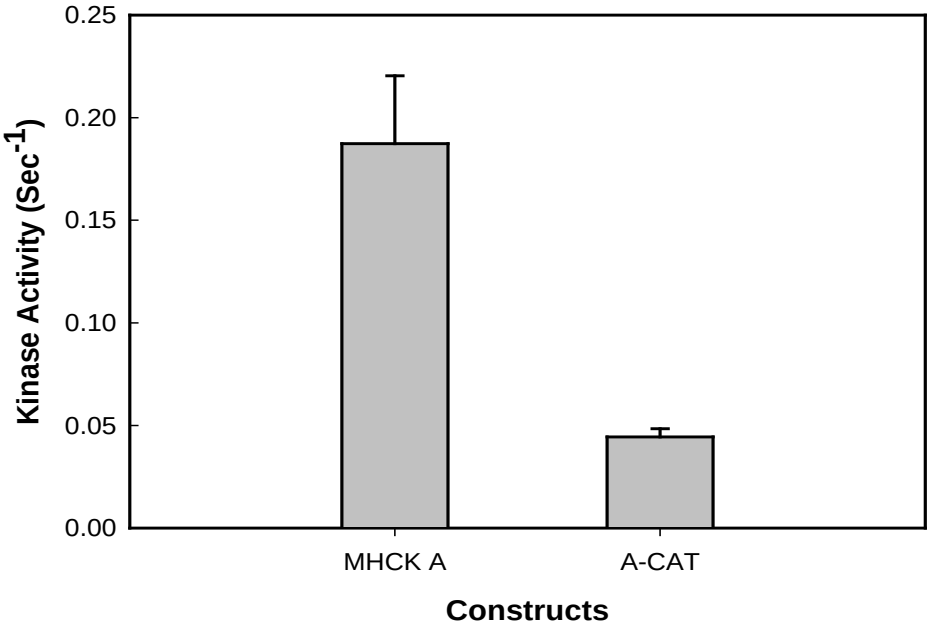

Figure 3-28. Kinase activity of full-length MHCK A and A-CAT. Assays were carried out as described in Materials and Methods.

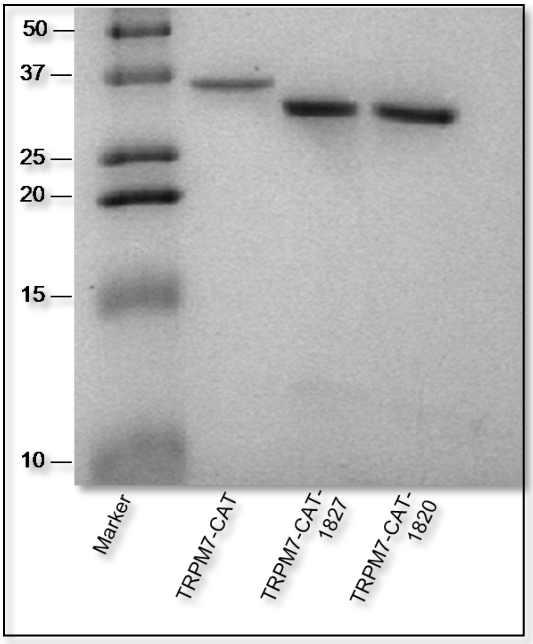

Figure 3-29. Coomassie Blue-stained SDS polyacrylamide gel of the purified bacterially-expressed constructs of TRPM7-CAT, TRPM7-CAT-1827 and TRPM7-CAT-1820.

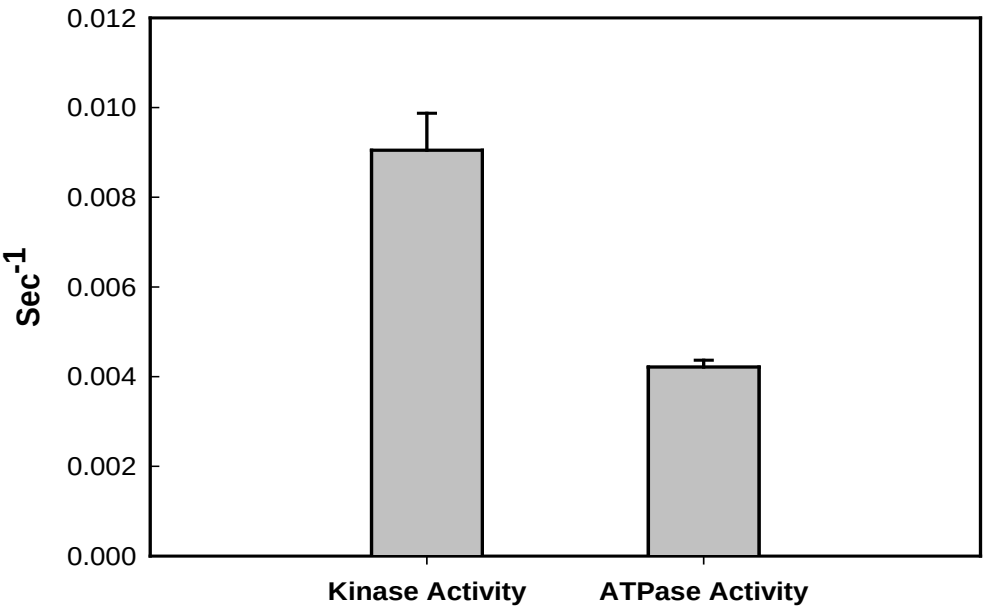

Figure 3-30. Kinase and ATPase activities of TRPM7-CAT. Assays were carried out as described in Materials and Methods.

substantially lower compared to the ATPase rate with value of 1.77 $x10^{-4}$ sec^{-1} (Table 3-1). These results show that TRPM7-CAT like A-CAT possess ATPase and ADPase activities in addition to kinase activity.

3.14. The C-Tail Sequence of TRPM7-CAT Plays an Important Catalytic Role

There is a high degree of similarity between the structures of TRPM7-CAT and A-CAT (Figures 1-6 and 1-9). Like A-CAT, electron density of residues 1828-1862 for the C-tail of TRPM7-CAT (residues 1819-1862) in the X-ray structure is missing. In order to investigate the importance of the C-tail region in TRPM7-CAT, truncation analysis of the TRPM7 C-tail sequence was performed (Figures 3-29 and 3-31).

Deletion of the entire C-tail sequence of TRPM7-CAT (TRPM7-CAT 1820) resulted in the loss of ~99% of kinase and ~54% of ATPase activity (Figure 3-32 and Table 3-1). The kinase and ATPase activities of TRPM7-CAT-1827 also decreased by ~97% and ~58%, respectively, indicating that the catalytically important segment of TRPM7 C-tail resides between residue 1827 and the end of the protein. These results demonstrate that like A-CAT, the C-tail region of TRPM7-CAT plays a critical role in the kinase activity and also indicates that the catalytically important segment of this C-tail resides between residue 1827 and the end of the protein. In contrast to A-CAT which is specific for the phosphorylation of threonine residues, TRPM7-CAT autophosphorylates predominantly serine residues [51;52;54;92]. In order to find the critical residue for the activity of TRPM7-CAT within the important C-tail region, a series of point-mutations (T1827A,

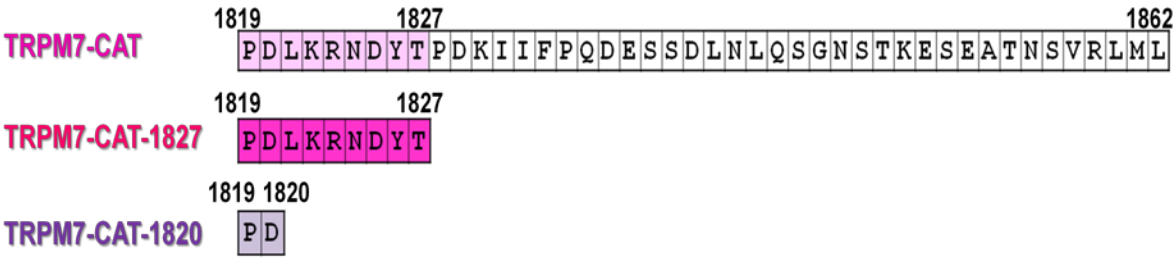

Figure 3-31. Sequences of the C-tail regions of the TRPM7-CAT, TRPM7-CAT-1827 and TRPM7-CAT-1820. The crystal structure of TRPM7-CAT has no defined electron density for residues 1828-1862 of the C-tail.

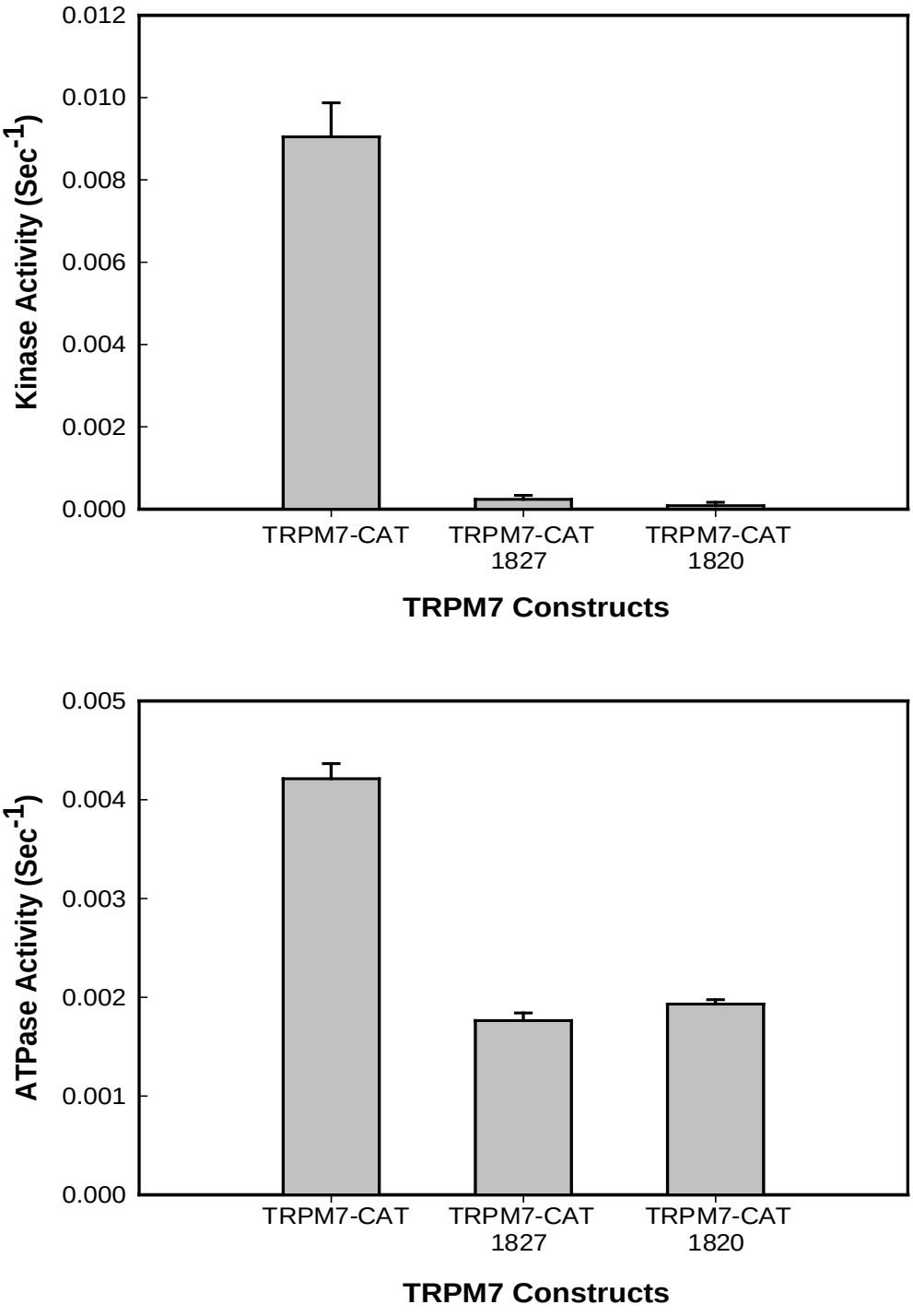

Figure 3-32. Kinase and ATPase activities of TRPM7-CAT, TRPM7-CAT-1827 and TRPM7-CAT-1820. Upper panel: Kinase activity. Lower panel: ATPase activity. Assays were carried out as described in Materials and Methods.

S1838A, S1839A, S1848A, and S1857A) and one double-mutation (S1838A-S1839A) were generated (Figures 3-33 and 3-34). Analysis of these mutants resulted in kinase rates close (~73-95%) to TRPM7-CAT (Figure 3-35 and Table 3-1) which shows that none of these sites are critical for TRPM7-CAT activity.

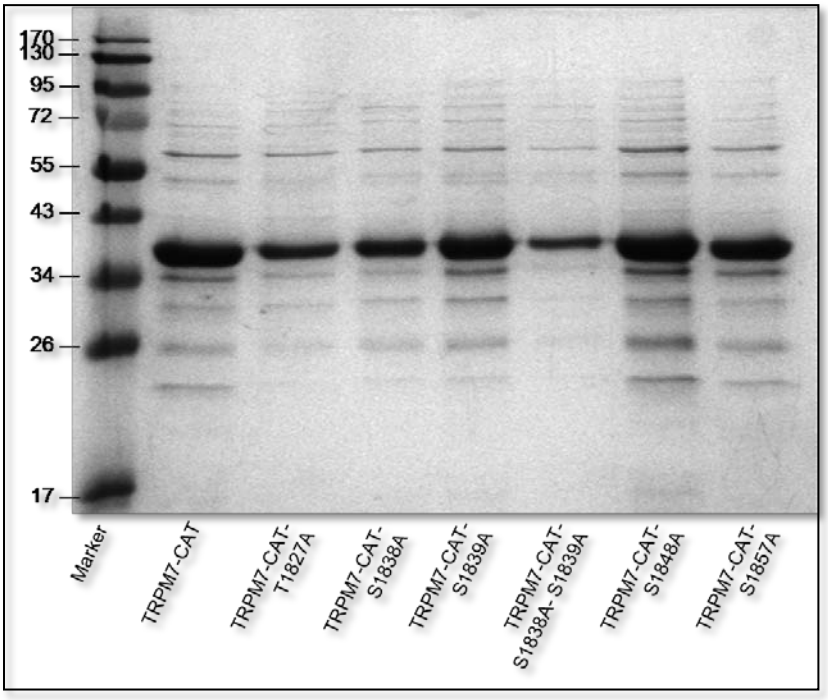

Figure 3-33. Coomassie Blue-stained SDS polyacrylamide gel of the purified bacterially-expressed TRPM7-CAT and its mutated constructs.

Figure 3-34. Sequences of the C-tail regions of TRPM7-CAT and its mutated constructs.

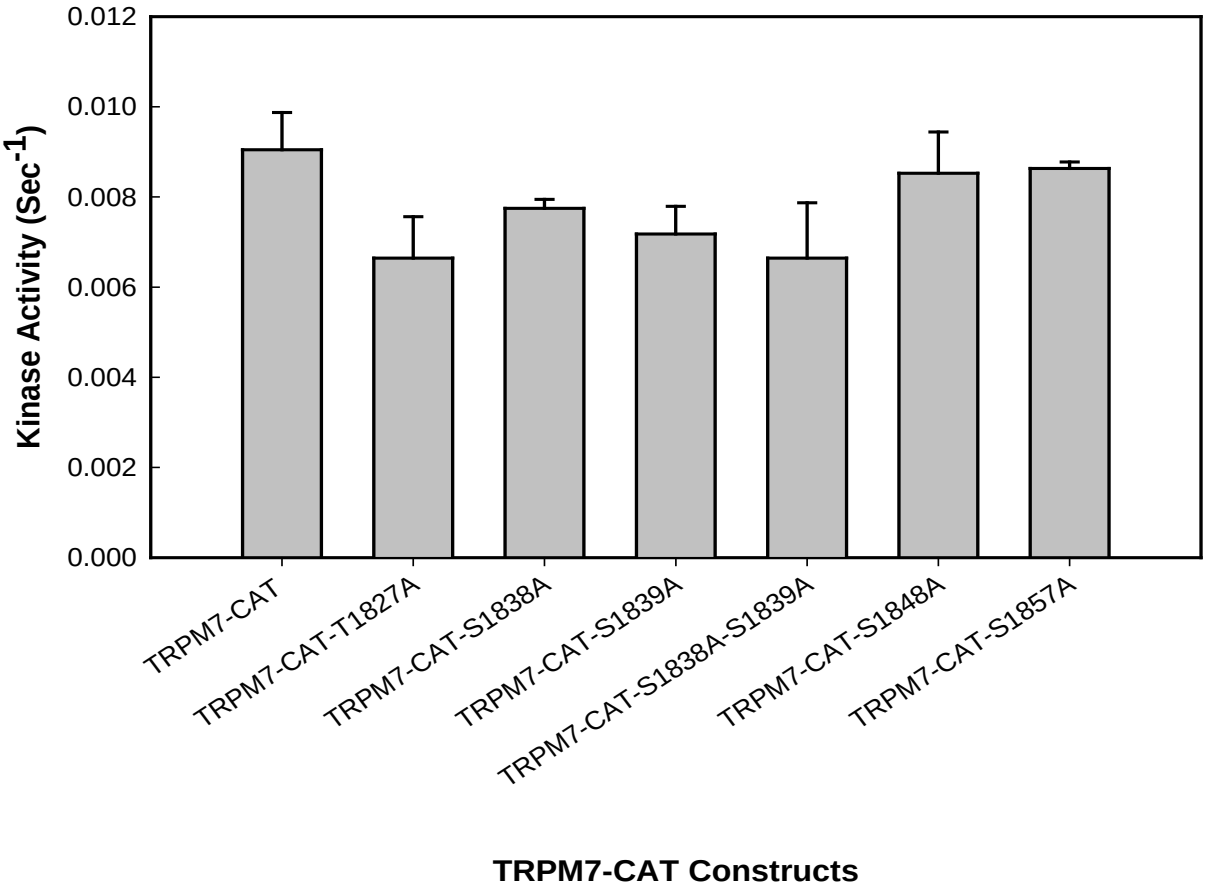

Figure 3-35. Kinase activity of TRPM7-CAT, and its mutated constructs. Assays were carried out as described in Materials and Methods.

CHAPTER 4

CONCLUSION AND DISCUSSION

The studies presented here have uncovered two novel observations about the alpha-kinase family. Firstly, in addition to possessing kinase activity, the catalytic domains of both MHCK A and TRPM7 possess potent ATPase activity. A-CAT and TRPM7-CAT possess also ADPase activity, although approximately 100 and 15 times lower than the ATPase activity, respectively. This result can explain why A-CAT crystallized in the presence of ATP contains AMP in the active site [8]. Some structures of A-CAT also contain adenosine in the active site [Ye, Q., unpublished observations]. The ability of A-CAT to hydrolyze AMP to adenosine has not been yet assayed. When the affinity of AMP or adenosine for the active site of A-CAT was investigated by kinase inhibition assays, the results showed no inhibition for AMP and only a slight inhibition for adenosine at the higher concentrations (0.1-1 mM) was found. These results indicate that AMP and adenosine have a lower affinity for A-CAT than ATP, which has a Km value of 50 μM [8]. Given the low affinity of AMP and adenosine for A-CAT, it is not clear why these nucleotides do not exchange for ATP in the A-CAT crystal. Measuring the concentration of ATP in the solution where the crystal has formed would show whether ATP hydrolysis to ADP, AMP and adenosine is a continuous progressive reaction in the A-CAT active site; that is it occurs without release of product. Alternatively, it is possible that A-CAT has hydrolyzed all ATP molecules in the crystallization solution to AMP or adenosine. This latter possibility seems unlikely, given the very slow rate of ADP hydrolysis measured here for A-CAT.

TRPM7 channel activity is inhibited by Mg^{2+} and Mg.ATP, both of which potentially interact with the alpha-kinase domain [52;65;77;78]. In contrast, millimolar levels of free Mg^{2+} or Mn^{2+} ions significantly increase the kinase activity of TRPM7-CAT [92]. The alpha-kinase domain structure itself, but not its intrinsic phosphotransferase activity, is required to regulate channel activity [52;78]. A local increase in the intracellular bulk free Mg^{2+} and Mg.ATP concentrations would close TRPM7 channels, resulting in a local decrease in free Mg^{2+} and a decrease in the phosphotransferase activity of the TRPM7 kinase domain [103]. The ability of the TRPM7 alpha-kinase domain to hydrolyze ATP to ADP or AMP may produce a feedback signal to promote channel opening. This new information can allow one to reassess the regulation of TRPM7 channel activity via its kinase domain.

Secondly, the results revealed that the unstructured sequence C-terminal to the alpha-kinase domains of both MHCK A (residues 806-841) and TRPM7 (residues 1819-1862) is necessary for catalytic activity. Deletion of the C-tail in A-CAT and TRPM7-CAT substantially reduced kinase activity by approximately 96% and 99%, and ATPase activity by approximately 97% and 55%, respectively. The decrease in ATPase activity indicates that the function of the C-tail is unlikely to involve protein/peptide substrate binding.

Crystal structure analysis of the truncated A-CAT-809 demonstrated that deletion of the C-tail region did not change the structure or fold of A-CAT, indicating that the C-tail sequence does not play a role in the overall structure stability of A-CAT. Indeed, A-CAT-809 crystallized more readily than A-CAT, suggesting that the flexible C-tail impairs crystal formation. It has been shown previously that A-CAT displays a strong

preference for the phosphorylation of threonine residues in substrates [51;54]. This study revealed that the C-tail is not involved in determining threonine specificity, since A-CAT-809 still prefers to phosphorylate threonine residues. From these results, we conclude that the C-tail may be directly involved in supporting a catalytically active state, perhaps by promoting ATP or Mg^{2+} binding.

The mutation of T825 to alanine eliminates the kinase and ATPase activities of A-CAT, revealing its critical role in catalytic activity. A threonine residue equivalent to T825 is conserved in a Gly-Thr-hydrophobic motif in all MHCK family members (Figure 3-10) in spite of the differences in length and variability of the residues in the C-tail regions. In addition, the kinase activity of A-CAT-802 was rescued by ligation of the C-tail sequence of B-CAT (A-CAT-B-CAT-Tail-Chimera). These results provide further evidence for a conserved activation sequence in the C-tail region. Studies of chimeric versions of A-CAT fused to the C-tail of MHCK C and MHCK D, or even that of TRPM7, may help in understanding this general mechanism for regulation of alpha-kinase activity. It will be important to investigate whether truncation of the C-tail or point-mutation of the conserved threonine residue in the C-tail sequences of MHCK B-D inhibits their catalytic activity.

The C-tail sequence needs to be in a specific orientation towards the active site in A-CAT, because addition of a free GST-A-CAT C-tail fragment did not increase the low kinase activity of A-CAT-809. The specific orientation of T825 with respect to the active site may explain why the activity of the kinase domain decreased when the length of the C-tail was reduced in two deletion constructs, in which residues 812-814 (A-CAT-ΔVLS) or 810-815 (A-CAT-ΔGGVLSG) were deleted. Unexpectedly, deletion of 10 residues

(810-819) in A-CAT-ΔGGVLSGNNKK, increased the kinase rate compared to the other deletion constructs. Possibly, this happened because T841 was brought closer to the active site, resulting in the functional substitution of T841 for T825. If this proposal is correct, we would predict that deletion of 16 residues (e.g. residues 810-825) of the C-tail, including T825, would also result in an active A-CAT. To confirm the importance of T841 in this construct, T841 could be mutated to alanine.

Autophosphorylation assays show that T825 accounts for approximately 30% of the total phosphate incorporated into A-CAT. A-CAT-5xAla, in which all of the autophosphorylation sites [8] are mutated to alanine except for T825, showed only a slight decrease in kinase and ATPase rates (~10% and ~17%, respectively). In contrast, as noted above, mutation of T825 to alanine decreased kinase activity by ~97%. The results raise the possibility that phosphorylation of T825 plays a role in the regulatory mechanism of A-CAT. Mutation of T825 to serine reduced A-CAT kinase activity by approximately 85%, which shows that this site is very specific for threonine. This is in agreement with previous studies which show that A-CAT strongly prefers to phosphorylate threonine residues in peptide and protein substrates [51;54]. Surprisingly, mutation of T825 to glutamic acid decreased kinase and ATPase activities by ~93% and ~96%, respectively.

In full-length MHCK A the C-tail is a part of the linker that connects the alpha-kinase domain to the WD repeat domain. T825 still plays an important role in the catalytic activity of MHCK A, since kinase assays of MHCK A-T825A and MHCK A-T825E showed a decrease in kinase activity by approximately 90%. The importance of

T825 phosphorylation in the context of full-length MHCK A activation *in* vivo could be examined by generating a phospho-specific antibody directed toward T825.

What is the exact role of the C-tail, and specifically T825, in supporting the catalytic activity of A-CAT? Does phosphorylation of T825 have any function in the regulation of catalytic activity of A-CAT? Answers to these questions are not clear yet. However, the requirement for the C-tail segment has lead us to speculate about its role.

The C-tail region of A-CAT was modeled using the residue builder in Pymol and was aligned onto the crystal structure of A-CAT (Figure 4-1). Given the length of the C-tail and assuming that it is unstructured and flexible, the model shows that the C-tail spans the entire distance of the alpha-kinase domain. It is very interesting that in this model T825 is located at a position that allows it to interact with the N/D loop or with the active site, including the active site pocket and the bound ATP (Figure 4-2). We can reassess the role of the chelated zinc atom found at the C-terminus of the alpha-kinase domain. Previously this zinc atom was thought to play a general role in maintaining the fold of the C-terminal lobe of the kinase domain. However, we now can hypothesize that the chelated zinc may also act to specifically orient the final exiting alpha-helix of the kinase domain in such a manner as to position the unstructured C-tail toward the active site (Figure 4-1).

It is not known whether the hydroxyl group of T825 or phosphorylation of T825 is the key requirement for catalytic activity. The further question in the case of phosphorylation is whether a stable autophosphorylation of T825 is needed to enhance kinase and ATPase activities, or whether a reversible phosphorylation of T825 is directly involved in the catalytic activity.

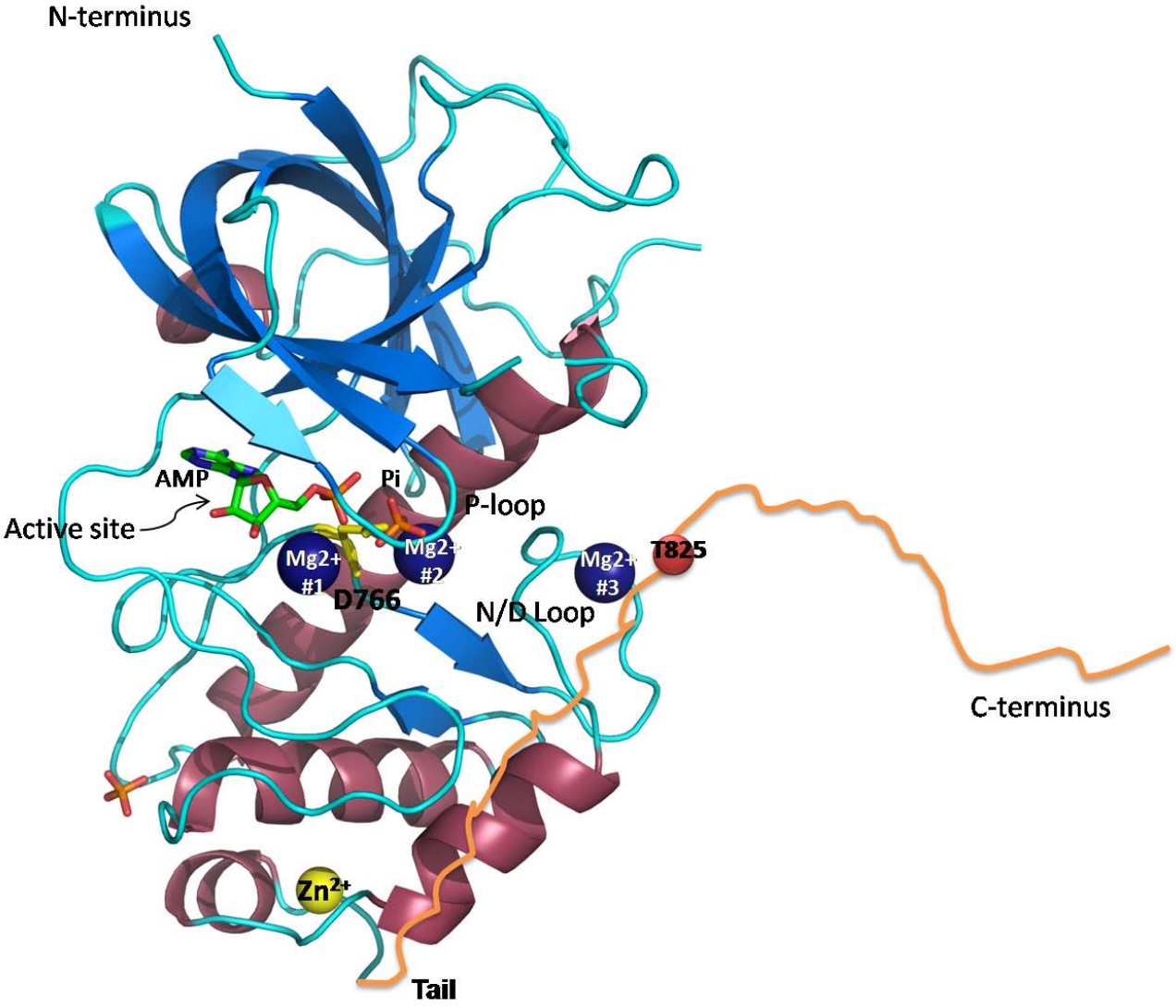

Figure 4-1. The structure of A-CAT with modeled C-tail sequence. The C-tail sequence has been shown in orange using Pymol. Mg^{2+} ions have been indicated as dark blue spheres, T825 as a red sphere, Zn^{2+} as a yellow sphere, and D766 as a yellow stick. AMP and Pi have been shown in sticks in the active site. Considering the length of the C-tail and its unstructured flexibility, it can be speculated that this long C-tail region can span the distance of the entire folded kinase domain.

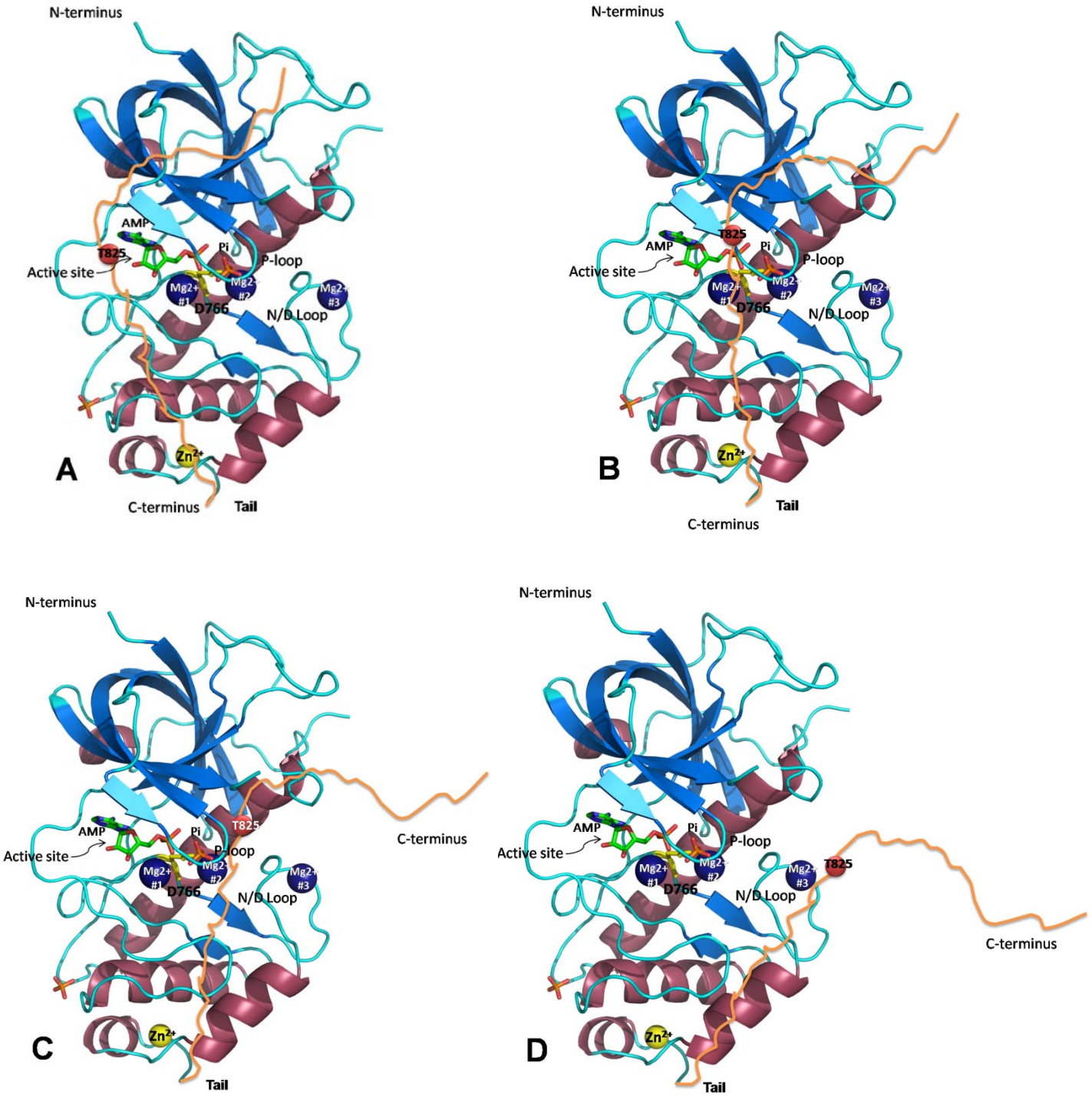

Figure 4-2. Model showing different possible structural locations of the flexible unstructured A-CAT C-Tail. Given the known length of the C-tail and assuming that it is highly flexible, it can be demonstrated that T825 may be able to interact with: A) Active site and the bound nucleotide, B) D766 in the active site and Mg^{2+}#1, C) Active site pocket and Mg^{2+}#2, or D) N/D loop and the bound Mg^{2+}#3.

It may be speculated that either the phosphorylated or unphosphorylated form of T825 may interact with the N/D loop and increase its affinity for binding divalent cations (Figures 4-1 and 4-2D). It is postulated that the conformation of the N/D loop, which forms one side of the active site pocket, is altered upon binding divalent cations. Direct evidence for a divalent-cation-mediated conformational change in the N/D-loop is lacking, although in TRPM7, the N/D loop is unstructured in the absence of nucleotide and undergoes a conformational change when nucleotide binds [93]. The presence of Mg^{2+}#3 in the crystal structure of A-CAT-809 shows that T825 is not required for binding of divalent cations to the N/D loop (Figure 3-7). The X-ray structure of A-CAT-AMP shows 5 bonds for the Mg^{2+}#1, meaning one bond is missing [8]. Mg^{2+}#1 is not present in the active site of A-CAT-809, which indicates that T825 may provide the extra bond that stabilizes the binding of Mg^{2+}#1 (Figures 3-7 and 1-6A). This may increase the affinity of the active site for ATP. The β-phosphate of ADP in the structure of A-CAT-809 forms a hydrogen bond (2.8 Å) with the 2' OH group of ribose, which does not leave enough space to accommodate the Mg^{2+}#1 (Figure 3-7).

The idea that the phosphate group on T825 is important for activity is not in accordance with the result showing that mutation of T825 to glutamic acid inactivates the kinase domain. It is possible that in this case glutamic acid does not exactly mimic a phosphorylated threonine. Mutation of T825 to aspartic acid or substitution of residues 824-826 with three glutamic acids may provide more clues in this regard.

Another possibility is that T825 is involved in the catalytic mechanism. It may be involved in transferring of the γ-phosphate of ATP to the active site D766 to form P-D766, or from P-D766 to the peptide substrate (Figure 4-2B). Such a role in a cycle of

phosphorylation/dephosphorylation would be in agreement with the results of mutational analysis which suggests that the residue at position 825 needs a hydroxyl group (Table 4-1).

In TRPM7-CAT, like A-CAT, the C-tail sequence is critical for activity. However, none of the serine and threonine residues mutated in this study (T1827, S1838, S1839, S1848 and S1857) were found to be necessary for catalytic activity. The mutated residues include both of the previously identified autophosphorylation sites (S1848 and S1857) in the TRPM7 C-tail [53]. An alignment map of the C-tail region of TRPM7 shows how these residues are conserved in different species (Figure 4-3). In future work, the other serine (S1845, S1852) and threonine (T1849, T1855) residues within the TRPM7 C-tail should be mutated to investigate their involvement in kinase activity. If one of these serine or threonine residues is found to be necessary for kinase activity, mass spectrometric studies may be carried out to determine if it is phosphorylated. It will be very important to determine whether the mechanism by which the C-tail regulates kinase activity is conserved between TRPM7 and MHCK A.

More experiments will be required to define the exact role of the C-tail region of the kinase domain. Defining the critical residue for the function of the C-tail of TRPM7-CAT will help to better understand the regulatory mechanism of the kinase domain by the C-tail region. Expansion of the project to the C-tail region of other alpha-kinases *in vitro* and *in vivo* will provide new insights into regulation of these important enzymes within the cell.

Table 4-1. Accordance of different states of T825 with the results of experiments. Check mark (√) indicates agreement with experiment and X indicates disagreement with experiment.

Activity Requirement	**Truncation of C-tail: Inactive**	**T825A: Inactive**	**T825E: Inactive**
Active when T825 has hydroxyl group	√	√	√
Active when T825 is phosphorylated	√	√	X*
Needs a cycle of phosphorylation/dephosphorylation	√	√	√

* Unless glutamic acid does not mimic the phosphorylated threonine here.

Figure 4-3. An alignment map of TRPM7 C-tail of different species. The conserved residues are shown in red. The residues of Mus musculus which have been mutated for this study (T1827, S1838, S1839, S1848, and S1857) are highlighted in slate in all species.

Reference List

1. Scheeff,E.D. and Bourne,P.E., Structural evolution of the protein kinase-like superfamily, PLoS. Comput. Biol., 1 (2005) 359-381.

2. Drennan,D. and Ryazanov,A.G., Alpha-kinases: analysis of the family and comparison with conventional protein kinases, Prog. Biophys. Mol Biol, 85 (2004) 1-32.

3. Manning,G., Plowman,G.D., Hunter,T., and Sudarsanam,S., Evolution of protein kinase signaling from yeast to man, Trends Biochem Sci, 27 (2002) 514-520.

4. Gough,J., Karplus,K., Hughey,R., and Chothia,C., Assignment of homology to genome sequences using a library of hidden Markov models that represent all proteins of known structure, J. Mol. Biol., 313 (2001) 903-919.

5. Ryazanov,A.G., Pavur,K.S., and Dorovkov,M.V., Alpha-kinases: a new class of protein kinases with a novel catalytic domain, Curr Biol, 9 (1999) R43-R45.

6. Swanson,R.V., Alex,L.A., and Simon,M.I., Histidine and aspartate phosphorylation: Two-component systems and the limits of homology, Trends Biochem Sci, 19 (1994) 485-490.

7. Pinna,L.A. and Ruzzene,M., How do protein kinases recognize their substrates?, Biochim. Biophys. Acta Mol. Cell Res., 1314 (1996) 191-225.

8. Ye,Q., Crawley,S.W., Yang,Y., Cote,G.P., and Jia.Z., Cystal Structure of the Alpah-kinase Domain of *Dictyostelium* Myosin Heavy Chain Kinase A, Science Signaling, In Press (2010).

9. Côté,G.P. and Bukiejko,U., Purification and characterization of a myosin heavy chain kinase from *Dictyostelium discoideum*, J Biol Chem, 262 (1987) 1065-1072.

10. Futey,L.M., Medley,Q.G., Côté,G.P., and Egelhoff,T.T., Structural analysis of myosin heavy chain kinase A from *Dictyostelium*. Evidence for a highly divergent protein kinase domain, an amino-terminal coiled-coil domain, and a domain homologous to the β-subunit of heterotrimeric G proteins, J Biol Chem, 270 (1995) 523-529.

11. Clancy,C.E., Mendoza,M.G., Naismith,T.V., Kolman,M.F., and Egelhoff,T.T., Identification of a protein kinase from *Dictyostelium* with homology to the novel catalytic domain of myosin heavy chain kinase A, J Biol Chem, 272 (1997) 11812-11815.

12. Nagasaki,A., Itoh,G., Yumura,S., and Uyeda,T.Q., Novel myosin heavy chain kinase involved in disassembly of myosin II filaments and efficient cleavage in mitotic dictyostelium cells, Mol Biol Cell, 13 (2002) 4333-4342.

13. Ryazanov,A.G., Elongation factor-2 kinase and its newly discovered relatives, FEBS Lett, 514 (2002) 26-29.

14. Yumura,S., Yoshida,M., Betapudi,V., Licate,L.S., Iwadate,Y., Nagasaki,A., Uyeda,T.Q., and Egelhoff,T.T., Multiple myosin II heavy chain kinases: roles in filament assembly control and proper cytokinesis in *Dictyostelium*, Mol Biol Cell, 16 (2005) 4256-4266.

15. Middelbeek,J., Clark,K., Venselaar,H., Huynen,M.A., and Van Leeuwen,F.N., The alpha-kinase family: an exceptional branch on the protein kinase tree, Cell Mol Life Sci, (2009).

16. Betapudi,V., Mason,C., Licate,L., and Egelhoff,T.T., Identification and characterization of a novel alpha-kinase with a von Willebrand factor A-like motif localized to the contractile vacuole and Golgi complex in *Dictyostelium discoideum*, Mol Biol Cell, 16 (2005) 2248-2262.

17. Runnels,L.W., Yue,L., and Clapham,D.E., TRP-PLIK, a bifunctional protein with kinase and ion channel activities, Science, 291 (2001) 1043-1047.

18. Schlingmann,K.P., Weber,S., Peters,M., Niemann,N.L., Vitzthum,H., Klingel,K., Kratz,M., Haddad,E., Ristoff,E., Dinour,D., Syrrou,M., Nielsen,S., Sassen,M., Waldegger,S., Seyberth,H.W., and Konrad,M., Hypomagnesemia with secondary hypocalcemia is caused by mutations in TRPM6, a new member of the TRPM gene family, Nat. Genet., 31 (2002) 166-170.

19. Ryazanov,A.G., Ward,M.D., Mendola,C.E., Pavur,K.S., Dorovkov,M.V., Wiedmann,M., Erdjument-Bromage,H., Tempst,P., Parmer,T.G., Prostko,C.R., Germino,F.J., and Hait,W.N., Identification of a new class of protein kinases represented by eukaryotic elongation factor-2 kinase, Proc Natl Acad Sci USA, 94 (1997) 4884-4889.

20. De La Roche,M.A. and Côté,G.P., Regulation of *Dictyostelium* myosin I and II, Biochim Biophys Acta, 1525 (2001) 245-261.

21. Sabry,J.H., Moores,S.L., Ryan,S., Zang,J.H., and Spudich,J.A., Myosin heavy chain phosphorylation sites regulate myosin localization during cytokinesis in live cells, Mol Biol Cell, 8 (1997) 2605-2615.

22. Krendel,M. and Mooseker,M.S., Myosins: tails (and heads) of functional diversity, Physiology. (Bethesda.), 20:239-51. (2005) 239-251.

23. Bresnick,A.R., Molecular mechanisms of nonmuscle myosin-II regulation, Curr Opin Cell Biol, 11 (1999) 26-33.

24. Robinson,D.N., Cavet,G., Warrick,H.M., and Spudich,J.A., Quantitation of the distribution and flux of myosin-II during cytokinesis, BMC. Cell Biol, 3 (2002) 4.

25. Chisholm,R.L., Rushforth,R.S., Pollenz,R.S., Kuczmarski,E.R., and Tafuri,S.R., *Dictyostelium discoideum* myosin: isolation and characterization of cDNAs encoding the essential light chain, Mol Cell Biol, 8 (1988) 794-810.

26. Tafuri,S.R., Rushforth,A.M., Kuczmarski,E.R., and Chisholm,R.L., *Dictyostelium discoideum* myosin: isolation and characterization of cDNAs encoding the regulatory light chain, Mol Cell Biol, 9 (1989) 3073-3080.

27. Warrick,H.M., De Lozanne,A., Leinwand,L.A., and Spudich,J.A., Conserved protein domains in a myosin heavy chain gene from *Dictyostelium discoideum*, Proc Natl Acad Sci USA, 83 (1986) 9433-9437.

28. Geeves,M.A. and Holmes,K.C., Structural mechanism of muscle contraction, Annu Rev Biochem, 68 (1999) 687-728.

29. Rayment,I., Holden,H.M., Whittaker,M., Yohn,C.B., Lorenz,M., Holmes,K.C., and Milligan,R.A., Structure of the actin-myosin complex and its implications for muscle contraction, Science, 261 (1993) 58-65.

30. Yumura,S. and Kitanishi-Yumura,T., Immunoelectron microscopic studies of the ultrastructure of myosin filaments in *Dictyostelium discoideum*, Cell Struct Funct, 15 (1990) 343-354.

31. Egelhoff,T.T., Lee,R.J., and Spudich,J.A., Dictyostelium myosin heavy chain phosphorylation sites regulate myosin filament assembly and localization in vivo, Cell, 75 (1993) 363-371.

32. Clark,K., Langeslag,M., Figdor,C.G., and Van Leeuwen,F.N., Myosin II and mechanotransduction: a balancing act, Trends Cell Biol, 17 (2007) 178-186.

33. Bosgraaf,L., Russcher,H., Smith,J.L., Wessels,D., Soll,D.R., and Van Haastert,P.J.M., A novel cGMP-signaling pathway mediating myosin assembly and chemotaxis in *Dictyostelium*., EMBO J, 21 (2002) 4560-4570.

34. Egelhoff,T.T., Croft,D., and Steimle,P.A., Actin activation of myosin heavy chain kinase A in *Dictyostelium*: a biochemical mechanism for the spatial regulation of myosin II filament disassembly, J Biol Chem, 280 (2005) 2879-2887.

35. Liang,W., Warrick,H.M., and Spudich,J.A., A structural model for phosphorylation control of *Dictyostelium* myosin II thick filament assembly, J Cell Biol, 147 (1999) 1039-1048.

36. Kuczmarski,E.R., Tafuri,S.R., and Parysek,L.M., Effect of heavy chain phosphorylation on the polymerization and structure of *Dictyostelium* myosin filaments, J Cell Biol, 105 (1987) 2989-2997.

37. Rosenberg,M., Straussman,R., Ben-Ya'acov,A., Ronen,D., and Ravid,S., MHC-IIB filament assembly and cellular localization are governed by the rod net charge, PLoS. ONE., 3 (2008) e1496.

38. Matsumura,F., Regulation of myosin II during cytokinesis in higher eukaryotes, Trends Cell Biol, 15 (2005) 371-377.

39. Stites,J., Wessels,D., Uhl,A., Egelhoff,T., Shutt,D., and Soll,D.R., Phosphorylation of the *Dictyostelium* myosin II heavy chain is necessary for maintaining cellular polarity and suppressing turning during chemotaxis, Cell Motil. Cytoskeleton, 39 (1998) 31-51.

40. Kolman,M.F., Futey,L.M., and Egelhoff,T.T., *Dictyostelium* myosin heavy chain kinase A regulates myosin localization during growth and development, J Cell Biol, 132 (1996) 101-109.

41. Vaillancourt,J.P., Lyons,C., and Côté,G.P., Identification of two phosphorylated threonines in the tail region of *Dictyostelium* myosin II, J Biol Chem, 263 (1988) 10082-10087.

42. Luck-Vielmetter,D., Schleicher,M., Grabatin,B., Wippler,J., and Gerisch,G., Replacement of threonine residues by serine and alanine in a phosphorylatable heavy chain fragment of *Dictyostelium* myosin II, FEBS Lett, 269 (1990) 239-243.

43. Côté,G.P., Luo,X., Murphy,M.B., and Egelhoff,T.T., Mapping of the novel protein kinase catalytic domain of *Dictyostelium* myosin II heavy chain kinase A, J Biol Chem, 272 (1997) 6846-6849.

44. Kolman,M.F. and Egelhoff,T.T., *Dictyostelium* myosin heavy chain kinase A subdomains - Coiled-coil and WD repeat roles in oligomerization and substrate targeting, J Biol Chem, 272 (1997) 16904-16910.

45. Steimle,P.A., Licate,L., Cote,G.P., and Egelhoff,T.T., Lamellipodial localization of *Dictyostelium* myosin heavy chain kinase A is mediated via F-actin binding by the coiled-coil domain, FEBS Lett, 516 (2002) 58-62.

46. Steimle,P.A., Naismith,T., Licate,L., and Egelhoff,T.T., WD repeat domains target *Dictyostelium* myosin heavy chain kinases by binding directly to myosin filaments, J Biol Chem, 276 (2001) 6853-6860.

47. Medley,Q.G., Gariepy,J., and Côté,G.P., *Dictyostelium* myosin II heavy-chain kinase A is activated by autophosphorylation: Studies with *Dictyostelium* myosin II and synthetic peptides, Biochemistry, 29 (1990) 8992-8997.

48. Medley,Q.G., Bagshaw,W.L., Truong,T., and Côté,G.P., *Dictyostelium* myosin II heavy-chain kinase A is activated by heparin, DNA and acidic phospholipids and inhibited by polylysine, polyarginine and histones, Biochim Biophys Acta, 1175 (1992) 7-12.

49. Steimle,P., Yumura,S., Côté,G.P., Medley,Q.G., Polyakov,M., Leppert,B., and Egelhoff,T.T., Recruitment of a myosin heavy chain kinase to actin-rich protrusions in *Dictyostelium*, Curr Biol, 11 (2001) 708-713.

50. Liang,W., Licate,L., Warrick,H., Spudich,J., and Egelhoff,T., Differential localization in cells of myosin II heavy chain kinases during cytokinesis and polarized migration, BMC. Cell Biol, 3 (2002) 19.

51. Crawley,S.W. and Cote,G.P., Determinants for Substrate Phosphorylation by *Dictyostelium* Myosin II Heavy Chain Kinases A and B and Eukaryotic Elongation Factor-2 Kinase, Biochim Biophys Acta, 1784 (2008) 908-915.

52. Matsushita,M., Kozak,J.A., Shimizu,Y., McLachlin,D.T., Yamaguchi,H., Wei,F.Y., Tomizawa,K., Matsui,H., Chait,B.T., Cahalan,M.D., and Nairn,A.C., Channel function is dissociated from the intrinsic kinase activity and autophosphorylation of TRPM7/ChaK1, J Biol Chem, 280 (2005) 20793-20803.

53. Clark,K., Middelbeek,J., Morrice,N.A., Figdor,C.G., Lasonder,E., and Van Leeuwen,F.N., Massive autophosphorylation of the Ser/Thr-rich domain controls protein kinase activity of TRPM6 and TRPM7, PLoS. ONE., 3 (2008) e1876.

54. Luo,X., Crawley,S.W., Steimle,P., Egelhoff,T.T., and Côté,G.P., Specific phosphorylation of threonine by the *Dictyostelium* myosin II heavy chain kinase family, J Biol Chem, 276 (2001) 17836-17843.

55. De Lozanne,A. and Spudich,J.A., Disruption of the *Dictyostelium* myosin heavy chain gene by homologous recombination, Science, 236 (1987) 1086-1091.

56. Manstein,D.J., Titus,M.A., De Lozanne,A., and Spudich,A., Gene replacement in *Dictyostelium*: generation of myosin null mutants, EMBO J, 8 (1989) 923-932.

57. Ruppel,K.M., Uyeda,T.Q.P., and Spudich,J.A., Role of highly conserved lysine 130 of myosin motor domain. *In vivo* and *in vitro* characterization of site specifically mutated myosin, J Biol Chem, 269 (1994) 18773-18780.

58. Wessels,D. and Soll,D.R., Myosin II heavy chain null mutant of *Dictyostelium* exhibits defective intracellular particle movement, J Cell Biol, 111 (1990) 1137-1148.

59. Wessels,D., Soll,D.R., Knecht,D.A., Loomis,W.F., De Lozanne,A., and Spudich,J.A., Cell motility and chemotaxis in *Dictyostelium* amebae lacking myosin heavy chain, Dev Biol, 128 (1988) 164-177.

60. Clapham,D.E., Runnels,L.W., and Strubing,C., The TRP ion channel family, Nat. Rev. Neurosci., 2 (2001) 387-396.

61. Clapham,D.E., TRP channels as cellular sensors, Nature, 426 (2003) 517-524.

62. Perraud,A.L., Knowles,H.M., and Schmitz,C., Novel aspects of signaling and ion-homeostasis regulation in immunocytes. The TRPM ion channels and their potential role in modulating the immune response, Mol. Immunol., 41 (2004) 657-673.

63. Jiang,L.H., Subunit interaction in channel assembly and functional regulation of transient receptor potential melastatin (TRPM) channels, Biochem Soc Trans, 35 (2007) 86-88.

64. Montell,C., An exciting release on TRPM7, Neuron, 52 (2006) 395-397.

65. Nadler,M.J., Hermosura,M.C., Inabe,K., Perraud,A.L., Zhu,Q., Stokes,A.J., Kurosaki,T., Kinet,J.P., Penner,R., Scharenberg,A.M., and Fleig,A., LTRPC7 is a Mg.ATP-regulated divalent cation channel required for cell viability, Nature, 411 (2001) 590-595.

66. Zhao,L., Wang,Y., Sun,N., Liu,X., Li,L., and Shi,J., Electroacupuncture regulates TRPM7 expression through the trkA/PI3K pathway after cerebral ischemia-reperfusion in rats, Life Sci., 81 (2007) 1211-1222.

67. Schlingmann,K.P., Weber,S., Peters,M., Niemann,N.L., Vitzthum,H., Klingel,K., Kratz,M., Haddad,E., Ristoff,E., Dinour,D., Syrrou,M., Nielsen,S., Sassen,M., Waldegger,S., Seyberth,H.W., and Konrad,M., Hypomagnesemia with secondary hypocalcemia is caused by mutations in TRPM6, a new member of the TRPM gene family, Nat. Genet., 31 (2002) 166-170.

68. Fonfria,E., Murdock,P.R., Cusdin,F.S., Benham,C.D., Kelsell,R.E., and McNulty,S., Tissue distribution profiles of the human TRPM cation channel family, J. Recept. Signal. Transduct. Res., 26 (2006) 159-178.

69. Walder,R.Y., Yang,B., Stokes,J.B., Kirby,P.A., Cao,X., Shi,P., Searby,C.C., Husted,R.F., and Sheffield,V.C., Mice defective in Trpm6 show embryonic mortality and neural tube defects, Hum Mol Genet, 18 (2009) 4367-4375.

70. Jin,J., Desai,B.N., Navarro,B., Donovan,A., Andrews,N.C., and Clapham,D.E., Deletion of Trpm7 disrupts embryonic development and thymopoiesis without altering Mg2+ homeostasis, Science, 322 (2008) 756-760.

71. Schmitz,C., Dorovkov,M.V., Zhao,X., Davenport,B.J., Ryazanov,A.G., and Perraud,A.L., The channel kinases TRPM6 and TRPM7 are functionally nonredundant, J Biol Chem, 280 (2005) 37763-37771.

72. Jiang,H., Tian,S.L., Zeng,Y., Li,L.L., and Shi,J., TrkA pathway(s) is involved in regulation of TRPM7 expression in hippocampal neurons subjected to ischemic-reperfusion and oxygen-glucose deprivation, Brain Res. Bull., 76 (2008) 124-130.

73. Iuga,A.O. and Lerner,E.A., TRP-ing up melanophores: TRPM7, melanin synthesis, and pigment cell survival, J. Invest Dermatol., 127 (2007) 1855-1856.

74. Montell,C. and Rubin,G.M., Molecular characterization of the Drosophila trp locus: a putative integral membrane protein required for phototransduction, Neuron, 2 (1989) 1313-1323.

75. Jiang,X., Newell,E.W., and Schlichter,L.C., Regulation of a TRPM7-like current in rat brain microglia, J Biol Chem, 278 (2003) 42867-42876.

76. Prakriya,M. and Lewis,R.S., Separation and characterization of currents through store-operated CRAC channels and Mg2+-inhibited cation (MIC) channels, J. Gen. Physiol, 119 (2002) 487-507.

77. Demeuse,P., Penner,R., and Fleig,A., TRPM7 channel is regulated by magnesium nucleotides via its kinase domain, J. Gen. Physiol, 127 (2006) 421-434.

78. Schmitz,C., Perraud,A.L., Johnson,C.O., Inabe,K., Smith,M.K., Penner,R., Kurosaki,T., Fleig,A., and Scharenberg,A.M., Regulation of vertebrate cellular Mg^{2+} homeostasis by TRPM7, Cell, 114 (2003) 191-200.

79. Thebault,S., Cao,G., Venselaar,H., Xi,Q., Bindels,R.J., and Hoenderop,J.G., Role of the alpha-kinase domain in TRPM6 channel and regulation by intracellular ATP, J Biol Chem, 283 (2008) 19999-20007.

80. Su,L.T., Agapito,M.A., Li,M., Simonson,W.T., Huttenlocher,A., Habas,R., Yue,L., and Runnels,L.W., TRPM7 regulates cell adhesion by controlling the calcium-dependent protease calpain, J Biol. Chem, 281 (2006) 11260-11270.

81. Clark,K., Langeslag,M., van Leeuwen,B., Ran,L., Ryazanov,A.G., Figdor,C.G., Moolenaar,W.H., Jalink,K., and Van Leeuwen,F.N., TRPM7, a novel regulator of actomyosin contractility and cell adhesion, EMBO J, 25 (2006) 290-301.

82. Clark,K., Middelbeek,J., Lasonder,E., Dulyaninova,N.G., Morrice,N.A., Ryazanov,A.G., Bresnick,A.R., Figdor,C.G., and Van Leeuwen,F.N., TRPM7 Regulates Myosin IIA Filament Stability and Protein Localization by Heavy Chain Phosphorylation, J Mol. Biol., 378 (2008) 788-801.

83. Clark,K., Middelbeek,J., Dorovkov,M.V., Figdor,C.G., Ryazanov,A.G., Lasonder,E., and Van Leeuwen,F.N., The alpha-kinases TRPM6 and TRPM7, but not eEF-2 kinase, phosphorylate the assembly domain of myosin IIA, IIB and IIC, FEBS Lett, 582 (2008) 2993-2997.

84. Bokoch,G.M., Biology of the p21-Activated Kinases, Annu Rev Biochem, 72 (2003) 743-781.

85. Roskoski,R., Jr., Src protein-tyrosine kinase structure and regulation, Biochem Biophys Res Commun, 324 (2004) 1155-1164.

86. Hubbard,S.R., Protein tyrosine kinases: autoregulation and small-molecule inhibition, Curr Opin Struct Biol, 12 (2002) 735-741.

87. Diggle,T.A., Seehra,C.K., Hase,S., and Redpath,N.T., Analysis of the domain structure of elongation factor-2 kinase by mutagenesis, FEBS Lett, 457 (1999) 189-192.

88. Pavur,K.S., Petrov,A.N., and Ryazanov,A.G., Mapping the functional domains of elongation factor-2 kinase, Biochemistry, 39 (2000) 12216-12224.

89. Diggle,T.A., Subkhankulova,T., Lilley,K.S., Shikotra,N., Willis,A.E., and Redpath,N.T., Phosphorylation of elongation factor-2 kinase on serine 499 by cAMP-dependent protein kinase induces Ca2+/calmodulin-independent activity, Biochem J, 353 (2001) 621-626.

90. Ryazanov,A.G., Ward,M.D., Mendola,C.E., Pavur,K.S., Dorovkov,M.V., Wiedmann,M., Erdjument-Bromage,H., Tempst,P., Parmer,T.G., Prostko,C.R., Germino,F.J., and Hait,W.N., Identification of a new class of protein kinases represented by eukaryotic elongation factor-2 kinase, Proc. Natl. Acad. Sci. U. S. A, 94 (1997) 4884-4889.

91. Nairn,A.C., Bhagat,B., and Palfrey,H.C., Identification of calmodulin-dependent protein kinase III and its major Mr 100,000 substrate in mammalian tissues, Proc Natl Acad Sci USA, 82 (1985) 7939-7943.

92. Ryazanova,L.V., Dorovkov,M.V., Ansari,A., and Ryazanov,A.G., Characterization of the protein kinase activity of TRPM7/ChaK1, a protein kinase fused to the transient receptor potential ion channel, J Biol Chem, 279 (2004) 3708-3716.

93. Yamaguchi,H., Matsushita,M., Nairn,A.C., and Kuriyan,J., Crystal structure of the atypical protein kinase domain of a TRP channel with phosphotransferase activity, Mol Cell, 7 (2001) 1047-1057.

94. Crawley,S.W. and Cote,G.P., Identification of Dimer Interactions Required for the Catalytic Activity of the TRPM7 Alpha-Kinase Domain, Biochem J, Published online 19 February 2009 doi:10.1042/BJ20081405 (2009).

95. Sambrook,J., Fritsch,E.F., and Maniatis,T., Molecular Cloning: A Laboratory Manual, Cold Spring Harbor Laboratory, Plainview, NY, 1989.

96. Levi,S., Polyakov,M., and Egelhoff,T.T., Green fluorescent protein and epitope tag fusion vectors for *Dictyostelium discoideum*, Plasmid, 44 (2000) 231-238.

97. Hadwiger,J.A. and Firtel,R.A., Analysis of $G_{\alpha}4$, a G-protein subunit required for multicellular development in *Dictyostelium*, Genes Dev., 6 (1992) 38-49.

98. Sussman,M., Cultivation and synchronous morphogenesis of *Dictyostelium* under controlled experimental conditions, Methods Cell Biol., 28 (1987) 9-29.

99. Knecht,D. and Pang,K.M., Electroporation of *Dictyostelium discoideum*, Methods Mol. Biol., 47 (1995) 321-330.

100. Casnellie,J.E., Assay of protein kinases using peptides with basic residues for phosphocellulose binding, Methods Enzymol, 200 (1991) 115-120.

101. Pollard,T.D. and Korn,E.D., *Acanthamoeba* myosin. I. Isolation from *Acanthamoeba castellanii* of an enzyme similar to muscle myosin, J Biol Chem, 248 (1973) 4682-4690.

102. Medley,Q.G., Lee,S.-F., and Côté,G.P., Purification and characterization of myosin II heavy chain kinase II A from *Dictyostelium*, Methods Enzymol, 196 (1991) 23-34.

103. Scharenberg,A.M., TRPM2 and TRPM7: channel/enzyme fusions to generate novel intracellular sensors, Pflugers Arch., 451 (2005) 220-227.